Sensor and Simulation Notes

Note 243

19 July 1978

Multipole Radiations: Formulation and Evaluation for Small EMP Simulators

Jiunn S. Yu
C-L. James Chen
Dikewood Industries, Inc.
Albuquerque, NM 87106

and

Carl E. Baum
Air Force Weapons Laboratory
Kirtland AFB, NM 87117

Abstract

Multipole radiations are formulated in terms of spherical harmonics for two small EMP simulators. Exact solutions for generalized multipole coefficients are obtained and shown to become mulitpole moments under quasi-static approximations. Strengths of multipoles are evaluated in exact and approximate forms for two simulators to evaluate their performance characteristics. Both simulators under quasi-static limit are shown to exhibit the desired $\vec{p}$ cross $\vec{m}$ features. General solutions including quadrupoles are also explicitly obtained. The desired features of $\vec{p}$ cross $\vec{m}$ are gradually degraded as the simulators become electrically larger. The numerical evaluations of multipole strengths have been prepared for the purpose of checking potential engineering models of the two simulators. Meanwhile, the exact formulations of

Sensor and Simulation Notes

Note 243

19 July 1978

Multipole Radiations: Formulation and Evaluation for Small EMP Simulators

Jiunn S. Yu
C-L. James Chen
Dikewood Industries, Inc.
Albuquerque, NM 87106

and

Carl E. Baum
Air Force Weapons Laboratory
Kirtland AFB, NM 87117

Abstract

Multipole radiations are formulated in terms of spherical harmonics for two small EMP simulators. Exact solutions for generalized multipole coefficients are obtained and shown to become mulitpole moments under quasi-static approximations. Strengths of multipoles are evaluated in exact and approximate forms for two simulators to evaluate their performance characteristics. Both simulators under quasi-static limit are shown to exhibit the desired $\vec{p}$ cross $\vec{m}$ features. General solutions including quadrupoles are also explicitly obtained. The desired features of $\vec{p}$ cross $\vec{m}$ are gradually degraded as the simulators become electrically larger. The numerical evaluations of multipole strengths have been prepared for the purpose of checking potential engineering models of the two simulators. Meanwhile, the exact formulations of

multipole strengths have been completed to allow more refined synthesis and design of potential simulators for generating uniform TEM illumination along the direction of maximum radiation.

CONTENTS

CONTENTS (Cont'd.)

ILLUSTRATIONS

ILLUSTRATIONS (Cont'd.)

SECTION I

INTRODUCTION

1. SMALL EMP SIMULATORS

Various types of large simulators have been built and operated to provide approximate simulations of nuclear EMP (electromagnetic pulse) environment. These simulators are large in that they are intended to provide a uniform illumination of EMP onto test objects such as aircraft or missiles.

As the EMP simulation and test technologies have advanced, the interaction mechanisms of EMP with various systems have also become better understood. When specific EMP penetration mechanisms into systems are known, means have been developed to reduce or eliminate the EMP couplings and penetrations. And, as a result, various systems can become hardened against vulnerability to EMP effects such as transient upsets or permanent damage to electronic equipment.

After each implementation of a new hardening concept or technique, an engineering test and evaluation is in order. To test a full-scale system in a large EMP simulator could be costly, time-consuming, and often impractical. For alleviating problems associated with full-scale testing, some types of small EMP simulators have been conceived (ref. 1) to provide localized illumination of EMP onto discrete POEs (ports of entry) of interest on systems.

---

1. Baum, C. E., "EMP Simulators for Various Types of Nuclear EMP Environment: An Interim Categorization," IEEE Trans. on Antennas and Propagation, January 1978. Also, "Some Types of Small EMP Simulators," AFWL Misc. Simulator Memos, No. 9, December 1976.

This report formulates and evaluates the potential performance characteristics of a particular type of small simulator of which the fields are to be produced purely by a pair of electric and magnetic dipoles.

2. THE $\vec{p}$ CROSS $\vec{m}$ CONCEPT AND LIMITATIONS

Should there be a pair of pure electric dipole $\vec{p}$ and pure magnetic dipole $\vec{m}$ placed perpendicular to each other and related properly in amplitude ($m = cp$ with c as the speed of light), their combined radiation would have a set of unique features to be formulated and discussed in this report (see Sections III and IV).

However, any radiating source has its physical limitations. That is, any "design" or synthesis of source distributions cannot be done by an arbitrary mathematical arrangement without considering its physical realizability. Physical limitations of electric- and magnetic-multipole sources including those of dipoles have been treated in reference 2. Since a production of dipoles by any source will also produce higher-order multipoles, one of the main tasks of this report is to formulate completely all the multipole strengths of a given source (see Section II and all Appendixes).

If a source region is made vanishingly small, an ideal $\vec{p}$ cross $\vec{m}$ source can be conceptually formulated (ref. 3) for wavefront propagation studies. In scattering phenomena, an ideal

---

2. Chu, L. J., "Physical Limitations of Omni-Directional Antennas," J. of Applied Physics, December 1948.

3. Rumsey, V. H., "Some New Forms of Huygens Principle," IRE Trans. on Antennas and Propagation, December 1959.

$\vec{p}$ cross $\vec{m}$ scatterer can be well approximated (ref. 4) by small spherical bodies of various material parameters. Of particular interest in radiation is that a resonant $\vec{p}$ cross $\vec{m}$ radiator can be approximated (ref. 5) by a microwave antenna of $\lambda^3/16$ with about 30% operating bandwidth. Finally, it is important to note that rigorous derivations (ref. 6) of the $\vec{p}$ cross $\vec{m}$ condition have also been previously performed under low-frequency approximations. The approach of this report is to formulate the exact solution in terms of multipoles of a radiation source. This approach will permit accurate evaluation of degradation effects by higher-order multipoles that are ever-present with varying degree of significance.

An ideal $\vec{p}$ cross $\vec{m}$ radiator has some unique features that are not found in other elemental radiators. They are summarized in part as follows:

a. Cardioid radiation pattern rotationally symmetric with the axis of maximum radiation.

b. Purely real power outflowing from any spherical surface enclosing the source region.

c. Twice the directivity of a purely electric or magnetic dipole.

---

4. Yu, J. S., "Electromagnetic Resonance, Invisibility, Non-Uniqueness, and Dipole Scattering of a Small Sphere," General Electric Tech. Information Series, No. R71EMH2; January 1971.

5. Yu, J. S., and H. Moriomoto, "Electromagnetic Dipole," General Electric Tech. Information Series, No. R71EMH3; January 1971.

6. Baum, C. E., "Some Characteristics of Electric and Magnetic Dipole Antennas for Radiating Transient Pulses," AFWL Sensors and Simulation Notes, No. 125; January 1971.

These desirable features are some of the goals to which small EMP simulators are to be designed.

3. MEDIUS (MAGNETIC AND ELECTRIC DIPOLE UNIFORM SIMULATORS) SYNTHESIS AND REALIZABILITY

The acronym MEDIUS (ref. 1) is adopted here to represent all small EMP simulators of which the fields are approximately those of an ideal $\vec{p}$ cross $\vec{m}$ radiator.

The synthesis problem of MEDIUS can be stated simply; that is, to find specific types of current distribution that would give rise to a pair of dipoles with proper amplitudes and orientations. Solution to this synthesis problem is known (e.g., ref. 4) to be non-unique; that is, there are indefinitely many distributions that may yield the same desired result, at least approximately.

Without going through mathematical formalisms, two possible current distributions (ref. 1) are selected for study in this report. Based on the fundamentals of electromagnetic theory (refs. 7-10) the arrangements shown in figures 1 and 2 are known to radiate dominantly both electric- and magnetic-dipole fields, if their

---

7. Stratton, J. A., Electromagnetic Theory, McGraw-Hill Book Co.; 1941.

8. Jackson, J. D., Classical Electrodynamics, John Wiley & Sons, Inc.; 1962.

9. King, R.W.P., Chapters 9 and 11 of Antenna Theory, Part 1, edited by R. E. Collins and F. J. Zucker, McGraw-Hill Book Co.; 1969.

10. Baum, C. E., "On the Singularity Expansion Method for the Solution of Electromagnetic Interaction Problems," AFWL Interaction Notes, No. 88; December 1971.

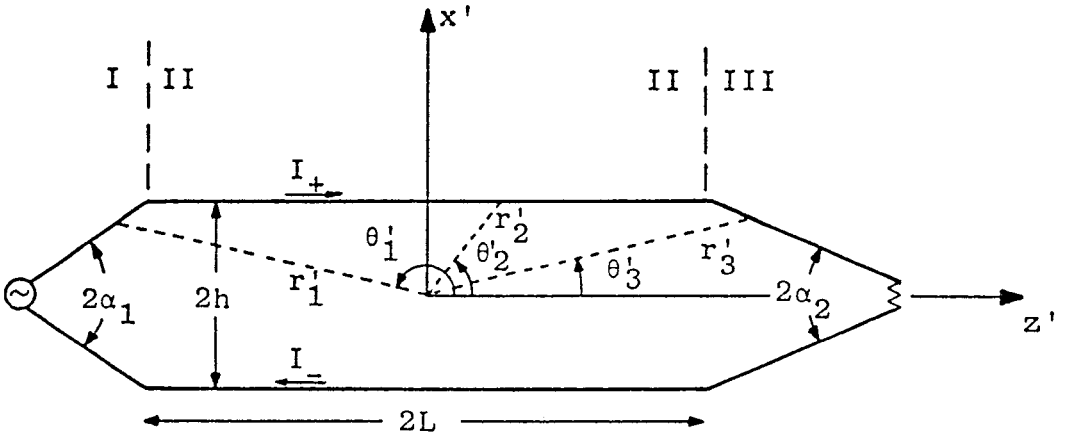

Figure 1. Transmission-Line MEDIUS and Its Source Coordinates (The y' axis is pointing out of the page. The driving power flow is along the (+z'), but the $\vec{p} \times \vec{m}$ radiation is along the (-z'), emphasizing "backward" radiation.)

Wire Radius = a

$2\ell n(2h/a) = 10$

$2\ell n(2\pi b/a) = 10$

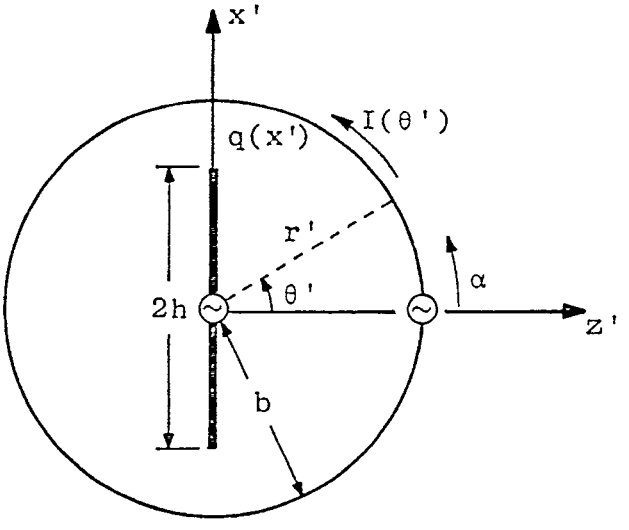

Figure 2. Collocated Linear and Circular Current Elements and Their Common Source Coordinates. (The y' axis is pointing out of the page. The $\vec{p} \times \vec{m}$ radiation is along the (+z').)

sizes are small measured in wavelength. Presently the transmission line is assumed to be perfectly matched, and the collocated current elements are assumed to have two independent but adjustable generators.

As soon as the locations of generators are selected for the conductors as arranged in figures 1 and 2, the current distributions will become unique and so will the radiated fields. The relative amplitudes and phases of the generators in figure 2 may be assumed, for the time being, to have unlimited ranges of flexibility. If the same assumption is also applied to the transmission line in general, the arrangements as shown in figures 1 and 2 could be considered physically realizable.

4. GENERALIZED MULTIPOLE COEFFICIENTS AND QUASI-STATIC MOMENTS

Two basic approaches are available for formulating multipole radiation. One is based on the Taylor series expansion of source contributions under the quasi-static approximation. This approach has been rigorously explored (ref. 6) leading to two leading terms for dipole moments. The other is based on the Bessel-Fourier series expansion that represents the source contribution in complete sets of spherical harmonics (refs. 7-10). This approach appears to have no previous work directed toward formulating the multipole radiation of the arrangements shown in figures 1 and 2. This report adopts the second approach to first formulate the generalized multipole radiation in full and then demonstrate asymptotically that generalized multipole coefficients are related to multipole moments for a small source region.

Coordinate systems for this report are conventional rectangular and spherical coordinates as shown in figures 1 and 2 for describing source regions. They are primed to designate specifically source coordinates. Multipole radiation in this report will use unprimed coordinate systems as shown in figure 3 for descriptions of all field vectors outside of source regions.

5. SIGNIFICANT RESULTS AND OBSERVATIONS

Since multipole radiation of the two selected structures appears to have no existing formulation in terms of spherical harmonics, a complete formulation has been carried out in this report. Section II serves as a summary for all the mathematical details derived in Appendixes A through E.

Multipole coefficients and quasi-static moments for the two selected simulators are evaluated in Sections III and IV where vector fields are also expressed in terms of radiated multipoles. Field patterns have been written out in full including contributions by dipoles and quadrupoles. Conditions for the ideal $\vec{p}$ cross $\vec{m}$ radiation are established for both simulators to demonstrate the desired unique features. The specific results and their associated significance are referred to Section V for more detailed discussions.

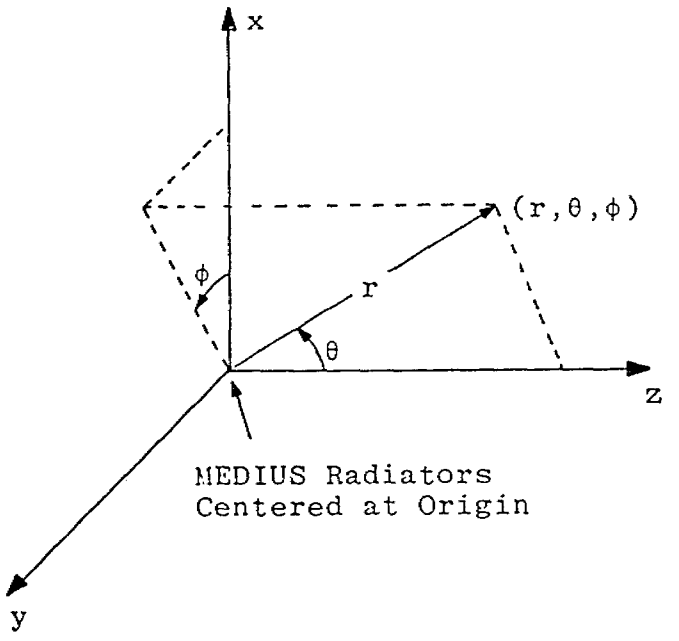

(These Cartesian coordinate axes are coincident with those of source coordinates in figure 2)

Figure 3. Conventional Spherical and Rectangular Coordinates for Fields and Potentials

SECTION II

MULTIPOLES OF DISTRIBUTED SOURCES

Solutions for Maxwell's equations have been developed in standard text books (refs. 7-9) with several techniques. A unique solution for a specific problem is assured when proper initial conditions and boundary conditions are applied to the general solution of the wave equations. The same unique solution can also be obtained by applying appropriate radiation conditions and boundary conditions to the general solution of the Helmholtz equations.

In the following, Helmholtz equations will be used for fields and potentials in the MKS system and in the frequency domain with $\exp(j\omega t)$ as the factor for time-harmonic description. If the complex plane s-domain is chosen, the factor $\exp(st)$ should be used.

1. HELMHOLTZ EQUATIONS FOR POTENTIALS

For the purpose of studying the $\vec{p}$ cross $\vec{m}$ concept, electromagnetic fields and potentials are desired in terms of multipoles. Multipole coefficients are to be formulated for distributed sources, while multipole moments are to be obtained asymptotically for small or point sources under quasi-static approximations. Both potentials and fields will first be written in Helmholtz equations for solving them in terms of multipoles.

Since the magnetic flux density $\vec{B}$ in the Maxwell's equations is solenoidal, it can be expressed as the curl of a vector potential $\vec{A}$ as

$$\vec{B} = \nabla \times \vec{A}, \quad \text{or} \quad \vec{H} = \mu^{-1} \nabla \times \vec{A} \tag{1}$$

where μ is the permeability of space being considered. Also, by the Maxwell's equation, the electric field intensity $\vec{E}$, when combined with $j\omega\vec{A}$ or $s\vec{A}$, becomes an irrotational vector. Let the combination be the gradient of a scalar potential Φ, the electric field intensity becomes

$$\vec{E} = -j\omega\vec{A} - \nabla\Phi , \quad \text{or} \quad \vec{E} = -s\vec{A} - \nabla\Phi \tag{2}$$

Equations (1) and (2) assure that both magnetic and electric fields are solved if the two potentials are uniquely determined.

Substitution of equations (1) and (2) into the Maxwell's equation, and application of the Lorentz condition

$$\nabla \cdot \vec{A} + j\omega\mu\varepsilon\Phi = 0, \quad \text{or} \quad \nabla \cdot \vec{A} + s\mu\varepsilon\Phi = 0 \tag{3}$$

will give rise to the desired Helmholtz equations for the two potentials as

$$(\nabla^2 + k^2)\vec{A} = -\mu\vec{J}, \quad \text{or} \quad (\nabla^2 - \gamma^2)\vec{A} = -\mu\vec{J} \tag{4}$$

$$(\nabla^2 + k^2)\Phi = -\varepsilon^{-1}\rho, \quad \text{or} \quad (\nabla^2 - \gamma^2)\Phi = -\varepsilon^{-1}\rho \tag{5}$$

where $k^2 = \omega^2\mu\varepsilon = \omega^2/c^2$, and $\gamma^2 = s^2/c^2$ with c as the speed of light and ε as the permittivity of space. The source term $\vec{J}$ and ρ are volumetric current and charge densities.

2. GREEN'S FUNCTION FOR POTENTIALS AND FIELDS

The Green's function G for equation (5) and for the rectangular components of equation (4) is defined to satisfy the Helmholtz

equations as

$$(\nabla^2 + k^2)\, G(\vec{r},\vec{r}') = -\delta(\vec{r} - \vec{r}') \tag{6}$$

Together with the Sommerfield's radiation condition

$$\lim_{|r-r'|\to\infty} \left(\frac{\partial}{\partial r} + jk\right) G(\vec{r},\vec{r}') = 0 \tag{7}$$

the time-harmonic Green's function takes the form

$$G(\vec{r},\vec{r}') = \frac{\exp(-jk|\vec{r} - \vec{r}'|)}{4\pi|\vec{r} - \vec{r}'|} \quad \begin{matrix}\text{with } k = \omega/c \\ \text{and } \vec{r} \neq \vec{r}'\end{matrix} \tag{8}$$

where $\vec{r}$ and $\vec{r}'$ are the position vectors of the field and source points. If the sources in equations (4) and (5) are first restricted to be elemental sources $[\vec{J}(\vec{r}')\, dv']\, \delta(\vec{r} - \vec{r}')$ and $[\rho(\vec{r}')\, dv']\, \delta(\vec{r} - \vec{r}')$, the solutions for the elemental potentials would also take the form of equation (8). By allowing the sources to be distributed, the solutions for the potentials become the integrated contributions from the entire source region as

$$\begin{aligned}\vec{A}(\vec{r}) &= \mu \int G(\vec{r},\vec{r}')\, \vec{J}(\vec{r}')\, dv' \\ &= \mu \int [\vec{\bar{I}}\, G(\vec{r},\vec{r}')] \cdot \vec{J}(\vec{r}')\, dv' \qquad (9) \\ &\quad \text{with } \vec{\bar{I}} = \vec{I}_x\vec{I}_x + \vec{I}_y\vec{I}_y + \vec{I}_z\vec{I}_z, \text{ and}\end{aligned}$$

$$\begin{aligned}\Phi(\vec{r}) &= \varepsilon^{-1} \int G(\vec{r},\vec{r}')\, \rho(\vec{r}')\, dv' \\ &= \frac{1}{j\omega\varepsilon} \int G(\vec{r},\vec{r}')\, \nabla' \cdot \vec{J}(\vec{r}')\, dv' \qquad (10)\end{aligned}$$

where the continuity equation is used in the second equality of equation (10). Solutions for the fields may also be expressed

using the Green's function by substituting equation (9) into equations (1) to (3). They are:

$$\vec{H} = \mu^{-1} \nabla \times \vec{A} = \int \nabla \times [\vec{\vec{I}}\, G(\vec{r},\vec{r}')] \cdot \vec{J}(\vec{r}')\, dv', \text{ and} \qquad (11)$$

$$\vec{E} = -j\omega\vec{A} - \nabla\Phi = -j\omega\vec{A} + \frac{1}{j\omega\mu\varepsilon} \nabla\nabla \cdot \vec{A}$$

$$= -j\omega\mu \int (\vec{\vec{I}} + k^{-2}\nabla\nabla)\, G(\vec{r},\vec{r}') \cdot \vec{J}(\vec{r}')\, dv' \qquad (12)$$

The potentials and fields as solved in equations (9) to (12) are next to be formulated in terms of multipoles.

3. MULTIPOLE EXPANSIONS OF POTENTIALS

The Green's function in equation (8) can first be written as the zeroth-order spherical Hankel function of the second kind $h_o^{(2)}$, and then expanded (ref. 7) into a complete set of spherical harmonics as

$$G(\vec{r},\vec{r}') = \frac{\exp(-jk|\vec{r} - \vec{r}'|)}{4\pi|\vec{r} - \vec{r}'|} = -\frac{jk}{4\pi} h_o^{(2)}(k|\vec{r} - \vec{r}'|)$$

$$= -\frac{jk}{4\pi} \sum_{\ell=0}^{\infty} (2\ell + 1)\, h_\ell^{(2)}(kr)\, j_\ell(kr')\, P_\ell(\cos\psi)$$

$$= -\frac{jk}{4\pi} \sum_{\ell=0}^{\infty} (2\ell + 1)\, h_\ell^{(2)}(kr)\, j_\ell(kr') \Big\{ P_\ell(\cos\theta)\, P_\ell(\cos\theta')$$

$$+ 2 \sum_{m=1}^{\ell} \frac{(\ell-m)!}{(\ell+m)!} \cdot P_\ell^m(\cos\theta)\, P_\ell^m(\cos\theta')$$

$$\cdot \Big[\cos(m\phi)\cos(m\phi') + \sin(m\phi)\sin(m\phi')\Big]\Big\} \qquad (13)$$

where j_ℓ are the spherical Bessel functions, P_ℓ are the Legendre

polynomials, P_ℓ^m are the associated Legendre polynomials, and $\cos\psi = \vec{1}_r \cdot \vec{1}_{r'}$. Substituting equation (13) into (9) and (10) gives rise to

$$\vec{A} = -\frac{jk\mu}{4\pi} \sum_{\ell=0}^{\infty} (2\ell + 1)\, h_\ell^{(2)}(kr) \int P_\ell(\cos\psi)\, j_\ell(kr')\, \vec{J}(\vec{r}')\, dv'$$

$$= \sum_{\ell=0}^{\infty} \vec{A}_\ell \qquad (14)$$

and

$$\Phi = -\frac{jk}{4\pi\varepsilon} \sum_{\ell=0}^{\infty} (2\ell + 1)\, h_\ell^{(2)}(kr) \int P_\ell(\cos\psi)\, j_\ell(kr')\, \rho(\vec{r}')\, dv'$$

$$= \sum_{\ell=0}^{\infty} \Phi_\ell \qquad (15)$$

These multipole expansions are valid for arbitrarily large source regions. Each term in the expansions has $(2\ell + 1)$ coefficients to be determined by the nature of source distributions. As illustrations, the first two terms in the potential expansions are first given in exact forms and then asymptotically expressed in terms of multipole moments. For the scalar potential

$$\Phi_o = -\frac{jk}{4\pi\varepsilon} h_o^{(2)}(kr) \int P_o(\cos\psi)\, j_o(kr')\, \rho(\vec{r}')\, dv'$$

$$\approx \frac{jk}{4\pi\varepsilon} h_o^{(2)}(kr) \int \rho(\vec{r}')\, dv', \text{ for } kr' << 1$$

$$= \frac{jk}{4\pi\varepsilon} h_o^{(2)}(kr)\, p_o, \quad \text{with } p_o = \int \rho(\vec{r}')\, dv' \qquad (16)$$

$$\Phi_1 = -\frac{jk}{4\pi\epsilon} h_1^{(2)}(kr) \int P_1(\cos\psi)\, j_1(kr')\, \rho(\vec{r}')\, dv'$$

$$\approx -\frac{jk}{4\pi\epsilon} h_1^{(2)}(kr) \int \vec{1}_r \cdot \vec{1}_{r'} \left(\frac{kr'}{3}\right) \rho(\vec{r}')\, dv', \text{ for } kr' << 1$$

$$= -\frac{jk}{4\pi\epsilon} h_1^{(2)}(kr)\, \vec{1}_r \cdot \vec{p}_1 \left(\frac{k}{3}\right), \text{with } \vec{p}_1 = \int \vec{r}'\, \rho(\vec{r}')\, dv' \qquad (17)$$

The first two terms of the vector potential are

$$\vec{A}_0 = -\frac{jk\mu}{4\pi} h_o^{(2)}(kr) \int P_o(\cos\psi)\, j_o(kr')\, \vec{J}(\vec{r}')\, dv'$$

$$\approx -\frac{jk\mu}{4\pi} h_o^{(2)}(kr) \int \vec{r}'(j\omega\rho(\vec{r}'))\, dv', \text{ for } kr' << 1$$

$$= -\frac{jk\mu}{4\pi} h_o^{(2)}(kr)(j\omega\vec{p}_1), \text{ with } \vec{p}_1 = \int \vec{r}'\, \rho(\vec{r}')\, dv' \qquad (18)$$

$$A_1 = -\frac{jk\mu}{4\pi} h_1^{(2)}(kr) \int P_1(\cos\psi)\, j_1(kr')\, \vec{J}(\vec{r}')\, dv'$$

$$\approx -\frac{jk\mu}{4\pi} h_1^{(2)}(kr) \int \vec{1}_r \cdot \vec{1}_{r'} \left(\frac{kr'}{3}\right) \vec{J}(\vec{r}')\, dv', \text{ for } kr' << 1$$

$$= -\frac{jk\mu}{4\pi} h_1^{(2)}(kr) \left[\vec{m}_1 \times \vec{1}_r + \frac{j\omega}{2} \vec{\vec{p}}_2 \cdot \vec{1}_r\right] \frac{k}{3}, \qquad (19)$$

with

$$\vec{m}_1 = \frac{1}{2} \int \vec{r}' \times \vec{J}(\vec{r}')\, dv' \qquad (19a)$$

and

$$(\vec{\vec{p}}_2)_{i,j} = \vec{1}_i \vec{1}_j \int x_i' x_j' \rho(\vec{r}')\, dv' \qquad (19b)$$

where equation (19a) defines the magnetic dipole moment and equation (19b) defines the components of electric quadrupole moments in a dyadic form. Further expansion of $\vec{A}_2$ involving the magnetic quadrupole moments (in dyadic form) can be found in Appendix A.

Also formulated there are the electric and magnetic fields contributed by all the dipole and quadrupole moments. A more general solution of fields in terms of multipoles is treated next.

4. MULTIPOLE EXPANSIONS OF FIELDS

Electromagnetic fields can be expanded (ref. 8) in terms of multipole coefficients. The derivations are somewhat lengthy and are treated in Appendixes B to D. In summary, the electric and magnetic fields due to a given source distribution $\vec{J}(\vec{r}')$ and $\rho(\vec{r}')$ have been obtained as

$$\vec{E} = \sum_{\ell=1}^{\infty} \frac{jk^{\ell+2}\sqrt{\mu/\varepsilon}}{(2\ell+1)!!}\left(\frac{\ell+1}{\ell}\right)^{\frac{1}{2}} \sum_{m=-\ell}^{\ell} (m_{\ell,m} - \frac{1}{\omega\mu\varepsilon} q_{\ell,m} \nabla\times) h_\ell^{(2)}(kr)\, \vec{X}_{\ell,m} \tag{20}$$

$$\vec{H} = \sum_{\ell=1}^{\infty} \frac{jk^{\ell+2}/\sqrt{\mu\varepsilon}}{(2\ell+1)!!}\left(\frac{\ell+1}{\ell}\right)^{\frac{1}{2}} \sum_{m=-\ell}^{\ell} (q_{\ell,m} + \frac{1}{\omega} m_{\ell,m} \nabla\times) h_\ell^{(2)}(kr)\, \vec{X}_{\ell,m} \tag{21}$$

where $\vec{X}_{\ell,m}$ and $\nabla\times(h_\ell^{(2)}\vec{X}_{\ell,m})$ are expanded in spherical coordinates in Appendix C. The electric multipole coefficients $p_{\ell,m}$ and the magnetic multipole coefficients $m_{\ell,m}$ are derived in Appendix B as

$$p_{\ell,m} = \frac{(2\ell+1)!!}{k^\ell(\ell+1)} \int Y^*_{\ell,m}(\theta',\phi')\left\{\rho(\vec{r}')\frac{d}{dr'}[r'j_\ell(kr')] + j\omega[\vec{r}\cdot\vec{J}(\vec{r}')]j_\ell(kr')\right\} dv' \tag{22}$$

and

$$m_{\ell,m} = -\frac{(2\ell+1)!!}{k^{\ell}(\ell+1)} \int \nabla'[Y^{*}_{\ell,m}(\theta',\phi')\, j_{\ell}(kr')] \cdot [\vec{r}' \times \vec{J}(\vec{r}')]dv' \tag{23}$$

where

$$(2\ell+1)!! = (2\ell+1)\cdot(2\ell-1)\cdots(5)\cdot(3)\cdot(1) \tag{24}$$

and

$$Y_{\ell,m}(\theta',\phi') = \sqrt{\frac{(2\ell+1)(\ell-m)!}{4\pi(\ell+m)!}}\, P^{m}_{\ell}(\cos\theta')\exp(jm\phi') \tag{25}$$

The electric dipole coefficients $p_{1,m}$ (with m = -1,0,+1), the electric quadrupole coefficients $p_{2,m}$ (with m = -2, =1, 0, +1, +2), the magnetic dipole coefficients $m_{1,m}$, and the magnetic quadrupole coefficients $m_{2,m}$ have all been expanded in Appendix D as integrals over the source region in spherical coordinates. Also in Appendix D, the coefficients are related to their corresponding moments when the source region kr' << 1.

5. ASYMPTOTIC MULTIPOLE COEFFICIENTS AND MULTIPOLE MOMENTS OF QUASI-STATIC SOURCES

Most radiators of given sizes can be electrically small for low frequencies but electrically large for high frequencies. The simulators under study may be operated from low frequencies up to their structural resonance frequencies. To assure that their characteristics can be developed in exact forms, it is appropriate to emphasize that the multipole coefficients in equations (22) to (25) are valid for arbitrarily large sources. These coefficients are exact and somewhat more complicated than their asymptotic approximations. When a source region is known to be small (i.e., kr' << 1) the coefficients can be asymptotically approximated as

$$p_{\ell,m} \approx \int (r')^{\ell}\, Y^{*}_{\ell,m}\, \rho(\vec{r}')\, dv' \tag{26}$$

$$m_{\ell,m} \approx \frac{1}{\ell+1} \int \nabla'((r')^{\ell}\, Y^{*}_{\ell,m}) \cdot [\vec{r}' \times \vec{J}(r')]\, dv' \tag{27}$$

The asymptotic electric-dipole coefficients are related (in Appendix D) to their corresponding moments in rectangular coordinates as

$$p_{1,0} \approx \sqrt{\frac{3}{4\pi}} \int r'(\cos\theta')\, \rho(r',\theta',\phi')\, dv'$$

$$= \sqrt{\frac{3}{4\pi}} \int z'\, \rho(x',y',z')\, dv' = \sqrt{\frac{3}{4\pi}}\; p_z \tag{28}$$

$$p_{1,\pm1} \approx \sqrt{\frac{3}{8\pi}} \int \mp r'(\sin\theta')\, \rho(r',\theta',\phi')\, \exp(\mp j\phi')\, dv'$$

$$= \sqrt{\frac{3}{8\pi}} \int \mp(x' \mp jy')\, \rho(x',y',z')\, dv' = \mp\sqrt{\frac{3}{8\pi}}\, (p_x \mp jp_y) \tag{29}$$

Similarly,

$$m_{1,0} \approx \frac{1}{2}\sqrt{\frac{3}{4\pi}} \int \vec{I}_{z'} \cdot [\vec{r}' \times \vec{J}(\vec{r}')]\, dv' = \sqrt{\frac{3}{4\pi}}\, m_z \tag{30}$$

$$m_{1,\pm1} \approx \frac{1}{2}\sqrt{\frac{3}{8\pi}} \int (\vec{I}_{x'} \mp j\vec{I}_{y'}) \cdot (\vec{r}' \times \vec{J})\, dv' = \mp\sqrt{\frac{3}{8\pi}}\, (m_x \mp jm_y) \tag{31}$$

The asymptotic electric-quadrupole coefficients are related (also in Appendix D) to their corresponding moments in rectangular coordinates as

$$p_{2,0} \approx \frac{1}{2}\sqrt{\frac{5}{4\pi}}\, (2p_{zz} - p_{xx} - p_{yy}) \tag{32}$$

$$p_{2,\pm1} \simeq \mp\sqrt{\frac{15}{8\pi}}\,(p_{xz} \mp jp_{yz}) \tag{33}$$

$$p_{2,\pm2} \simeq \frac{1}{2}\sqrt{\frac{15}{8\pi}}\,(p_{xx} - p_{yy} \mp j2p_{xy}) \tag{34}$$

where

$$p_{x_i x_j} = \int x_i x_j\, \rho(x',y',z')\, dv' \tag{35}$$

Finally, the asymptotic magnetic-quadrupole coefficients are:

$$m_{2,0} \simeq \frac{1}{3}\sqrt{\frac{5}{4\pi}}\,(2m_{zz} - m_{xx} - m_{yy}) \tag{36}$$

$$m_{2,\pm1} \simeq \mp\frac{2}{3}\sqrt{\frac{15}{8\pi}}\,(m_{xz} \mp jm_{yz}) \tag{37}$$

$$m_{2,\pm2} \simeq \frac{1}{3}\sqrt{\frac{15}{8\pi}}\,(m_{xx} - m_{yy} \mp j2m_{xy}) \tag{38}$$

where

$$m_{x_i x_j} = \frac{1}{2}\int \left[x_i(\vec{r}' \times \vec{J}) \cdot \vec{I}_j + x_j(\vec{r}' \times \vec{J}) \cdot \vec{I}_i\right] dv \tag{39}$$

This section has formulated the potentials and fields in terms of multipoles of a given source region. The general solutions have also been asymptotically formulated for quasi-static sources whose kr' is vanishingly small. These solutions are to be applied to two specific simulators in the following two sections.

SECTION III

TRANSMISSION-LINE MEDIUS PERFORMANCE

The simulator source coordinates of the transmission-line MEDIUS is shown in figure 1. To maintain a good transmission line mode, the height to length ratio h/L is restricted to be no larger than 0.2, and the height h is intended to be a small fraction of the operating wavelength. The flat portion of the transmission is designated as region II, while the slant portions at the source and load ends are respectively designated as regions I and III. Presently the entire line is assumed to have been perfectly impedance-matched. That is, the driving source, the terminating load and the bends are assumed to have no impedance discontinuity. Under this assumption, the current and charge distributions are first to be formulated. The multipole strengths will then be formulated and evaluated before the simulator field characteristics are discussed.

1. CURRENT AND CHARGE DISTRIBUTIONS

The driving source in figure 1 is assumed to send a traveling-wave current propagating along the entire line and terminating at the load end without any reflection. Let the amplitude of the current be I_o, and let the upper- and lower-half currents of the structure be $I_{\pm}$. The current distributions can be written by assuming a lossless transmission line as

$$I_{\pm}(z') = \begin{cases} I_o[\sin(\alpha_1)\hat{I}_{x'} \pm \cos(\alpha_1)\hat{I}_{z'}]\exp[-jk(z'+L)\sec(\alpha_1) + jkL] & \text{in I} \\ \pm I_o \hat{I}_{z'} \exp(-jkz') & \text{in II} \\ I_o[-\sin(\alpha_2)\hat{I}_{x'} \pm \cos(\alpha_2)\hat{I}_{z'}]\exp[-jk(z'-L)\sec(\alpha_2) - jkL] & \text{in III} \end{cases} \quad (40)$$

Use of the continuity equation on these currents will result in linear charge densities $q_{\pm}$ on the upper and lower parts:

$$q_{\pm}(z') = \begin{cases} \pm(I_o/c)\exp[-jk(z'+L)\sec(\alpha_1) + jkL] & \text{in I} \\ \pm(I_o/c)\exp(-jkz') & \text{in II} \\ \pm(I_o/c)\exp[-jk(z'-L)\sec(\alpha_2) - jkL] & \text{in III} \end{cases} \quad (41)$$

Equations (40) and (41) complete the current and charge descriptions for $x' > 0$ and $x' < 0$ in figure 1. They are the sources for the multipoles of interest.

2. THE MULTIPOLE COEFFICIENTS

The generalized multipole coefficients, defined in equations (22) through (25), are valid for an arbitrarily large source region. If the basic property of the associated Legendre polynomials is applied to equation (25), it can be shown that $Y_{\ell,-m} = (-1)^m Y^*_{\ell,m}$. This identity can in turn be applied to equations (22) and (23) to show that

$$p_{\ell,-m} = (-1)^m p^*_{\ell,m}, \quad \text{and} \quad m_{\ell,-m} = (-1)^m m^*_{\ell,m} \quad (42)$$

Thus only $p_{\ell,m}$ and $m_{\ell,m}$ need be explicitly formulated for the evaluations of multipole coefficients.

The line sources in equations (40) and (41) can now be used in equations (22) and (23) to give the multipole coefficients of the transmission line in figure 1. They are:

$$p_{\ell,m} = \frac{(2\ell + 1)!!}{k^{\ell}(\ell + 1)} \int Y^{*}_{\ell,m}(\theta',\phi') \left\{ q_{\pm}(z') \left[kr' j_{\ell-1}(kr') - \ell j_{\ell}(kr') \right] \right.$$

$$\left. + j\omega [\vec{r}' \cdot \vec{I}_{\pm}(z')] \, j_{\ell}(kr') \right\} dz' \qquad (43)$$

and

$$m_{\ell,m} = \frac{(2\ell + 1)!!}{k^{\ell}(\ell + 1)} \int \nabla' [Y^{*}_{\ell,m}(\theta',\phi') \, j_{\ell}(kr')] \cdot [\vec{r}' \times \vec{I}_{\pm}(z')] \, dz'$$

$$= \frac{(2\ell + 1)!!}{k^{\ell}(\ell + 1)} (-jm) \int \frac{j_{\ell}(kr')}{r' \sin\theta'} Y^{*}_{\ell,m}(\theta',\phi') \left\{ \vec{I}_{\phi'} \cdot [\vec{r}' \times \vec{I}_{\pm}(z')] \right\} dz' \qquad (44)$$

where the second identity for $m_{\ell,m}$ is the result of recognizing that $\vec{r}' \times \vec{I}_{\pm}$ of the transmission line have only ϕ' components. The line integrals in equations (43) and (44) are along the upper half of the transmission line when the sources are subscripted by (+) as defined in equations (40) and (41). Naturally, the integrals have to include also the path along the lower half of the transmission line with the sources subscripted by (-).

Referring to equations (40) and (41) in conjunction with figure 1, the source terms in equation (43) have the following properties:

$$q_{+}(z') = -q_{-}(z'), \quad \text{and} \quad \vec{r}' \cdot \vec{I}_{+}(z') = -[\vec{r}' \cdot \vec{I}_{-}(z')] \qquad (45)$$

Also, equation (25) can be applied to figure 1 to show that

$$Y^*_{\ell,m}(\theta',\phi'=0) = Y^*_{\ell,m}(\theta',\phi'=\pi) \quad \text{for } m = 0,2,4,... \tag{46}$$

Therefore, for m even, the $q_{\ell,m}$ in equation (43) become identically zero for the transmission line. On the other hand,

$$Y^*_{\ell,m}(\theta',\phi'=0) = -Y^*_{\ell,m}(\theta',\phi'=\pi), \quad \text{for } m = 1,3,5,... \tag{47}$$

Thus, for m odd, the upper- and lower-half contributions for $q_{\ell,m}$ in equation (43) are equal, and the line integration can be carried out only along the upper-half of the transmission line. The magnetic multipole coefficients $m_{\ell,m}$ in equation (44) can be demonstrated to be similar to $p_{\ell,m}$ by recognizing that

$$\vec{r}' \times \vec{I}_+(z') = -\vec{r}' \times \vec{I}_-(z') \tag{48}$$

In summary, the transmission line MEDIUS (in fig. 1) has only odd multipole coefficients with m = 1,3,5,... in equations (43) and (44). Moreover, their total contributions from the complete line integrations are simply twice the integrations along the upper half of the transmission line using only the sources $q_+(z')$ and $\vec{I}_+(z')$.

3. THE ELECTRIC AND MAGNETIC DIPOLES

The electric dipole coefficient $p_{1,1}$ by equation (43) is

$$\begin{aligned} p_{1,1} &= \frac{3}{k} \int Y^*_{1,1}(\theta',\phi'=0) \left\{ q_+(z')\left[kr'j_o(kr') - j_1(kr')\right] \right. \\ &\qquad \left. + j\omega\left[\vec{r}' \cdot \vec{I}_+(z')\right] j_1(kr') \right\} dz' \\ &= (p_{1,1})_I + (p_{1,1})_{II} + (p_{1,1})_{III} \end{aligned} \tag{49}$$

where the integration is decomposed into three regions according to the sources defined in equations (40) and (41). Substitutions of these sources into equation (49) give rise to

$$(p_{1,1})_I = \frac{3}{k}\int_{-L-h\cot(\alpha_1)}^{-L} Y^*_{1,1}(\theta_1',0)\left\{f[q_+(z',\alpha_1)],\vec{I}(z',\alpha_1),r_1'\right\} \cdot \sec(\alpha_1)\,dz' \tag{50a}$$

$$(p_{1,1})_{III} = \frac{3}{k}\int_{L}^{L+h\cot(\alpha_2)} Y^*_{1,1}(\theta_3',0)\left\{f[q_+(z',\alpha_2)],\vec{I}(z',\alpha_2),r_3'\right\} \cdot \sec(\alpha_2)\,dz' \tag{50b}$$

$$(p_{1,1})_{II} = \frac{3}{k}\int_{-L}^{L} Y^*_{1,1}(\theta_2',0)\left\{f[q_+(z')],\vec{I}(z'),r_2'\right\} dz' \tag{50c}$$

The above integrations are considerably simplified if a special case is made for $\alpha_1 = \alpha_2 = \alpha$. The results are:

$$(p_{1,1})_{II} = -\sqrt{\frac{3}{8\pi}}\frac{3}{k}\int_{-L}^{L}(I_o/c)\sin(\theta_2')\exp(-jkz')[kr_2'j_o(kr_2') - j_1(kr_2') + jkz'\,j_1(kr_2')]\,dz' \tag{51}$$

$$(p_{1,1})_{I+III} = (p_{1,1})_I + (p_{1,1})_{III}$$

$$= -\sqrt{\frac{3}{8\pi}}\frac{6}{k}\int_{-L-h\cot(\alpha)}^{-L}(I_o/c)\sin(\theta_1')\left\{\cos(\Omega)[kr_1'j_o(kr_1') - j_1(kr_1')] - \sin(\Omega)[kz'\sec(\alpha) + k(L\tan(\alpha) + h)\sin(\alpha)]j_1(kr_1')\sec(\alpha)\right\}dz' \tag{52}$$

where the variables in terms of z' are:

$$\Omega = kL - k(z'+L)\sec(\alpha) \quad , \tag{53}$$

$$r_1' = \left\{ z'^2 + \left[(L+z')\tan(\alpha) + h \right]^2 \right\}^{\frac{1}{2}} \quad , \tag{54}$$

and

$$\sin(\theta_1') = \left[(L+z')\tan(\alpha) + h \right] / r_1' \tag{55}$$

Numerical integrations of equations (51) and (52) have been performed and their normalized results are plotted as the primed quantities in the bottom set of figure 4 for $\alpha = 45^{\circ}$ and $h/L = 0.1$. The normalization factor for these curves is $(-\sqrt{3/8\pi}\ A\ I_o/c)$ with A as the area of the transmission line in the x'z' plane, i.e.,

$$A = 4Lh + 2h^2 \cot\alpha \tag{56}$$

The factor $(-\sqrt{3/8\pi})$ was used in equation (29) to relate the spherical dipole coefficient $p_{1,1}$ and the Cartesian dipole moments. The dipole moments for the transmission line are derived in detail in Appendix F. Equations (20) and (21) of Appendix F indicate that the dipole moment has only the x-component p_x:

$$p_x = (p_x)_I + (p_x)_{II} + (p_x)_{III} \tag{57a}$$

with

$$(p_x)_{I+III} = (p_x)_I + (p_x)_{III}$$

$$= (I_o/c)\left\{ \frac{8}{k^2} \sin(\alpha) \sin\left[\frac{kh\ \csc(\alpha)}{2} \right] \sin\left[kL + \frac{kh\ \csc(\alpha)}{2} \right], \right.$$

$$\left. -(4h/k)\sin(kL) \right\} \tag{57b}$$

and

$$(p_x)_{II} = (I_o/c)\frac{4h}{k}\sin(kL) \tag{57c}$$

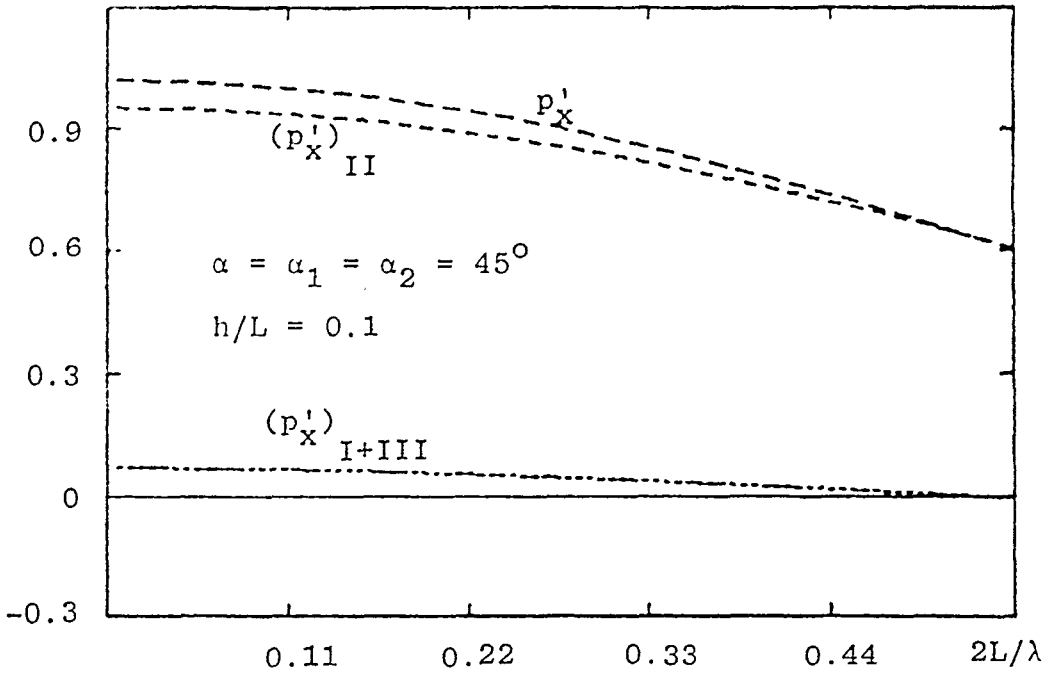

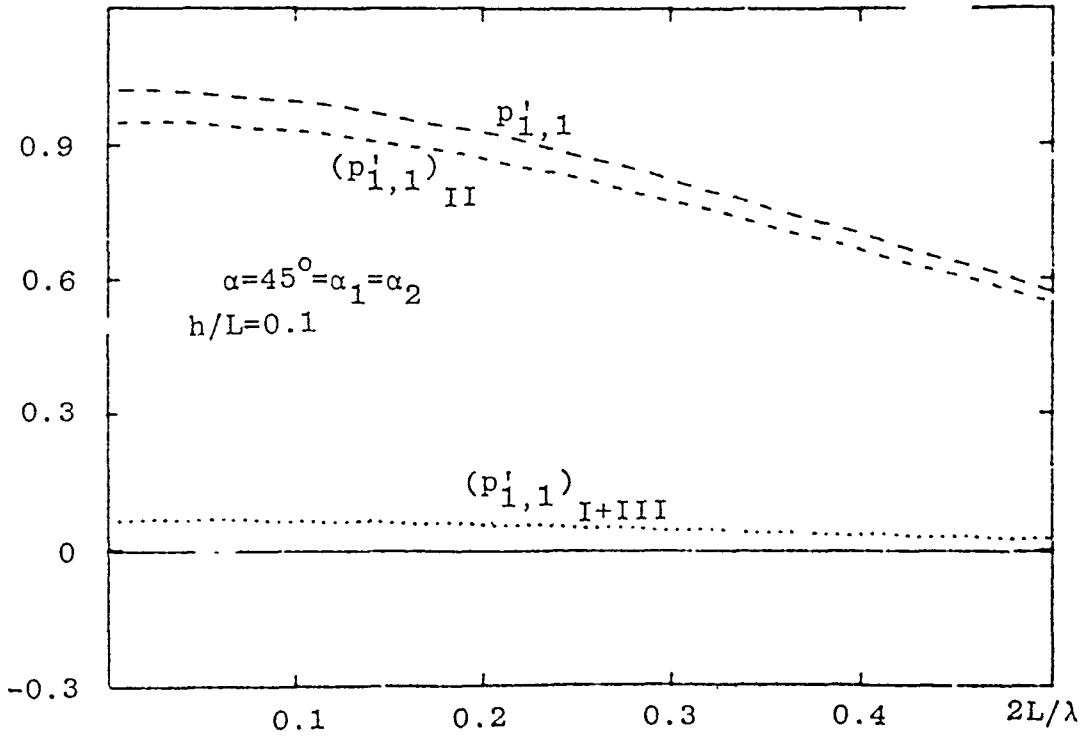

Figure 4. Normalized Electric-Dipole Moments (Top Curves) and Electric-Dipole Coefficients (Bottom Curves) of the Transmission-Line MEDIUS (in fig. 1) with $2L/\lambda < 0.5$

Using a normalization factor ($A\ I_o/c$) for the above equations, their normalized curves are plotted as the primed quantities shown in the top set of figure 4.

A comparison between the two sets of curves in figure 4 indicates clearly that the dipole moments for the transmission line approximate very closely the generalized dipole coefficients if $2L/\lambda$ with λ as the wavelength is restricted to less than 0.5. However, this conclusion is not true for larger values of $2L/\lambda$. Figure 5 shows that the generalized dipole coefficients are monotonically decreasing with the length $2L/\lambda$. On the other hand, the moments under quasi-static approximations are seen to deviate from the exact solutions significantly for $2L/\lambda > 0.5$ and become oscillatory. Therefore, the dipole moments as obtained in equation (57) can not be accurately used to represent the dipole fields of the MEDIUS if $2L/\lambda$ becomes larger than 0.5.

Formulation and evaluation of the magnetic dipole for MEDIUS are considered next. Use of equation (44) will follow closely the procedures performed in using equation (43). The magnetic dipole coefficients can be obtained similar to equations (51) and (52) as

$$m_{1,1} = (m_{1,1})_I + (m_{1,1})_{II} + (m_{1,1})_{III} \tag{58a}$$

with

$$(m_{1,1})_{II} = -j\sqrt{\frac{3}{8\pi}}\,\frac{3}{k}\int_{-L}^{L} I_o[j_1(kr_2')/r_2'] \exp(-jkz')\, dz' \tag{58b}$$

and

$$(m_{1,1})_{I+III} = (m_{1,1})_I + (m_{1,1})_{III}$$

$$= -j\sqrt{\frac{3}{8\pi}}\,\frac{6}{k}\int_{-L-h\cot(\alpha)}^{-L} \cos(\Omega)[L\tan(\alpha) + h][j_1(kr_1')/r_1']dz' \tag{58c}$$

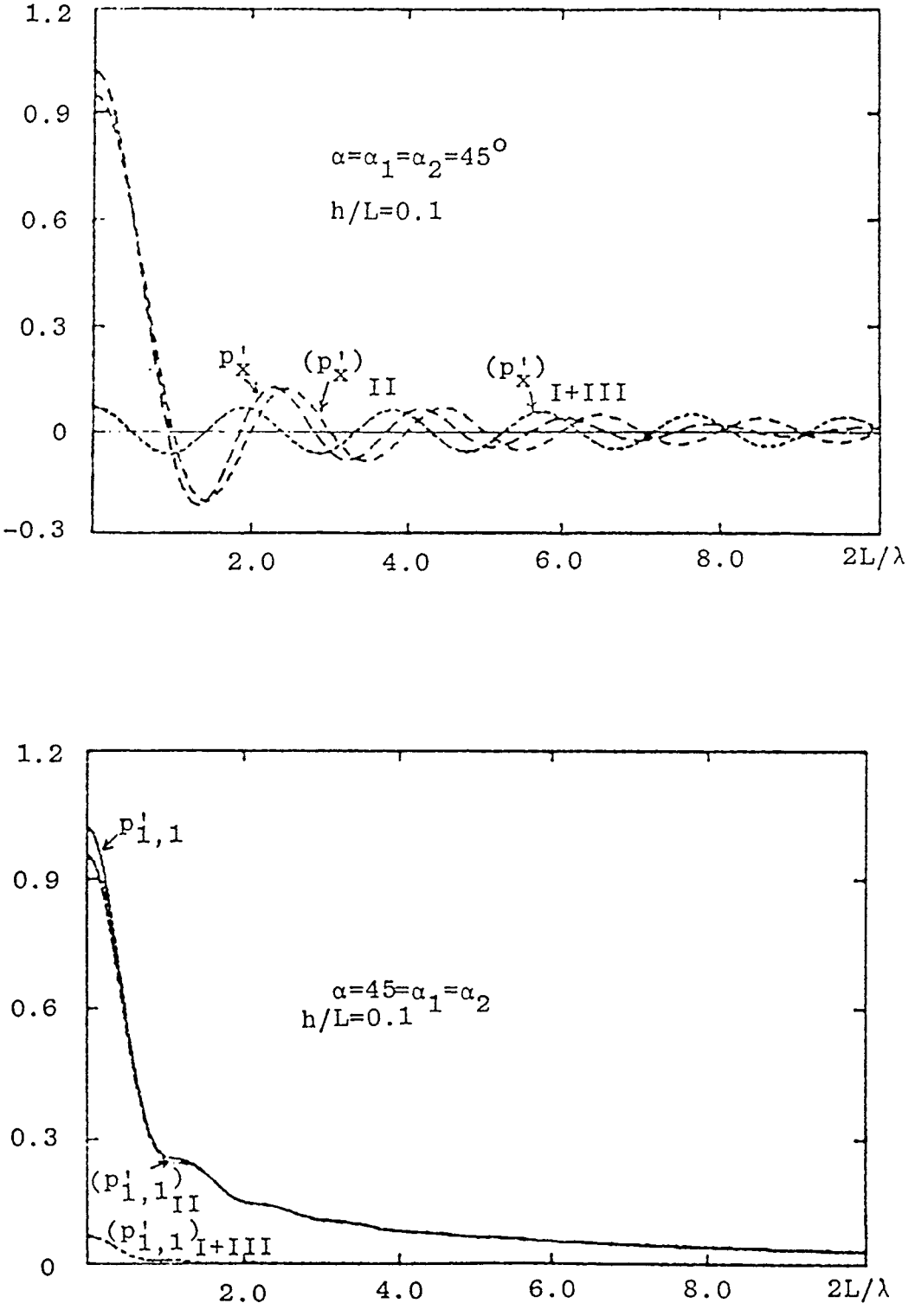

Figure 5. Normalized Electric-Dipole Moments (Top Curves) and Electric-Dipole Coefficients (Bottom Curves) of the Transmission Line with $2L/\lambda < 10$

Referring to equations (31) and (56), the normalization factor ($j\sqrt{3/8\pi}\ I_o A$) is applied to the above equations. Their normalized curves are plotted as the primed quantities in the bottom set of figure 6 for $\alpha = 45^\circ$ and $h/L = 0.1$.

Quasi-static approximation of the magnetic-dipole coefficients leads to the magnetic-dipole moments which are derived in detail in Appendix F. As can be seen in equations (31) and (33) of Appendix F, the transmission line has only the y-component moments as

$$m_y = (m_y)_I + (m_y)_{II} + (m_y)_{III} \tag{59a}$$

and

$$(m_y)_{II} = -I_o\left(\frac{2h}{k}\right) \sin(kL) \tag{59b}$$

and

$$(m_y)_{I+III} = (m_y)_I + (m_y)_{III}$$

$$= -I_o\ 4[L + h\ \cot(\alpha)]\ \frac{\sin(\alpha)}{k}\ \sin\left[\frac{kh\ \csc(\alpha)}{2}\right]$$

$$\cdot\ \cos\left[kL + \frac{kh\ \csc(\alpha)}{2}\right] \tag{59c}$$

Using a normalization factor ($I_o A$) with A defined in equation (56), the normalized moments are plotted in the top set of figure 6. Comparison between the moments and the coefficients indicates that an excellent agreement exists for $2L/\lambda > 0.5$, as was also observed in figure 4. However, significant error would occur if the coefficients for $2L/\lambda > 0.5$ were to be used for the fields of the transmission line. This observation is illustrated in figure 7 where the magnetic coefficients are plotted in absolute values. While

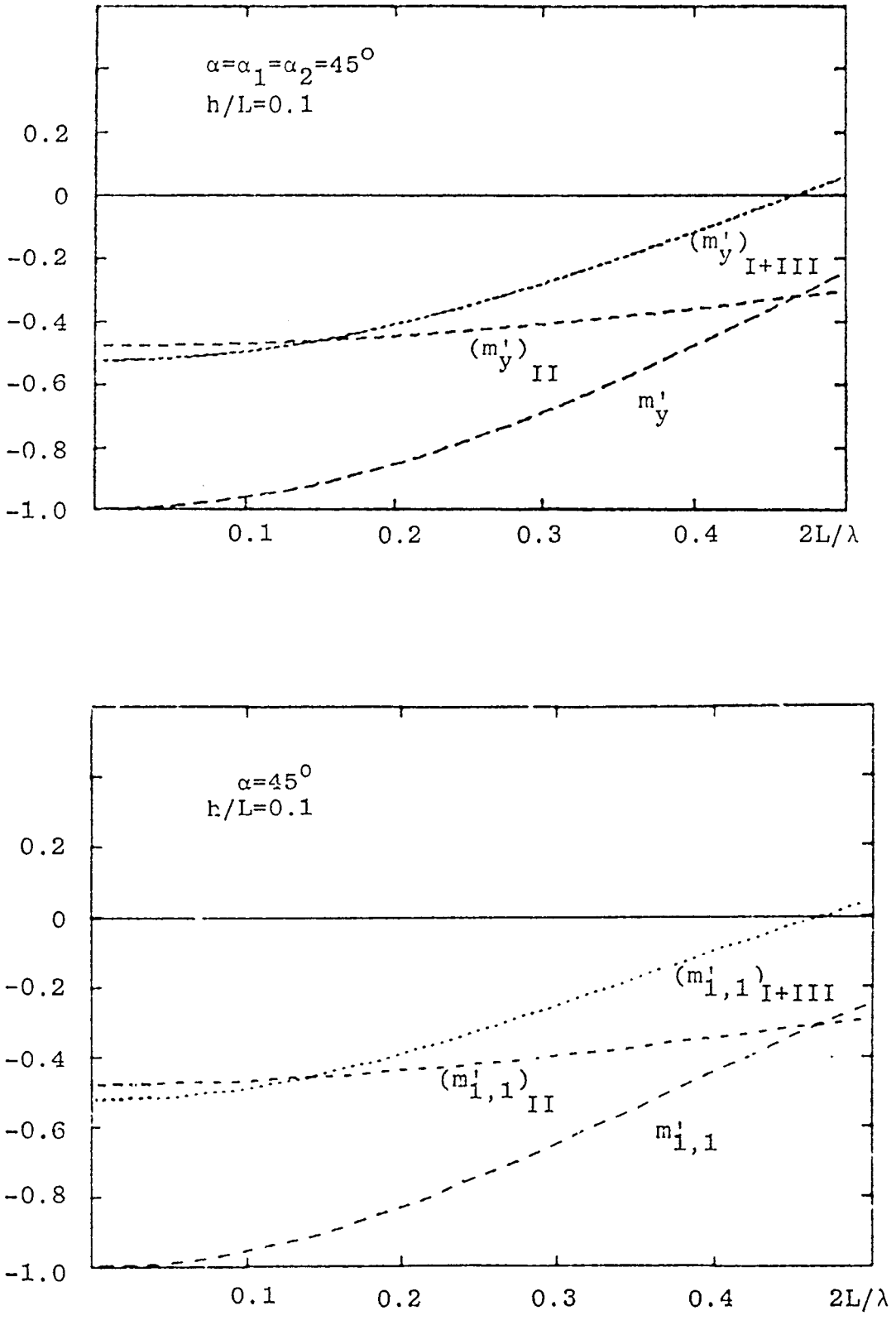

Figure 6. Normalized Magnetic-Dipole Moments (Top Curves) and Magnetic-Dipole Coefficients (Bottom Curves) of the Transmission-Line MEDIUS (in fig. 1) with $2L/\lambda < 0.5$

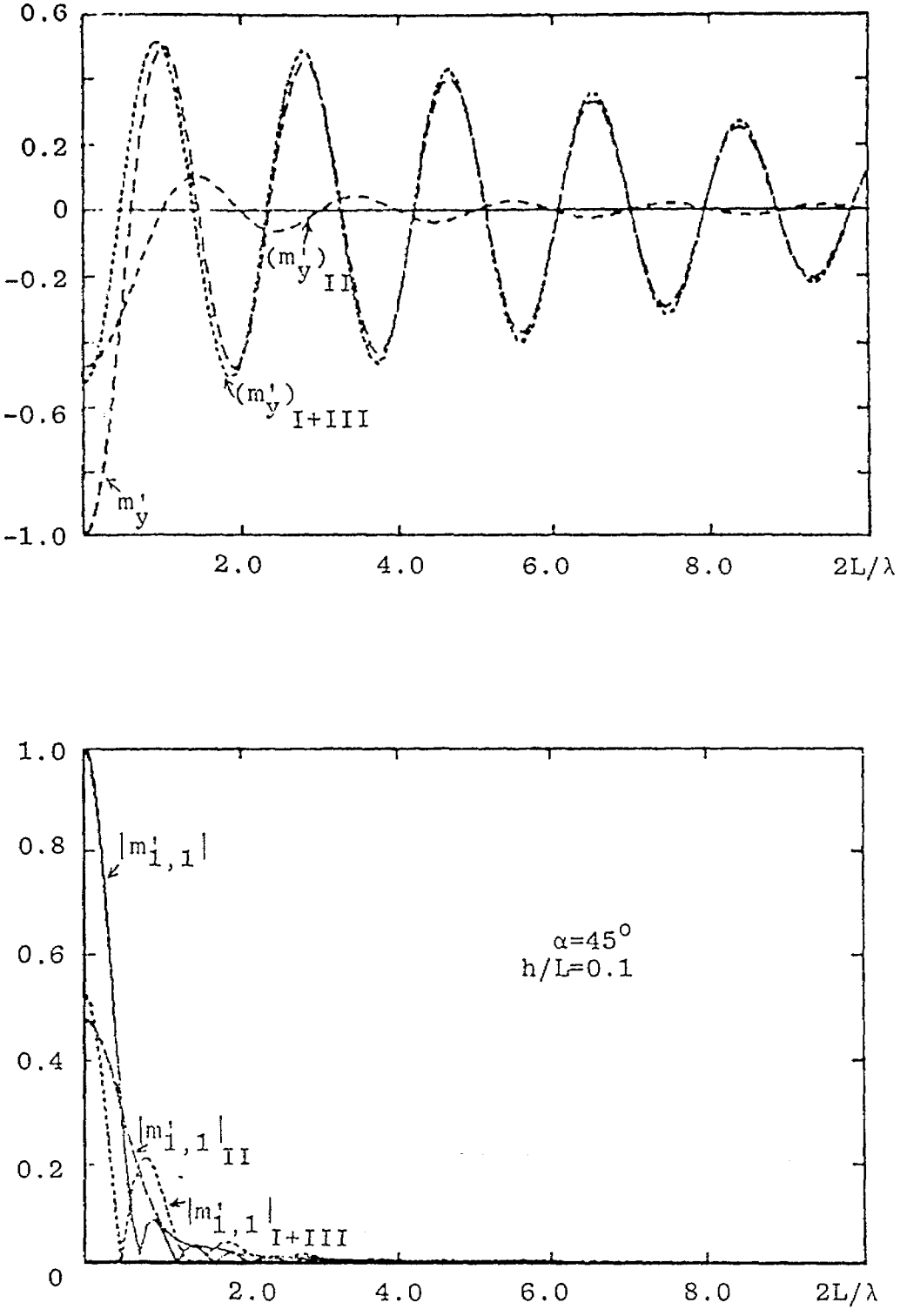

Figure 7. Normalized Magnetic-Dipole Moments (Top Curves) and Magnetic-Dipole Coefficients (Bottom Curves) of the Transmission Line with $2L/\lambda < 10$

the combined coefficient decreases rapidly for $2L/\lambda > 0.5$, the combined moment is seen to oscillate with a much slower rate of decrease. Therefore, if fields are to be described in terms of a magnetic dipole, the use of the magnetic-dipole coefficient in its exact form becomes necessary for $2L/\lambda > 0.5$.

4. THE ELECTRIC AND MAGNETIC QUADRUPOLES

Following the same procedures in obtaining the dipole coefficients, the electric-quadrupole coefficients for the transmission line can be obtained from equation (43) as

$$p_{2,1} = (p_{2,1})_I + (p_{2,1})_{II} + (p_{2,1})_{III} \tag{60a}$$

with

$$(p_{2,1})_{II} = -\frac{5}{k^2}\sqrt{\frac{15}{8\pi}} \int_{-L}^{L} (I_o/c) \sin(2\theta_2') \exp(-jkz') \left[kr_2' j_1(kr_2') - 2j_2(kr_2') + jkz' j_2(kr_2')\right] dz' \tag{60b}$$

and

$$(p_{2,1})_{I+III} = (p_{2,1})_I + (p_{2,1})_{III}$$

$$= -\frac{j10}{k^2}\sqrt{\frac{15}{8\pi}} \int_{-L-h\cot(\alpha)}^{-L} (I_o/c) \sin(2\theta_1') \Big\{\sin(\Omega)\left[kr_1' j_1(kr_1') - 2j_2(kr_1')\right] + \cos(\Omega)\left[kz' \sec(\alpha) + (kL\tan(\alpha) + kh)\sin(\alpha)\right] j_2(kr_1')\Big\} dz' \tag{60c}$$

An appropriate normalization factor for $p_{2,1}$ is $(-j\sqrt{15/8\pi}\, AI_o L_e/c)$ with L_e as the effective length defined as

$$L_e = A/2h = 2L = h\cot(\alpha) \tag{61}$$

Normalized curves for these coefficients are plotted in the bottom sets of figures 8 and 9 for $\alpha = 45^o$ and $h/L = 0.1$.

The corresponding moments under quasi-static approximation have been obtained in equation (44) of Appendix F as $(p_{xz})_{II}$, and in equation (46) of Appendix F as $(p_{xz})_{I+III}$. The normalization factor for these moments is $(jA\, I_o L_e/c)$. Normalized plots for these moments are shown in the top sets of figures 8 and 9.

Magnetic-quadrupole coefficients can be obtained from equation (44) as

$$m_{2,1} = (m_{2,1})_I + (m_{2,1})_{II} + (m_{2,1})_{III} \tag{62a}$$

with

$$(m_{2,1})_{II} = -j\,\frac{15}{k^2}\left(\frac{2}{3}\sqrt{\frac{15}{8\pi}}\right)\int_{-L}^{L} I_o h\cos(\theta_2')\,\frac{j_2(kr_2')}{r_2'}\,\exp(-jkz')\,dz' \tag{62b}$$

$$(m_{2,1})_{I+III} = (m_{2,1})_I + (m_{2,1})_{III}$$

$$= \frac{30}{k^2}\left(\frac{2}{3}\sqrt{\frac{15}{8\pi}}\right)\int_{-L-h\cot(\alpha)}^{-L} I_o(\cos\theta_1')\sin(\Omega)$$

$$[L\tan(\alpha) + h]\cdot\frac{j_2(kr_1')}{r_1'}\,dz' \tag{62c}$$

An appropriate normalization factor for the above quantities is $(-\frac{2}{3}\sqrt{15/8\pi}\, AI_o L_e)$ according to equation (37) with $m_{xz} = 0$. Their normalized curves are plotted in the bottom sets of figures 10 and 11. The top sets of figures 10 and 11 are plotted with a

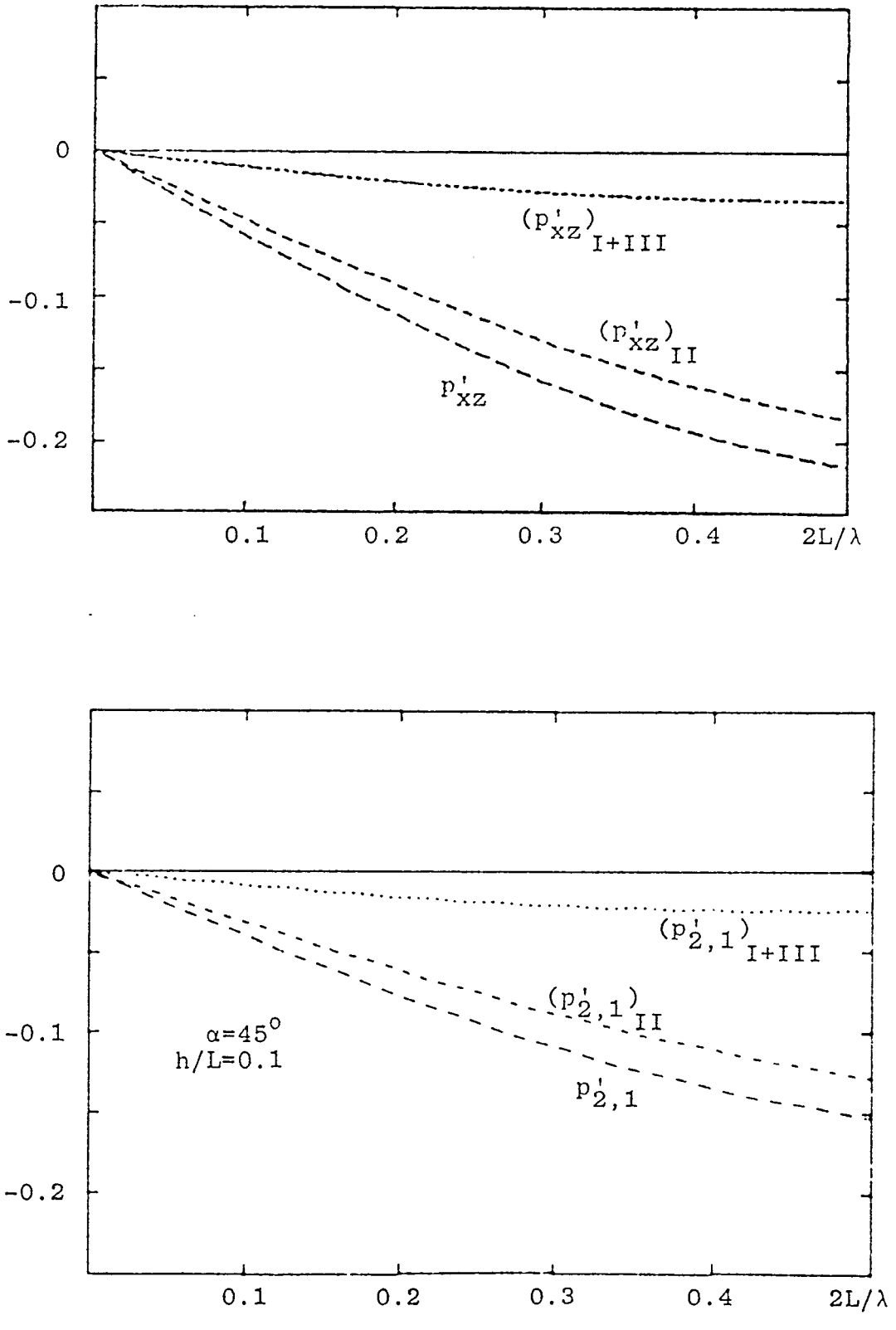

Figure 8. Normalized Electric-Quadrupole Moments (Top Curves) and Electric-Quadrupole Coefficients (Bottom Curves) of the Transmission-Line MEDIUS (in fig. 1) with $2L/\lambda < 0.5$

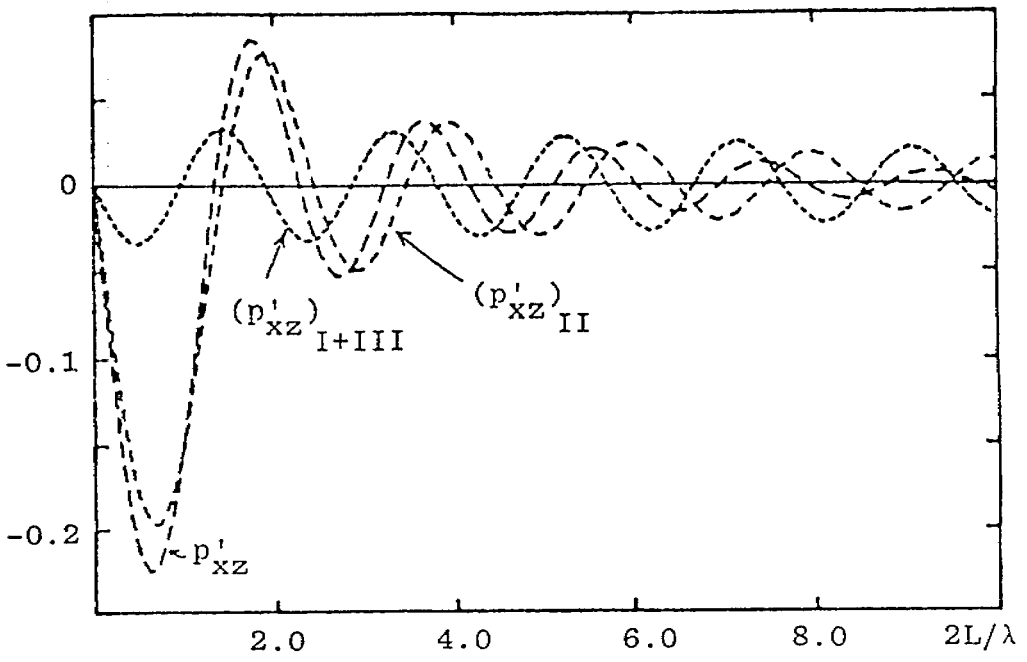

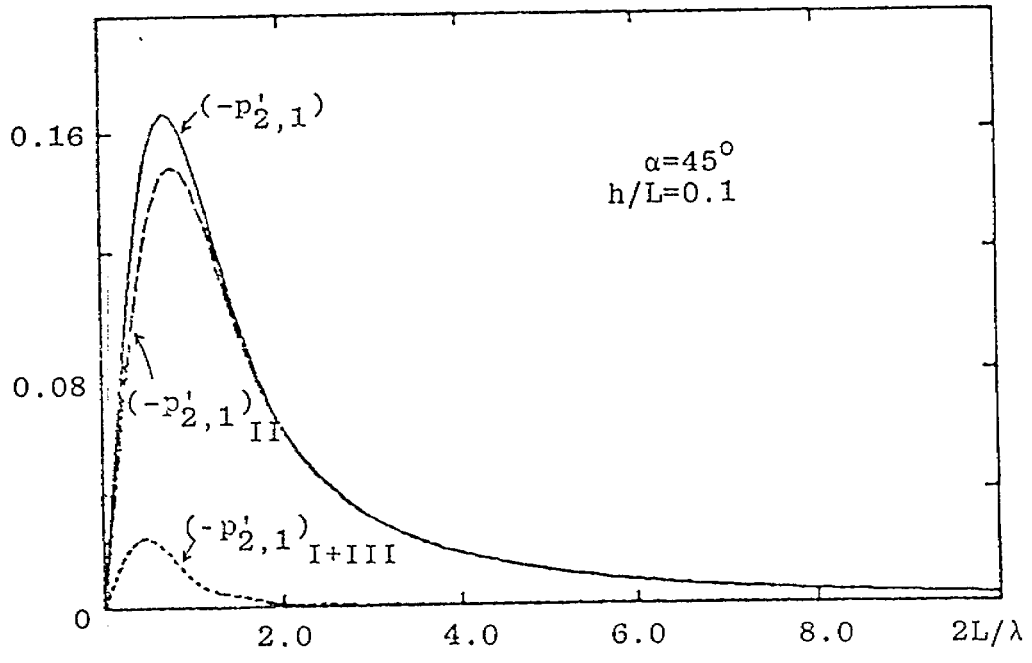

Figure 9. Normalized Electric-Quadrupole Moments (Top Curves) and Electric-Quadrupole Coefficients (Bottom Curves) of the Transmission Line with $2L/\lambda < 10$

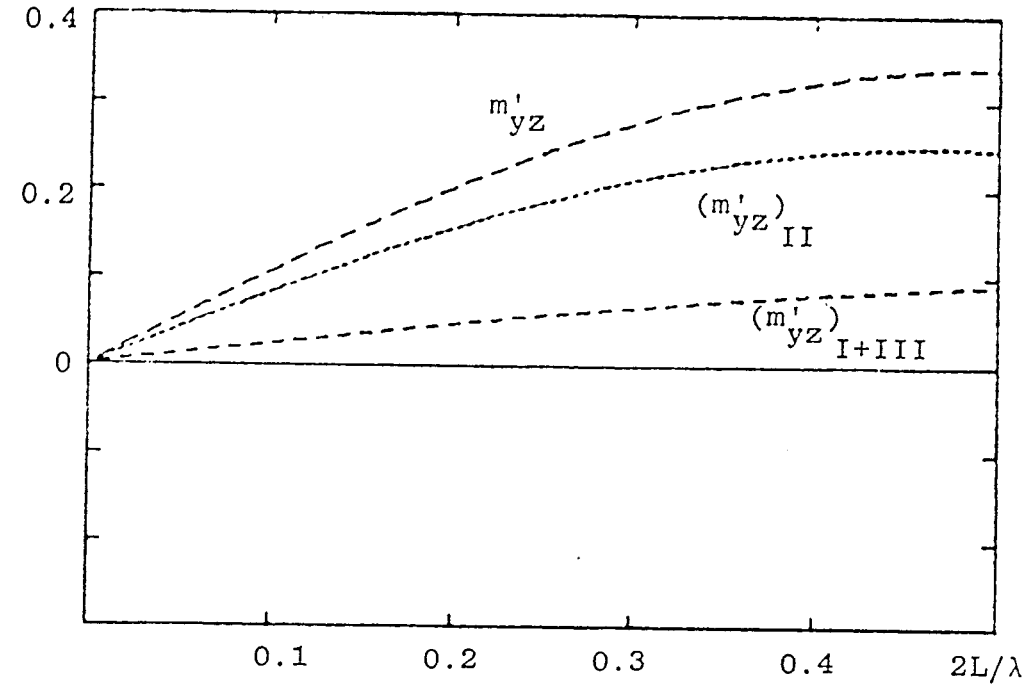

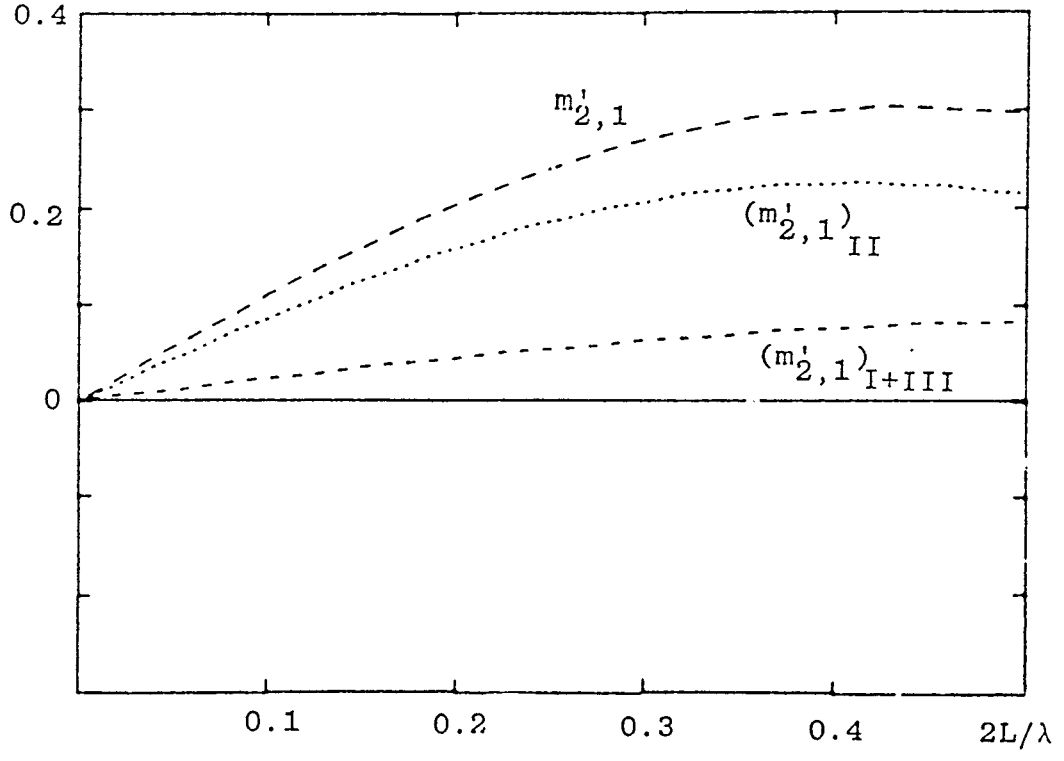

Figure 10. Normalized Magnetic-Quadrupole Moments (Top Curves) and Magnetic-Quadrupole Coefficients (Bottom Curves) of the Transmission-Line MEDIUS (in fig. 1) with $2L/\lambda < 0.5$

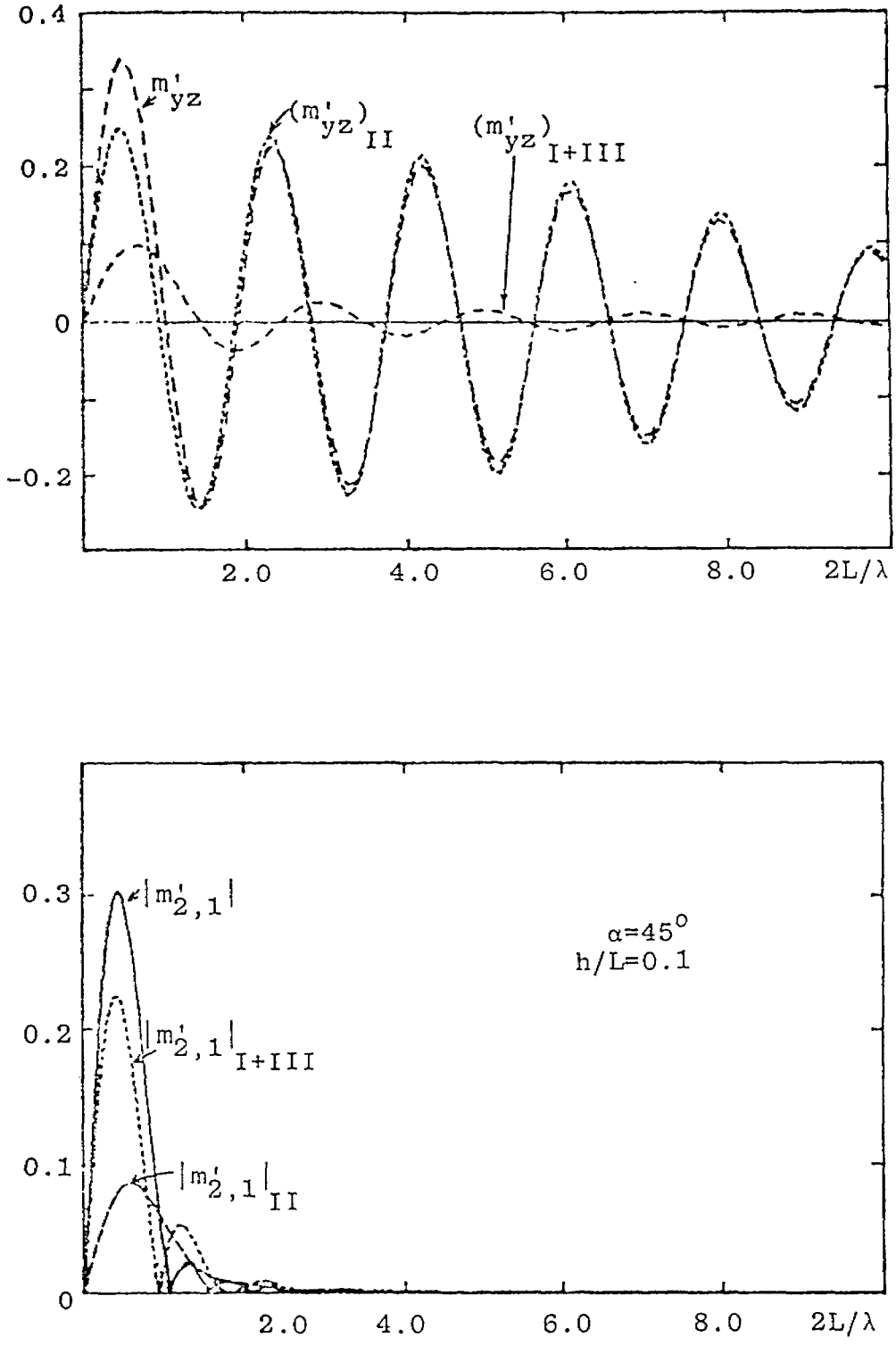

Figure 11. Normalized Magnetic-Quadrupole Moments (Top Curves) and Magnetic-Quadrupole Coefficients (Bottom Curves) of the Transmission Line with $2L/\lambda < 10$

normalization factor (jAI_oL_e) for the quasi-static quadrupole moments $(m_{yz})_{II}$ in equation (57) of Appendix F, and $(m_{yz})_{I+III}$ in equation (59) of Appendix F.

5. PARAMETRIC VARIATIONS OF MULTIPOLES

The dipole and quadrupole moments have been demonstrated as accurate approximations of the generalized coefficients, if $2L/\lambda$ is restricted to less than 0.5. One area of particular interest in studying the $\vec{p}$ cross $\vec{m}$ concept is the sensitivity of multipole moments with respect to the transmission-line parameters.

Figure 12 shows that the amplitudes and rates of variation of the normalized electri-dipole moments are varying with different combinations of the parameters. Should the maximum amplitude and the minimum rate of change with respect to $2L/\lambda$ be the most desirable features, the choice of $h/L = 0.1$ and $\alpha = 45^o$ would be a good one. The parametric curves can also be plotted using quation (61) and letting $L_e/\lambda = 2L/\lambda[1 + h/2L \tan(\alpha)]$ be the abscissa. This transformation of abscissa will indicate that all the parametric curves are essentially the same for $L_e/\lambda < 0.5$. Further detailed study may shed some more light on this optimization question.

The variations (fig. 13) of normalized magnetic-dipole coefficient also indicate the same conclusion. That is, the various combinations of h/L and α give rise to essentially the same normalized magnetic-dipole coefficients for $L_e/\lambda < 0.5$. A choice of small α will reduce the impedance mismatch of the transmission line.

Parametric variations of the normalized electri-quadrupole moment are also given in figure 14 with $2L/\lambda$ as the abscissa.

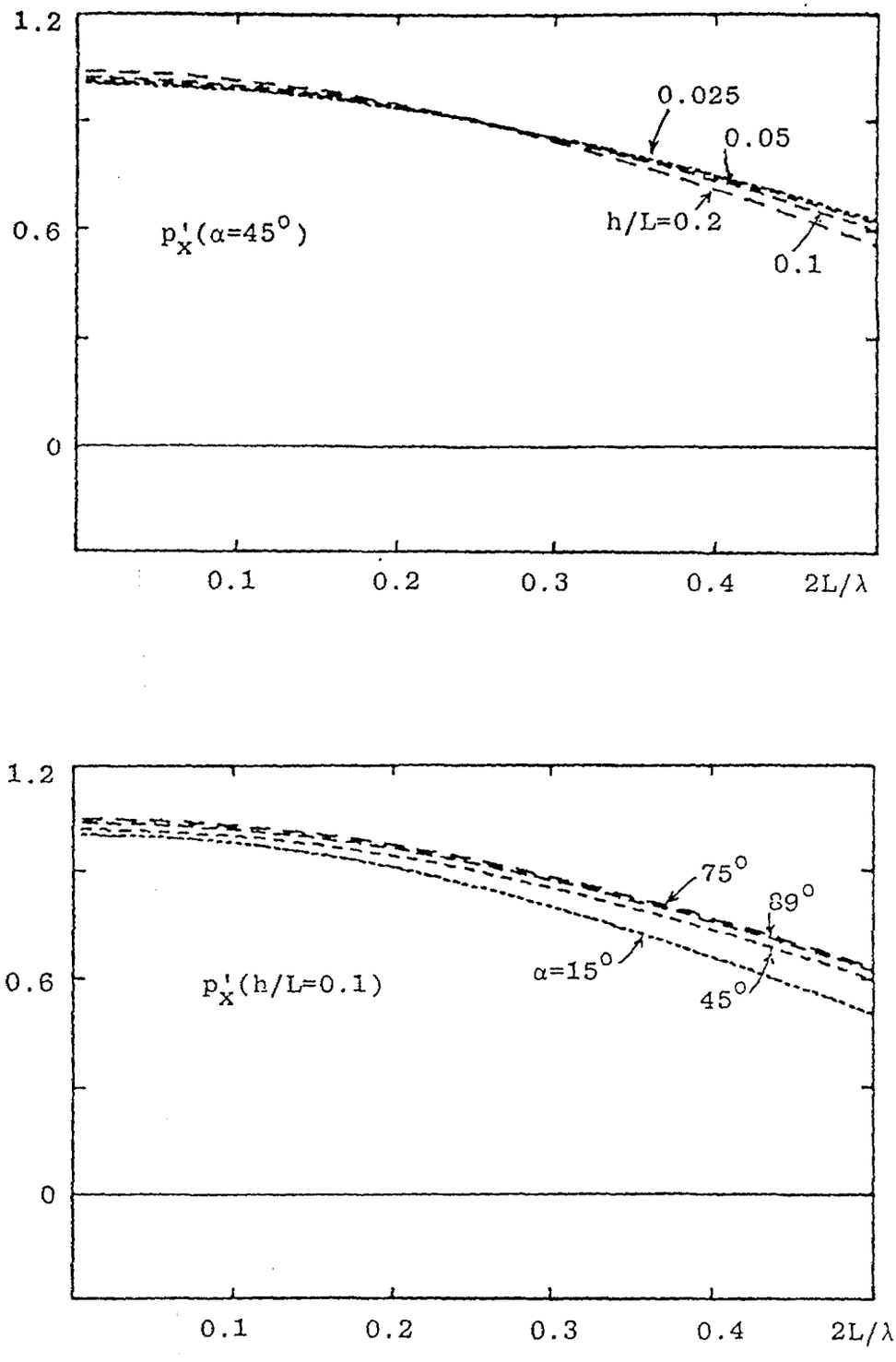

Figure 12. Variations of the Normalized Electric-Dipole Moments with h/L and α as Parameters

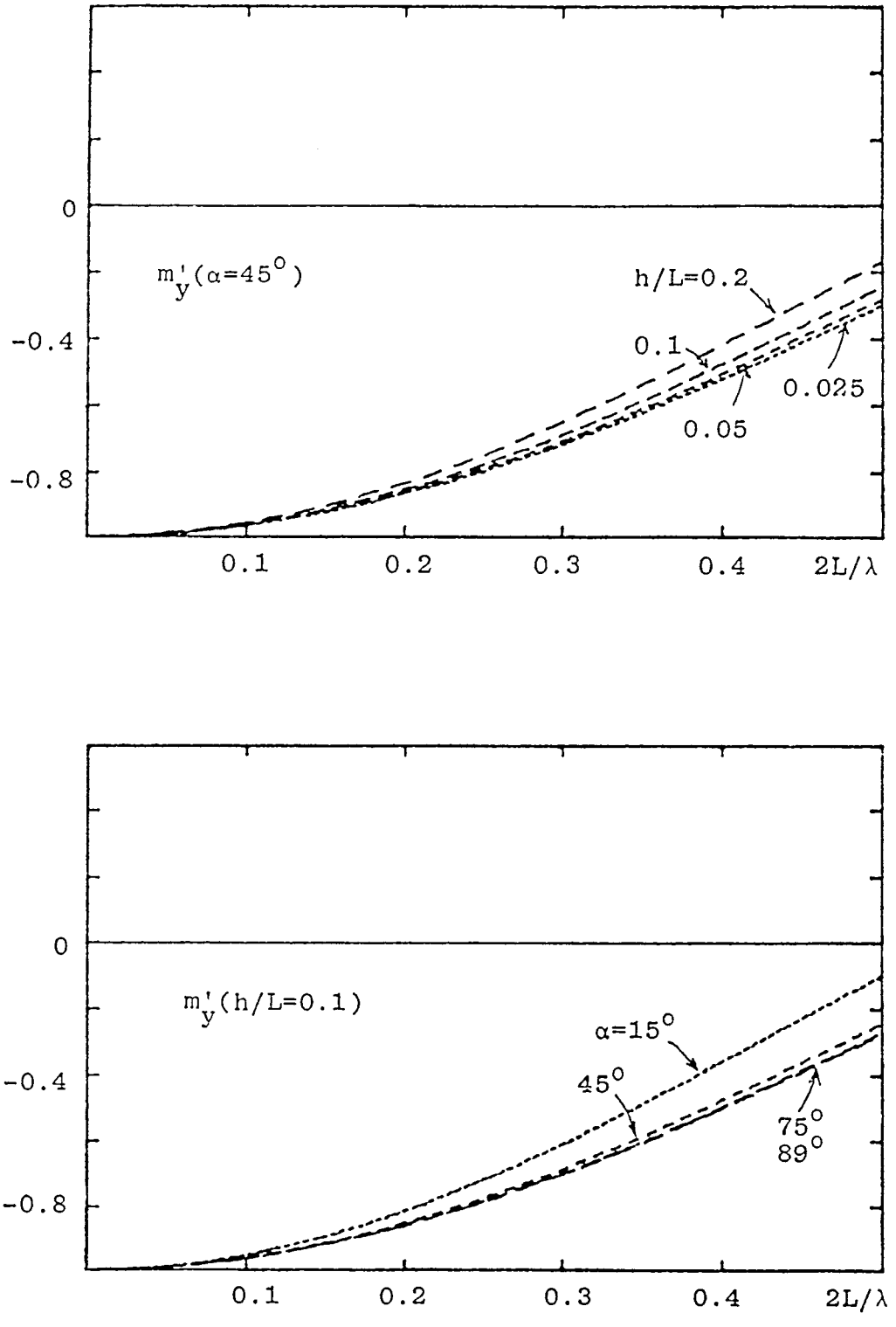

Figure 13. Variations of the Normalized Magnetic-Dipole Coefficients with h/L and α as Parameters

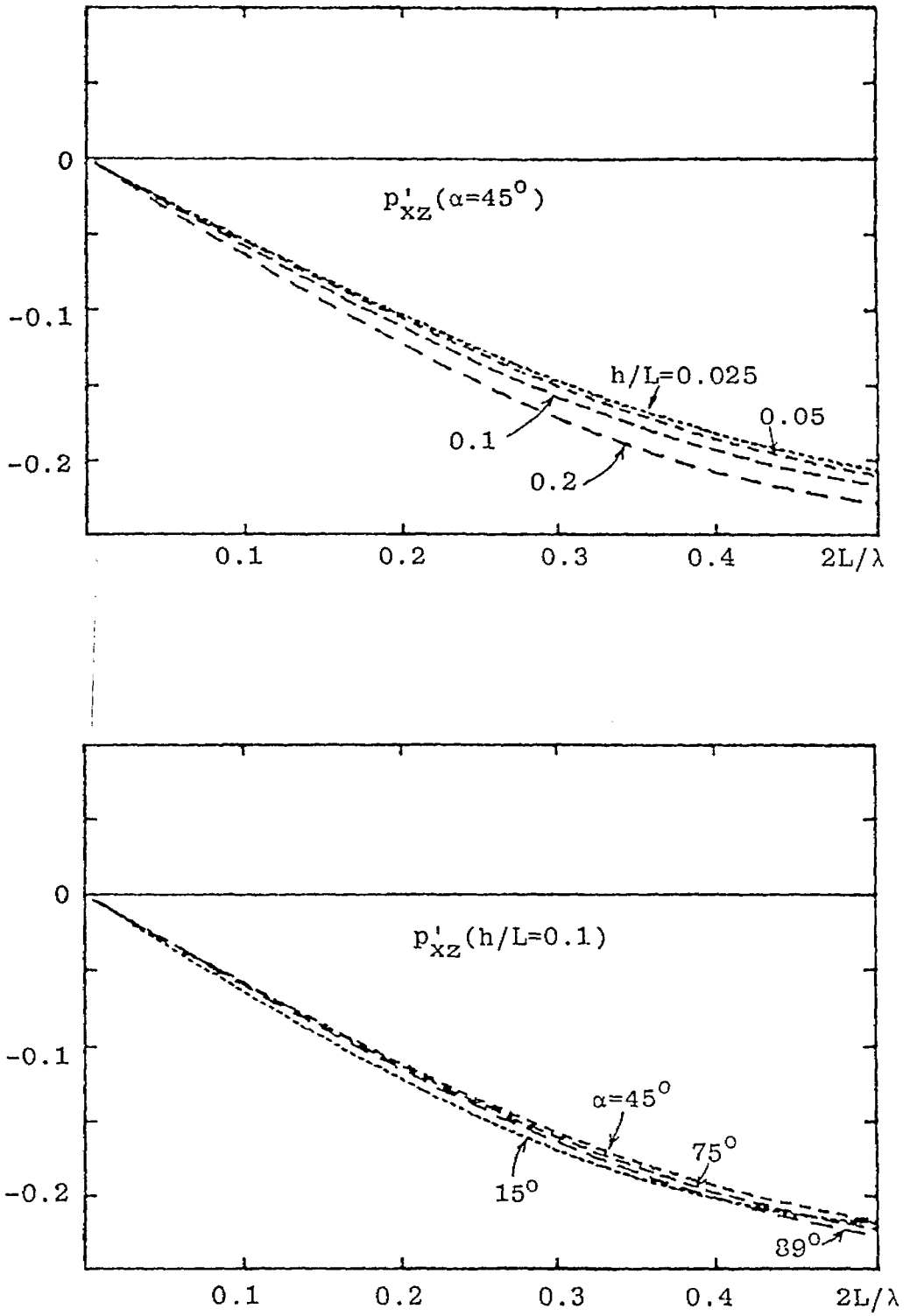

Figure 14. Variations of the Normalized Electric-Quadrupole Moments with h/L and α as Parameters

The transformation of the abscissa to L_e/λ will indicate that the normalized curves are essentially the same in that a good $\vec{p}$ cross $\vec{m}$ condition is to have insignificant higher-order moments for $L_e/\lambda < 0.5$. The same observation can also be made for the normalized magnetic-quadrupole moments shown in figure 15.

6. FIELD PATTERNS OF THE SIMULATOR

The eventual performance characteristics of interest are the fields generated by the simulator (of which multipole strengths and their parametric variations have been formulated and evaluated). Making use of equations (20) through (25), the fields can be expressed in terms of multipole coefficients $p_{\ell,m}$ and $m_{\ell,m}$. For the dipole and quadrupole coefficients the asymptotic relationships with their moments in rectangular coordinates have been given in equations (28) through (39). Since the moments are good approximations for the coefficients when $2L/\lambda < 0.5$, as shown in figures 4 through 11, and since the dipole moments begin to reach zero rapidly for the simulator to be about one-half wavelength, use of the moments for field description is presently adequate for the simulator.

The electric and magnetic fields in spherical coordinates can be obtained using only the dipole and quadrupole moments as:

$$\vec{E} = \frac{\sqrt{\mu/\epsilon}\ k^2 m_y}{4\pi r}\left[\hat{1}_r\left(\frac{1}{kr}\right)\left\{\frac{2cp_x}{m_y}\, g_1(kr)\sin(\theta) + \frac{3kcp_{xz}}{m_y}\, g_2(kr)\, \sin(\theta)\cos(\theta)\right\}\right.$$
$$\cdot \cos(\phi) + \hat{1}_\theta\left\{\left[g_1(kr) + \frac{cp_x}{m_y}\, g_3(kr)\cos(\theta)\right] + j\left[\frac{km_{yz}}{2m_y}\, g_2(kr)\cos(\theta)\right.\right.$$
$$\left.\left. + \frac{kcp_{xz}}{2m_y}\, g_4(kr)\cos(2\theta)\right]\right\}\cos(\phi) - \hat{1}_\phi\left\{ g_1(kr)\cos(\theta)\right.$$
$$\left.\left. + j\left[\frac{km_{yz}}{2m_y}\, g_2(kr)\cos(2\theta) + \frac{kcp_{xz}}{2m_y}\, g_4(kr)\cos(\theta)\right]\right\}\sin(\phi)\right] \exp(-jkr) \qquad (63a)$$

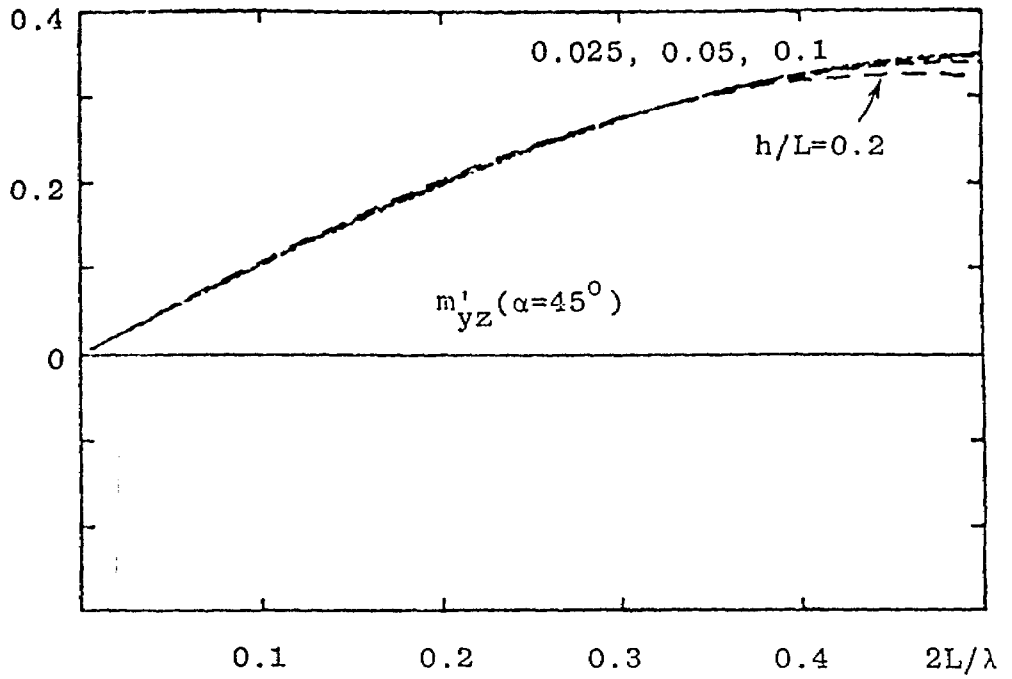

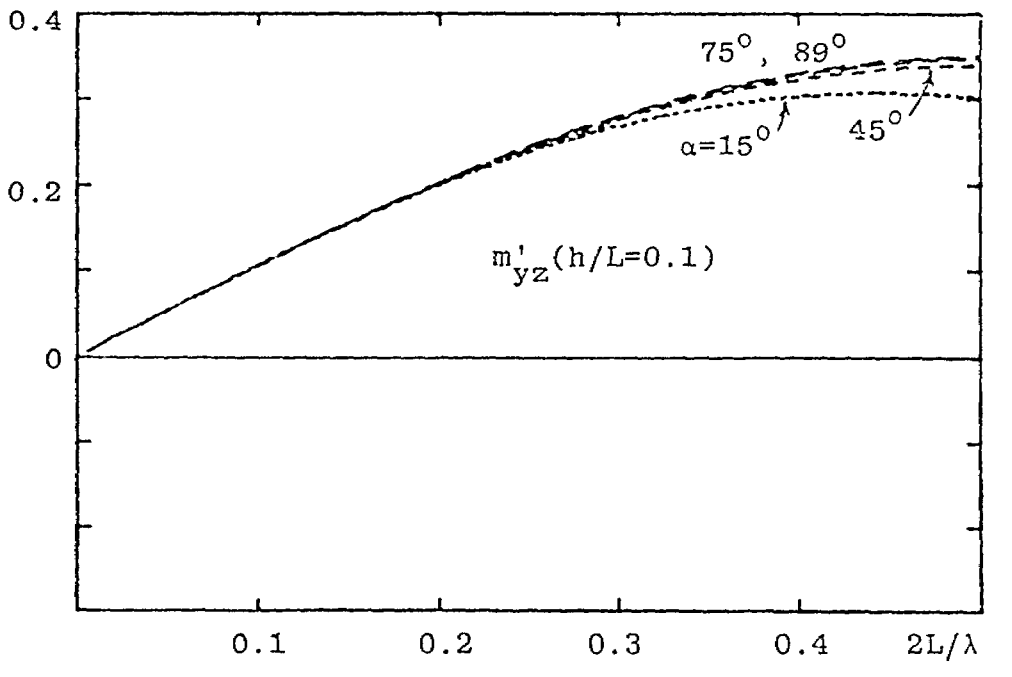

Figure 15. Variations of the Normalized Magnetic-Quadrupole Moments with h/L and α as Parameters

$$\vec{H} = \frac{k^2 m_y}{4\pi r}\left[\hat{1}_r\left(\frac{1}{kr}\right)\left\{g_1(kr)\sin(\theta) + \frac{3km_{yz}}{m_y}\, g_2(kr)\sin(\theta)\cos(\theta)\right\}\sin(\phi)\right.$$

$$+ \hat{1}_\theta\left\{\left[\frac{cp_x}{m_y}\, g_1(kr) + g_3(kr)\cos(\theta)\right] + j\left[\frac{kcp_{xz}}{2m_y}\, g_2(kr)\cos(\theta)\right.\right.$$

$$\left.\left. + \frac{km_{yz}}{2m_y}\, g_4(kr)\cos(2\theta)\right]\right\}\sin(\phi) + \vec{1}_\phi\left\{\left[\frac{cp_x}{m_y}\, g_1(kr)\cos(\theta) + g_3(kr)\right]\right.$$

$$\left.\left. + j\left[\frac{kcp_{xz}}{2m_y}\, g_2(kr)\cos(2\theta) + \frac{km_{yz}}{2m_y}\, g_4(kr)\cos(\theta)\right]\right\}\cos(\phi)\right]\exp(-jkr) \tag{63b}$$

where

$$g_1(kr) = 1 - \frac{1}{kr} \tag{64a}$$

$$g_2(kr) = \left[1 - \frac{3}{(kr)^2}\right] - \frac{j3}{kr} \tag{64b}$$

$$g_3(kr) = \left[1 - \frac{1}{(kr)^2}\right] - \frac{j}{kr} \tag{64c}$$

and

$$g_4(kr) = \left[1 - \frac{6}{(kr)^2}\right] - j3\left[\frac{1}{kr} - \frac{2}{(kr)^3}\right] \tag{64d}$$

It is noted that the fields are written with the magnetic dipole coefficient m_y as a common factor. The normalized m_y is $m_y' = m_y/AI_o$ with A given in equation (56). If the transmission line were made sufficiently short that $2L/\lambda \leq 0.1$, the quadrupole moments would be negligibly small, and the dipole moments would be approximately related as $m_y \simeq -cp_x$. These approximations simplify the fields in equation(63) as

$$\vec{E} \simeq \frac{\pi I_o\sqrt{\mu/\varepsilon}}{r}\,(m_y'\, A/\lambda^2)\left\{\vec{1}_r\left[\frac{j2}{kr}\, g_1(kr)\sin(\theta)\right]\cos\phi + \vec{1}_\theta[g_1(kr)\right.$$

$$\left. - g_3(kr)\cos(\theta)]\cos\phi - \vec{1}_\phi[g_1(kr)\cos(\theta) - g_3(kr)]\sin\phi\right\}\exp(-jkr) \tag{65a}$$

$$\vec{H} \approx \frac{\pi I_o}{r}(m_y' A/\lambda^2)\left\{\vec{I}_r\left[\frac{j2}{kr} g_1(kr)\sin(\theta)\right]\sin\phi - \vec{I}_\theta\left[g_1(kr)\right.\right.$$

$$\left.\left. - g_3(kr)\cos(\theta)\right]\sin\phi - \vec{I}_\phi\left[g_1(kr)\cos(\theta) - g_3(kr)\right]\cos\phi\right\}\exp(-jkr) \quad (65b)$$

The fields represent the desired radiation from a combination of x-directed electric-dipole moment p_x and y-directed magnetic-dipole $m_y = cp_x$. With the aid of equations (64a) and (64c), the fields are valid in all regions outside of the source region. The component $E_\theta(\theta, \phi=0)$ is seen to have a pattern identical to the $H_\theta(\theta, \phi=\pi/2)$. Similarly, the patterns $E_\phi(\theta, \phi=-\pi/2)$ and $H_\phi(\theta, \phi=0)$ are also identical. As $kr \to \infty$, the r components of fields vanish rapidly and the other components have a simple $(1+\cos\theta)$ variation that is characteristics of a $\vec{p}$ cross $\vec{m}$ radiator.

Both dipole moments of interest are given in equations (57) and (59). In the low frequency limits where $2L/\lambda$ and $h\csc(\alpha)$ approach zero, the moments take the forms:

$$p_x \approx \frac{4I_o hL}{c} + \frac{2h^2 I_o \csc(\alpha)}{c}$$

and

$$m_y \approx -4I_o hL - 2I_o h^2 \cot(\alpha)$$

Thus

$$-cp_x/m_y = \frac{4L + 2h\csc(\alpha)}{4L + 2h\cot(\alpha)} = 1, \text{ if } \alpha = 0 \quad (66)$$

The field strengths in equation (65) can be readily obtained if the transmission line area is given. For example, consider the case of $2L/\lambda = 0.1$ in figure 6 where m_y' is found to be about 0.96.

For $\alpha = 45^{o}$, the area in equation (56) gives $A/\lambda^2 = 0.00105$. Substitution of these values into the common factor in equation (65a) gives

$$\frac{\pi I_o \sqrt{\mu/\varepsilon}}{r} (m'_y \, A/\lambda^2) \simeq 1.2 \, \frac{I_o}{r}$$

Therefore an electric field intensity of 12 V/m at r = 10 m would be induced by a current $I_o = 100$ amperes flowing in the electrically small ($A = 0.00105 \, \lambda^2$) transmission line.

If the transmission line is allowed to become electrically large, the quadrupole moments would be increasingly significant, and the field patterns given in equation (63) would have to be used. For this situation the field strengths would become larger and field patterns deviate gradually from the ideal case given in equation (65). The field strengths for $2L/\lambda < 0.5$ can also be readily estimated by using the normalized curves in figures 4, 6, 8, and 10.

For the convenience of using equation (63) in estimating the field strengths for $2L/\lambda < 0.5$, figure 16 shows the relative value of cp_x/m_y used in the equation. The other relative values used in the equation are shown on the top curves of figures 17 and 18. The latter curve can be used in conjunction with figure 16 to obtain km_{yz}/m_y. Bottom curves of figures 17 and 18 are plotted using the generalized quadrupole and dipole coefficients. Since they are exact solutions they may be used for more accurate evaluation of equation (63). Of course, the exact values of the normalized $p_{1,1}$ and $m_{1,1}$ in figures 4 and 6 will have to be used for this purpose.

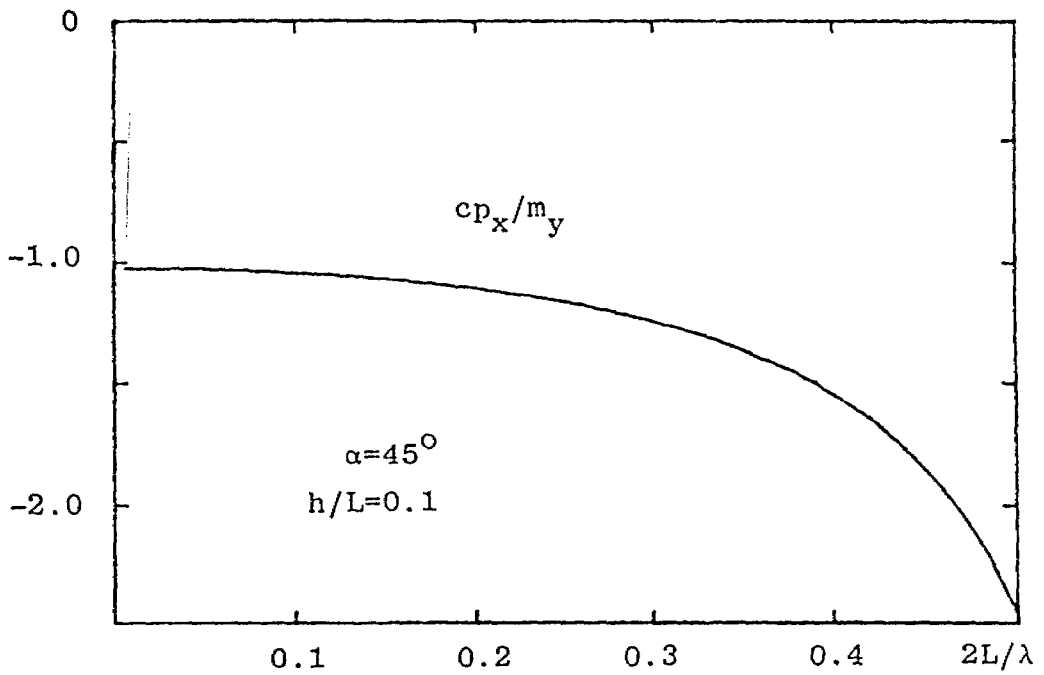

Figure 16. Relative Value of cp_x/m_y for $2L/\lambda < 0.5$

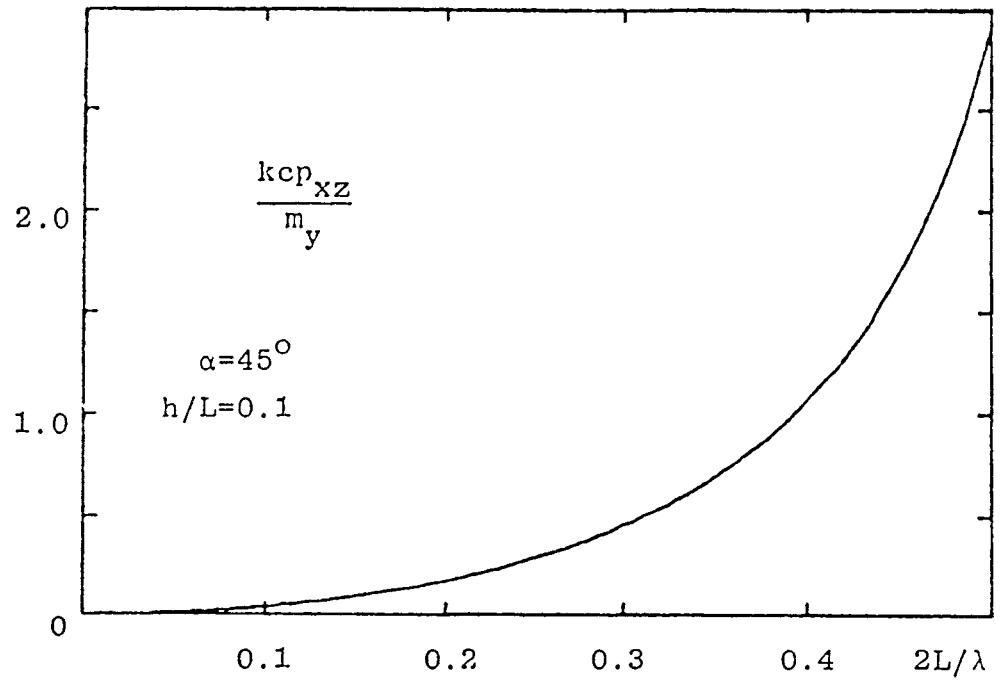

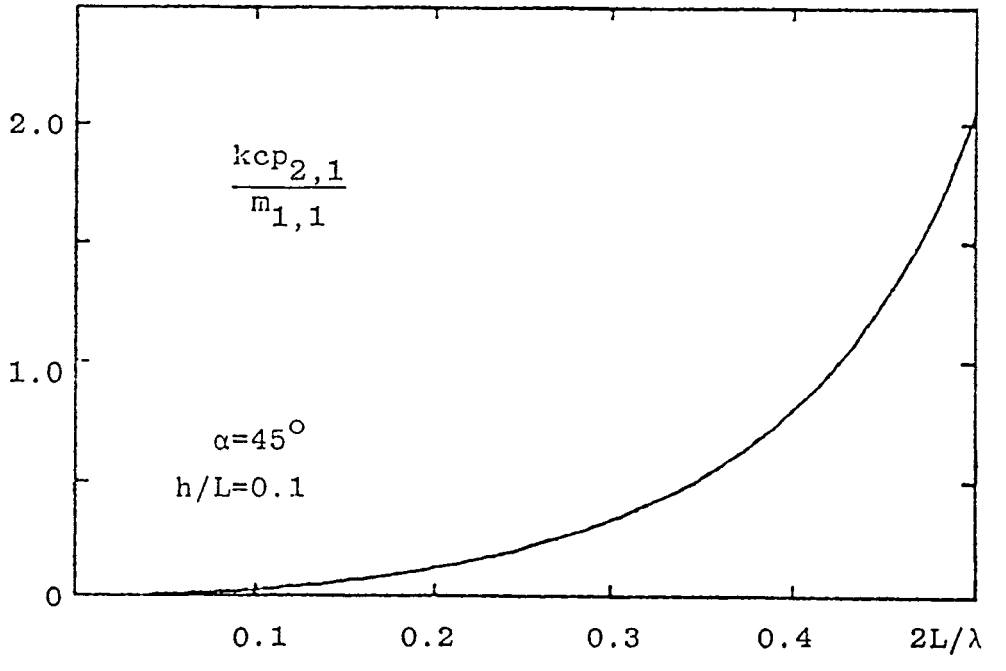

Figure 17. Relative Value of kcp_{xz}/m_y Used in Equation (63) And Its Corresponding Plot Without Quasi-static Approximation

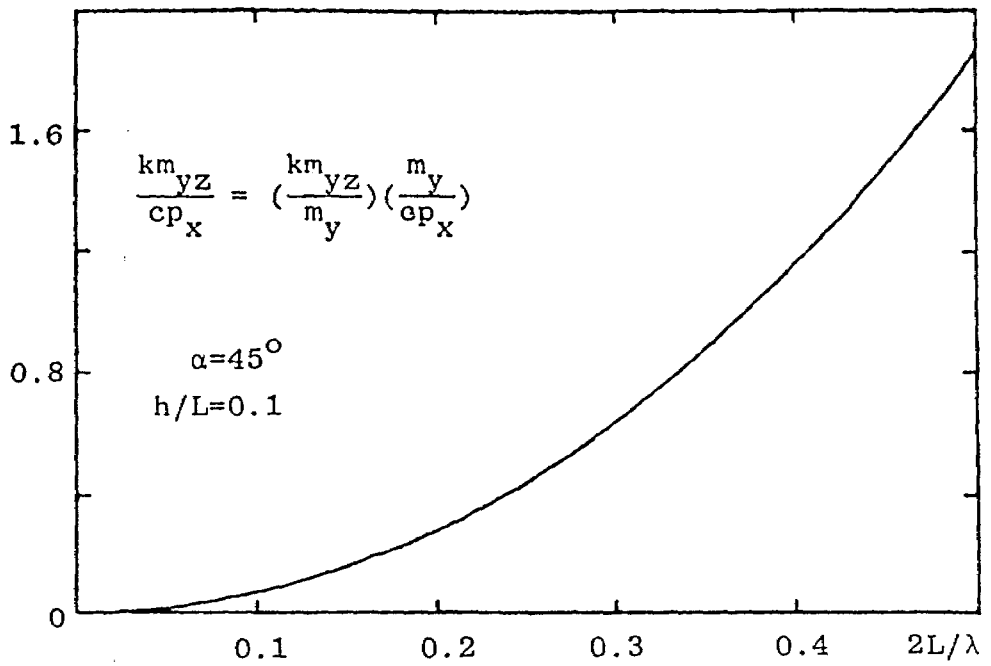

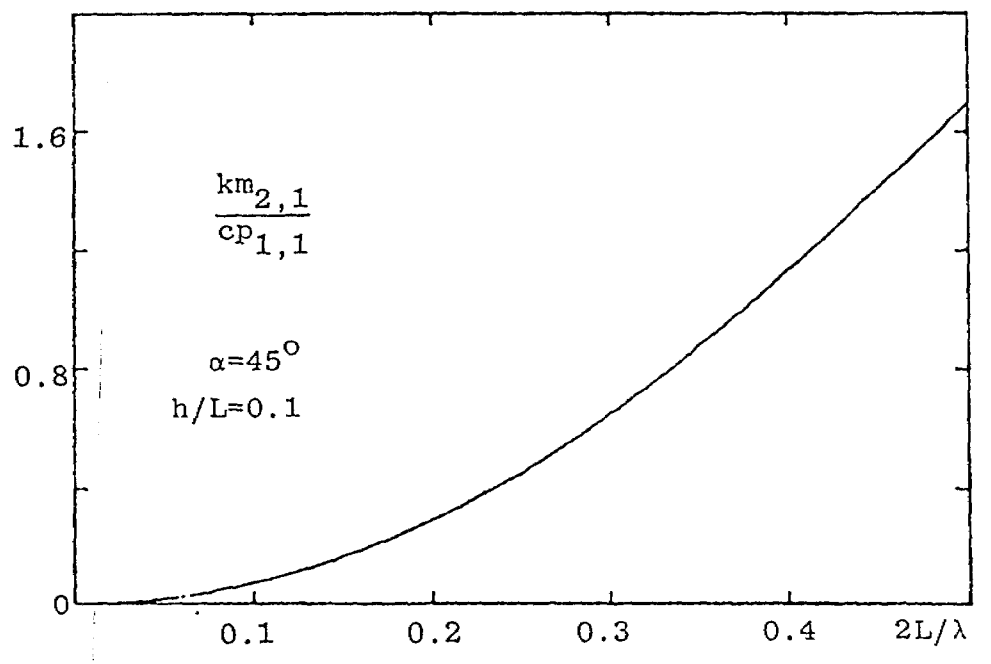

Figure 18. Relative Value of km_{yz}/cp_x and Its Corresponding Plot Without Quasi-static Approximation

7. THE $\vec{p}$ CROSS $\vec{m}$ CONDITIONS

For the transmission line to be short ($2L/\lambda \leq 0.1$), the field components in equation (65) can be used to show that

$$\frac{E_\theta(\theta=\pi,\phi=0)}{H_\phi(\theta=\pi,\phi=0)} = \sqrt{\mu/\varepsilon} = \frac{E_\phi(\theta=\pi,\phi=\pi/2)}{-H_\theta(\theta=\pi,\phi=\pi/2)} \tag{67}$$

This is the first p_x cross m_y condition stating that the fields produced by the transmission line (fig. 1) are pure TEM (Transverse Electromagnetic) waves propagating outward in the (-z) direction. This condition is a unique property that assures a nearly uniform plane wave around $\theta = \pi$ along all distance outside of the source region. For an EMP simulator, this property allows near-zone and especially quasi-near-zone illumination of a test object. Even for a longer transmission line with $2L/\lambda < 0.5$, equation (63) can be used to show that the above property still holds approximately true.

The second unique property of the $\vec{p}$ cross $\vec{m}$ condition is that the total outflowing power is purely real in all space outside the source region. That is

$$P_{p\times m} = \frac{k^4 m_y^2 \sqrt{\mu/\varepsilon}}{6\pi} = P_p + P_m = 2\mathrm{Re}(P_p) = 2\mathrm{Re}(P_m) \tag{68}$$

A derivation of this result is given in Appendix E where P_p is the complex outflowing power of p_x and P_m is that of $m_y = -cp_x$. Both P_p and P_m are complex but are conjugate of each other. The property of $P_{\vec{p}\times\vec{m}}$ is an important property for a small radiator in that there is no reactive power outside the source region.

Consequently when a $\vec{p}\times\vec{m}$ condition is realized, the difficult problem of feeding a highly reactive small radiator could be alleviated from the reactive loading of a purely electric or purely magnetic radiator.

The third important property of a $\vec{p}\times\vec{m}$ radiator is the directivity defined as

$$D = \frac{E_\theta(\theta=\pi,\phi=0) \times H^*(\theta=\pi,\phi=0)}{P_{\vec{p}\times\vec{m}}/4\pi} = 3.0 \text{ for } r \to \infty \qquad (69)$$

It means that in the far zone, the directivity of a $\vec{p}\times\vec{m}$ radiator is twice that of a pure electric or magnetic dipole. An increase of the directivity by a factor of 2 is significant in that the maximum power density is increased by a factor of 4 while the total radiated power is increased only by a factor of 2.

The three unique features of a $\vec{p}\times\vec{m}$ radiator are well assured by a small transmission MEDIUS. These properties degrade gradually for the MEDIUS if the length is restricted to $2L/\lambda < 0.5$. In other words, these features are closely approximated in the region around $\theta = \pi$, even though the transmission line is operated above $2L/\lambda = 0.1$ but limited to $2L/\lambda < 0.5$.

SECTION IV

COMBINED LINEAR AND CIRCULAR CURRENT ELEMENTS

1. CURRENT AND CHARGE DISTRIBUTIONS

The linear and circular elements of figure 2 are collocated as an attempt to produce a pair of crossed electric and magnetic dipoles. Assuming no interaction between the two elements, their current and charge distributions can be obtained from reference 9. For the linear current element, the distributions of current and linear charge density (coulomb/m) are

$$\vec{I}(x') = \vec{I}_{x'}(I_o)\left\{\sin(kh - k|x'|) + A[\cos(kx') - \cos(kh)] + B[\cos(kx'/2) - \cos(kh/2)]\right\} \tag{70a}$$

$$q(x' \gtrless 0) = (q_o)[\pm\cos(kh - k|x'|) + A\sin(kx') + \frac{B}{2}\sin(kx'/2)] \tag{70b}$$

$$q_o = j(I_o/c) \tag{70c}$$

where the coefficients A and B are dependent of the length and diameter of the linear wire. Evaluation of their values using $2\ell n(2h/a) = 10$ are available from reference 9. The current and charge distributions of the circular current element are:

$$\vec{I}(\theta') = \vec{I}_{\theta'}(I_o)\left[\frac{1}{a_o} + 2\sum_{n=1}^{\infty}\frac{\cos(n\theta')}{a_n}\right] = \vec{I}_{\theta'}\left[I'_o + 2\sum_{n=1}^{\infty} I'_n\cos(n\theta')\right] \tag{71a}$$

and

$$q(\theta') = \frac{2}{jkb}\left(\frac{I_o}{c}\right)\sum_{n=1}^{\infty}\frac{n\sin(n\theta')}{a_n} = \frac{2}{jkb}\sum_{n=1}^{\infty}(I'_n/c)\sin(n\theta') \tag{71b}$$

where the coefficients $(1/a_n)$ are plotted in reference 9 and the value of I_o is $(-jV/\pi\sqrt{\mu/\varepsilon})$ with V as the applied voltage.

2. STRENGTHS OF ELECTRIC AND MAGNETIC DIPOLES

Full derivation of the multipole coefficients and moments is given in Appendix G. For the linear current element the magnetic multipoles are all zero assuming the wire is sufficiently thin such that $ka \to 0$. Also, assuming the wire length $2h/\lambda < 0.5$, all the higher-order electric multipoles are negligibly small. Since the linear element is center-fed, the electric quadrupole also vanishes. The only nonzero multipole is the electric-dipole with a coefficient

$$p_{1,1} = -\frac{3}{k}\sqrt{\frac{3}{8\pi}} \int_o^h q(x')\left[kx' j_o(kx') - j_1(kx')\right] dx' \qquad (72)$$

where equation (70b) should be used for evaluation. Asymptotically with $kx' << 1$, the electric-dipole moment p_x can be obtained as

$$p_x = j\frac{2I_o}{k^2 c}\left[1 - \cos(kh)\right] \approx j\frac{I_o}{c}h^2 = q_o h^2 \qquad (73)$$

The normalized electric-dipole strength can be done in the manner as in the last section. Figure 19 shows that for $2h/\lambda < 0.4$ the exact and asymptotic definitions are identical.

The electric and magnetic dipoles for the circular loop are obtained in Appendix G as

$$p_{1,1} = \left(-\frac{I_1'}{c}\sqrt{\frac{3}{8\pi}}\right)\left(\frac{3\pi}{jk^2}\right)\left(kbj_o(kb) - j_1(kb)\right) \qquad (74)$$

and

$$m_{1,1} = \left(I_o'\sqrt{\frac{3}{8\pi}}\right)\left(\frac{j3\pi b}{k}\right) j_1(kb) \qquad (75)$$

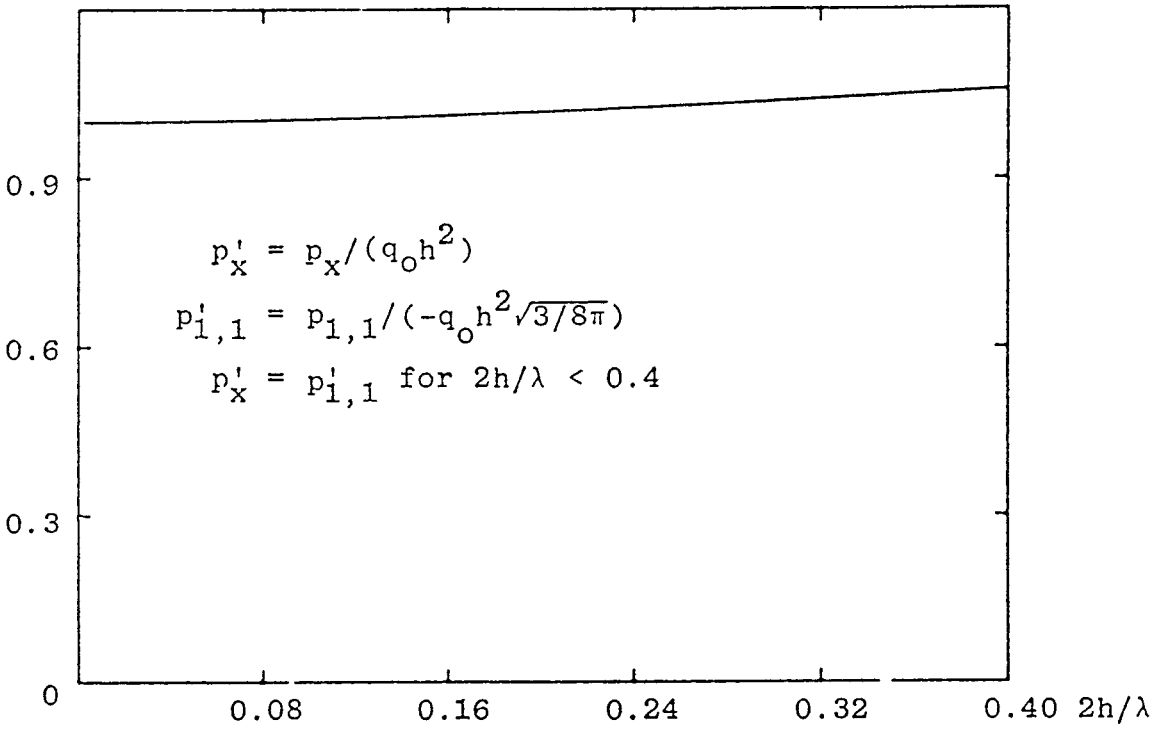

Figure 19. Normalized Dipole Moment and Dipole Coefficient of the Linear Current Element in Figure 2

They become the dipole moments p_x and m_y (without the factor $\sqrt{3/8\pi}$) under the quasi-static approximations of the spherical Bessel functions with kb << 1. Their normalized absolute values are plotted in figure 20 using the values of $(1/a_o)$ and $(1/a_1)$ given in reference 9. The value of $(1/a_1)$ is complex and approaches zero as kb approaches zero. When $p_{1,1}$ or p_x is normalized by πb^2, they approach about 2 as b approaches zero. This is caused by the real part of $(1/a_o)$ which diverges as b becomes zero (see ref. 9).

3. STRENGTH OF ELECTRIC AND MAGNETIC QUADRUPOLES

As mentioned earlier, the linear element is center-fed and its electric quadrupole is zero. The electric and magnetic quadrupole coefficients of the loop can be obtained from the results of Appendix G as

$$p_{2,1} = \left(-\frac{I_2'}{c}\sqrt{\frac{15}{8\pi}}\right)\left(\frac{10\pi}{jk^3}\right)(kbj_1(kb) - 2j_2(kb)) \tag{76}$$

and

$$m_{2,1} = \left(I_1'\sqrt{\frac{15}{8\pi}}\right)\left(\frac{j10\pi b}{k^2}\right)j_2(kb) \tag{77}$$

If kb << 1, they become the quadrupole moments p_{xz} and m_{yz} without the factor $\sqrt{15/8\pi}$. Their normalized curves are given in figure 21 where resonance phenomena are associated with the coefficients $(1/a_1)$ and $(1/a_2)$ as given in reference 9.

4. FIELD PATTERNS OF THE ELEMENTS

As the multipole coefficients have been formulated and evaluated, their substitution into equation (63) will give the field patterns of the combined elements assuming no interaction.

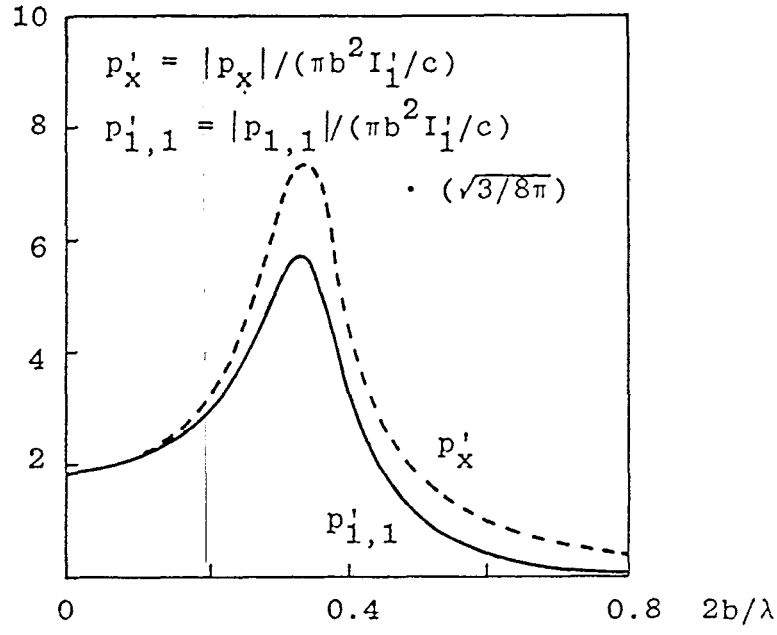

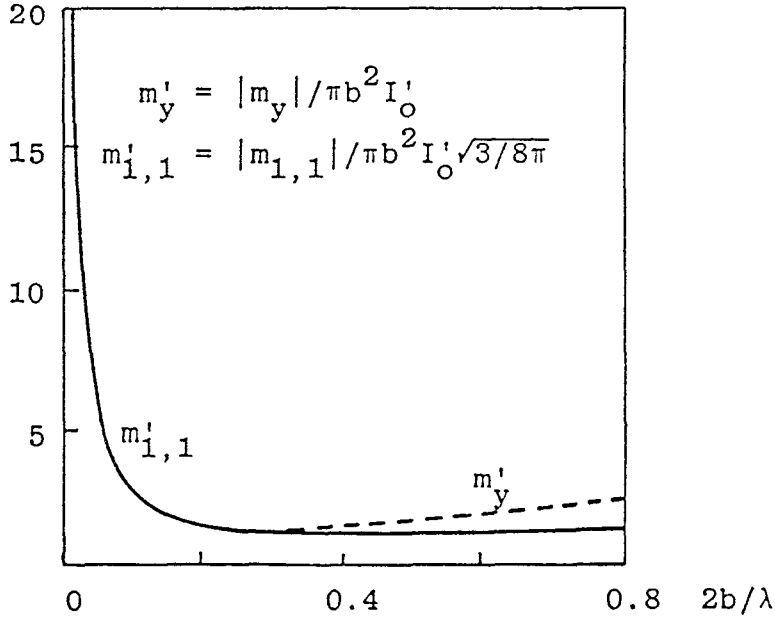

Figure 20. Normalized Dipole Coefficients and Dipole Moments of the Circular Current Element Shown in Figure 2

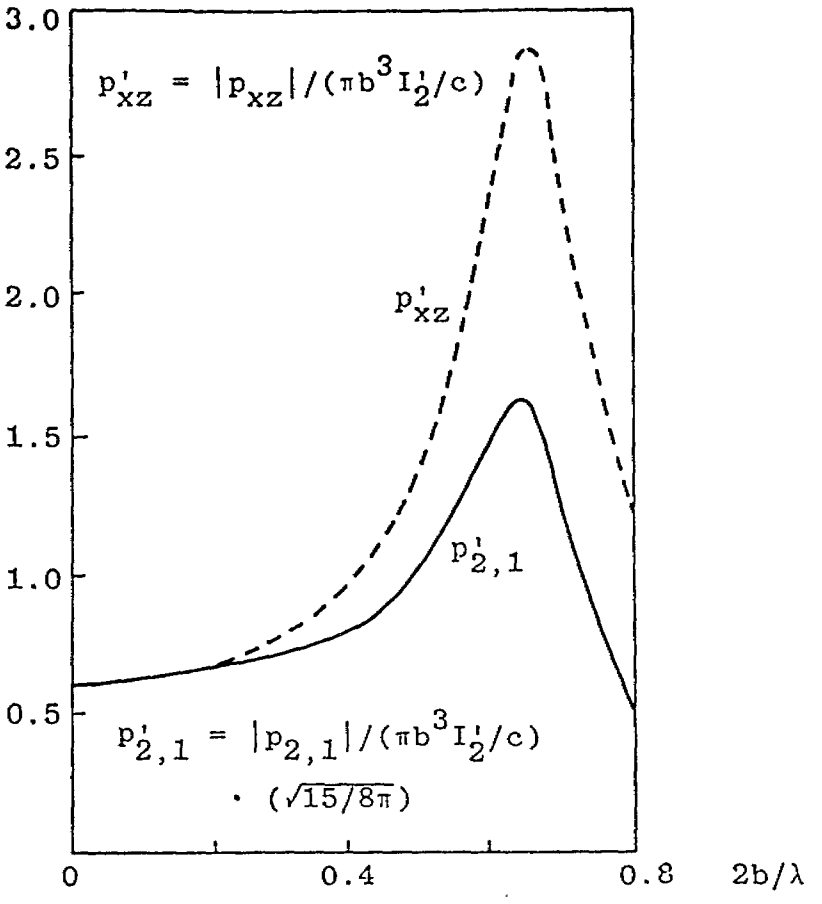

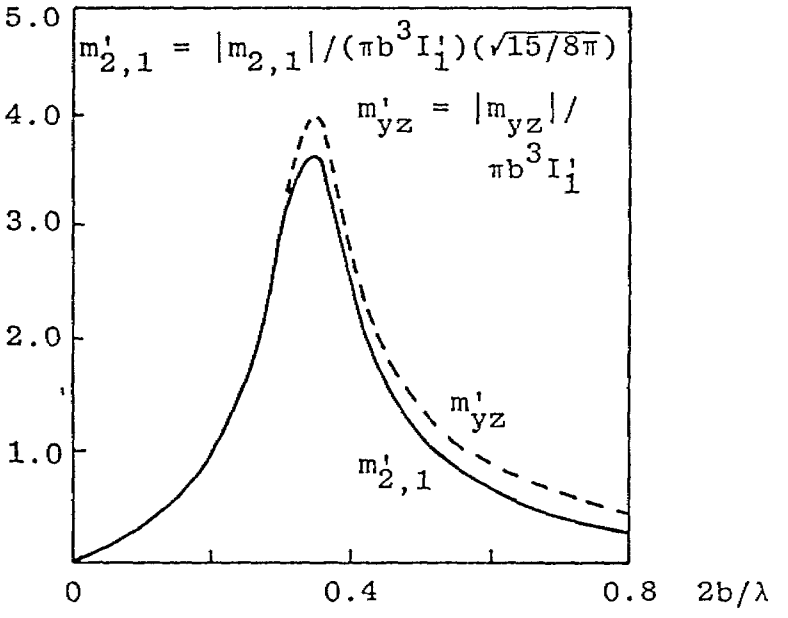

Figure 21. Normalized Quadrupole Coefficients and Moments of the Circular Current Element

For $2b/\lambda < 0.8$ the relative strengths of the quadrupole coefficients are plotted in figure 22 for the circular loop. Since the loop also contributes to electric-dipole field, the total electric dipole coefficient of the combined elements should be the sum of those in equations (72) and (74). For $kb << 1$, their sum becomes $(p_x)_s$ for the combined elements as

$$(p_x)_s = (p_x)_1 + (p_x)_2$$

$$\approx \frac{j2(I_o)_1}{ck^2}(1 - \cos(kh)) + j\frac{2\pi kb^3(I_o')_2}{c} \qquad (78)$$

if (I_1') in equation (74) is approximated as $(-k^2b^2I_o')$ for kb vanishingly small. The designations $(p_x)_1$ and $(p_x)_2$ are used to distinguish the electric-dipole moments for the linear and circular currents. Meanwhile, the magnetic moment m_y can be obtained from equation (75) as

$$m_y \approx (\pi b^2)(I_o')_2 \qquad (79)$$

One condition of particular interest is the relationship between $(I_o)_1$ of the linear element and $(I_o')_2$ of the circular element such that $c(p_x)_s = m_y$. Use of the above two equations gives the required ratio as

$$(I_o)_1/(I_o')_2 \approx -j\pi(b^2/h^2)(1 - j2kb), \text{ or}$$

$$(cq_o)_1/(I_o')_2 \approx \pi b^2/h^2 , \quad \text{for } 2kb << 1 \qquad (80)$$

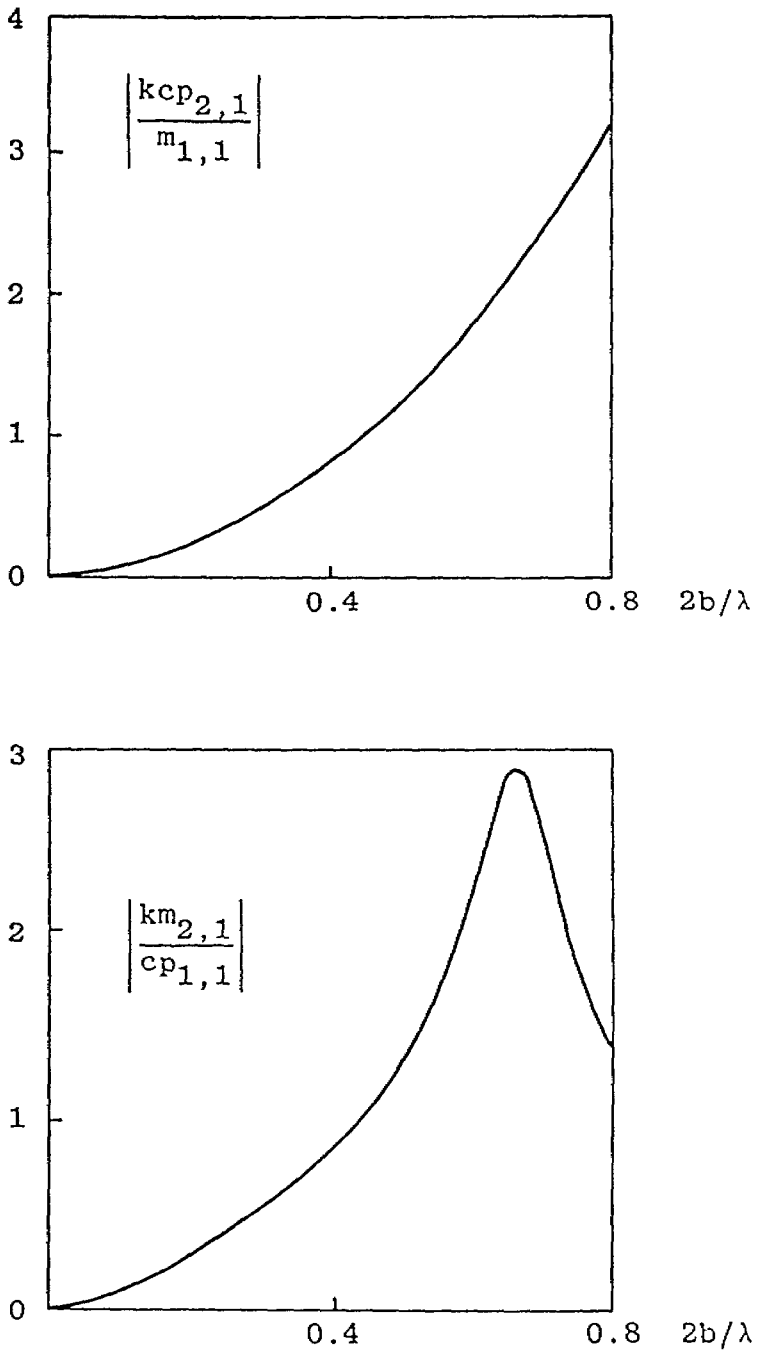

Figure 22. The Quadrupole Coefficients Normalized by the Dipole Coefficients of the Circular Current Element

This indicates that, if the two currents could be maintained independently, the linear current would have to lag 90^{o} in phase and be proportional to $\pi b^2/h^2$ in amplitude with respect to the circular current. Should the value of $(I_o)_1$ in equation (80) be used in equation (78), the $(p_x)_s$ would be dependent of $(I_o')_2$ only and the combined element would exhibit an ideal p cross m condition.

Similar to the transmission-line MEDIUS, the patterns for the combined elements with $2b/\lambda < 0.1$ are completely described by equation (65). Also, all the p cross m conditions discussed in connection with the transmission line are equally applicable to the combined elements. The only exception is that the maximum radiation now takes place at $\theta = 0$ instead of $\theta = \pi$ for the transmission line. As for the field strength, the combined elements would yield considerably more than the transmission line if the same amount of current could be maintained. This observation becomes quite clear by comparing the normalized magnetic-dipole moments in figures 6 and 20. For instance, the loop element with $2b/\lambda = 0.0366$ will have the same area as the transmission line with $2L/\lambda = 0.1$, $\alpha = 45^{o}$, and $h/L = 0.1$. While m_y' for the transmission line is nearly unity, the m_y' for the loop is about 10 as can be seen in figure 20. Therefore, if the same amplitude of current were maintained in the loop and the linear current were maintained as in equation (80), the combined elements would produce 10 times higher fields than those by the transmission line.

SECTION V

CONCLUSION AND OBSERVATION

1. MULTIPOLE RADIATION

Due to the apparent absence of previous work, a complete description of multipole radiation has been formulated for the two selected simulators. The spherical vector functions used are those of references 7, 8, and 10.

Multipole radiation has been solved exactly for an arbitrarily large source. The solution is exact in that the complete set of spherical harmonics is used and the harmonic coefficients are formulated by integrals over the entire source region. These harmonic coefficients have been treated in this report as the generalized multipole coefficients.

Considerable amount of vector operations on the spherical harmonic functions has been found necessary, as was found in reference 10, to lead to the complete formulation of multipole radiation. Some of the benefits of this formulation are listed as follows:

- Generalized multipole coefficients can now be evaluated in their exact forms for an arbitrarily large and complex source, and their asymptotic approximations can be directly identified with the multipole moments developed under quasi-static solutions.
- Generalized dipole coefficients can now be used to systematically perform a source-synthesis procedure by which their strengths can be maximized with appropriate relationships. (This benefit is to alleviate the restriction of a vanishingly small source region, which is inherent in quasi-static source synthesis.)

- For a relatively large and complex source, the generalized higher-order-pole coefficients can now be used to systematically minimize their radiation contributions when only the ideal $\vec{p}$ cross $\vec{m}$ radiation is desired.

The first benefit has been demonstrated for the two selected simulators. Effort to demonstrate the last two benefits remains to be attempted in the future.

2. TRANSMISSION-LINE MEDIUS

The first simulator (fig. 1) is a backward radiator in that its maximum radiation is along $\theta' = \pi$ or $(-z')$ axis if the line length is restricted to be small. A complete evaluation of its dipole and quadrupole moments has been performed and compared with their generalized coefficients. Figures 4 through 11 are their normalized plots for direct comparisons between exact solutions and quasi-static approximations.

Parametric variations of the multipole coefficients have also been evaluated as shown in figures 12 through 15. The results indicate that the variations with geometric parameters of the simulator are relatively insignificant when h/L is restricted to less than 0.2.

Radiation patterns of various field components are concisely formulated in equations (63) and (65). The fields are the exact solutions valid everywhere outside of the source region. They are relatively simple functions of the spherical coordinates when the values of multipole coefficients are evaluated as has been done in this report. For the convenience of using these equations to estimate field strengths and patterns, the relative values of

multipoles are also plotted in figures 16 through 18. Patterns of field vectors are considerably simplified when the radiation is predominantly of dipole moments. For $2L/\lambda \leq 0.1$ the field vectors in equation (65) are an accurate representation of the simulator radiation which is closely that of the ideal $\vec{p}$ cross $\vec{m}$ condition desired.

The ideal $\vec{p}$ cross $\vec{m}$ conditions are discussed in conjunction with equations (67) through (69). These conditions are presently confined to a small simulator $2L/\lambda < 0.1$. However, when the simulator becomes larger, the conditions are degraded gradually. For example, the half-power-density beamwidth of an ideal $\vec{p}$ cross $\vec{m}$ radiator can be obtained as about 131° from equation (65) with $kr \to \infty$. Earlier work (ref. 5) on a resonant electromagnetic dipole has a range of 108° to 177° half-power-density beamwidths for approximately equal E- and H-plane patterns.

3. LINEAR AND CIRCULAR CURRENT ELEMENTS

The second simulator (fig. 2) is the collocated current elements. It is a forward radiator in that the maximum radiation is in the (+z) direction with $\theta = 0$, if the conditions of equation (80) are met.

Assuming the wires are thin compared to their lengths, the normalized dipole and quadrupole strengths have been evaluated as shown in figures 19 through 21. The currents in both elements were assumed to be independent for the multipole evaluations. This assumption would be valid if the generators could be adjusted including their mutual impedances to support the required currents.

Radiation field vectors and the patterns of field components are the same as equations (63) through (65), provided the multipole moments are replaced by those obtained for the combined current elements. These equations are valid also for larger simulators using multipole coefficients when the relationships given in equations (28) through (39) were properly used.

Again for the convenience of using equation (63), the relative strength of the multipoles are plotted in figure 22. Perhaps it is worth noting that all the multipoles of second simulator are complex, instead of being purely real or imaginary for the first simulator.

4. LIMITATION AND REALIZABILITY

Physical limitations of the two simulators are imposed by the assumptions made in their formulations. The first simulator is assumed to have been perfectly impedance-matched. The second simulator is assumed to have its currents maintained independently. The former assumption is not severe and the required generator is clearly realizable in practice, although the radiator is extremely inefficient in that most power would be delivered to the terminating load. The latter assumption is quite severe in that both generators are connected to highly reactive loads including the mutual coupling effects. Thus the realizability of the required generators is not immediately clear. However, if the generators were realizable in practice, the radiation efficiency of the second simulator would be much higher than that of the

first simulator. Also the second simulator has the flexibility of separating the linear and circular elements. This flexibility could be explored for optimizing the simulator performance in conjunction with generator requirements. One possibility is to separate the current elements as was suggested in reference 6. This would allow the linear element to radiate without being strongly affected by the presence of circular loop. All the data and formulations presented in this report can be used directly even for this arrangement, except that a phase factor has to be introduced to account for spatial separation. This is true if one recalls that the two elements were assumed to have no interaction and were driven independently.

REFERENCES

1. Baum, C. E., "EMP Simulators for Various Types of Nuclear EMP Environment: An Interim Categorization," IEEE Trans. on Antennas and Propagation, January 1978. Also, "Some Types of Small EMP Simulators," AFWL Misc. Simulator Memos, No. 9, December 1976.

2. Chu, L. J., "Physical Limitations of Omni-Directional Antennas," J. of Applied Physics; December 1948.

3. Rumsey, V. H., "Some New Forms of Huygens Principle," IRE Trans. on Antennas and Propagation; December 1959.

4. Yu, J. S., "Electromagnetic Resonance, Invisibility, Non-uniqueness, and Dipole Scattering of a Small Sphere," General Electric Tech. Information Series, No. R71EMH2, January 1971.

5. Yu, J. S., and H. Morimoto, "Electromagnetic Dipole," General Electric Tech. Information Series, No. R71EMH3, January 1971.

6. Baum, C. E., "Some Characteristics of Electric and Magnetic Dipole Antennas for Radiating Transient Pulses," AFWL Sensor and Simulation Notes, Note 125; January 1971.

7. Stratton, J. A., Electromagnetic Theory, McGraw-Hill Book Co., 1941.

8. Jackson, J. D., Classical Electrodynamics, John Wiley & Sons, Inc., 1962.

9. King, R.W.P., Chapters 9 and 11 of Antenna Theory, Part 1, edited by R. E. Collin and F. J. Zucker, McGraw-Hill Book Co.; 1969.

10. Baum, C. E., "On the Singularity Expansion Method for the Solution of Electromagnetic Interaction Problems," AFWL Interaction Notes, Note 88; December 1971.

APPENDIX A

DERIVATION OF MULTIPOLE MOMENTS FOR POTENTIALS AND FIELDS

Fields and potentials can be expressed in terms of multipole coefficients or multipole moments. This Appendix will first show that the vector potential can be expressed as an infinite series. The first three lowest-order terms are to be expanded in terms of electric and magnetic multipole moments by restricting the source region to be small.

After the potentials are derived, the associated fields due to dipole and quadrupole moments are given to show how each moment is contributing to the near and far fields.

1. VECTOR POTENTIAL SERIES

The vector potential for the current distribution $\vec{J}(\vec{r}')$ is given by

$$\vec{A}(\vec{r}) = \frac{\mu_o}{4\pi} \int \vec{J}(\vec{r}') \frac{e^{-jk|\vec{r} - \vec{r}'|}}{|\vec{r} - \vec{r}'|} dv \qquad (A1)$$

Expanding the integrand of the above integral yields

$$\vec{A}(\vec{r}) = \frac{jk\mu_o}{4\pi} \sum_{\ell=0}^{\infty} (2\ell+1)\, h_\ell^{(2)}(kr) \int \vec{J}(\vec{r}')\, j_\ell(kr')\, P_\ell(\cos\psi)\, dv \qquad (A2)$$

where j_ℓ are the spherical Bessel functions, P_ℓ are the Legendre polynomials, $h_\ell^{(2)}$ are the spherical Hankel functions of the second kind, and ψ is the angle between $\vec{r}$ and $\vec{r}'$.

2. ZERO-ORDER POTENTIAL

The zero-order vector potential is

$$\vec{A}_o(\vec{r}) = - \frac{jk\mu_o}{4\pi} h_o^{(2)}(kr) \int \vec{J}(\vec{r}') \, j_o(kr') \, dv \tag{A3}$$

which can be approximated by retaining only the first term of $j_o(kr')$ expanded in Taylor series, i.e.,

$$\vec{A}_o(\vec{r}) \simeq -\frac{\mu_o e^{-jkr}}{4\pi r} \int \vec{J}(\vec{r}') \, dv \tag{A4}$$

It can be shown by using the continuity equation that

$$\int \vec{J} \, dv = - j\omega \int \vec{r}' \rho \, dv \tag{A5}$$

Hence

$$\vec{A}_o(\vec{r}) = \frac{j\omega\mu_o e^{-jkr}}{4\pi r} \int \vec{r}' \, \rho \, dv \tag{A6}$$

Since the quasi-static definition of an electric dipole moment is

$$\vec{p} = \int \vec{r}' \, \rho \, dv \tag{A7}$$

the zero-order potential can be written

$$\vec{A}_o(\vec{r}) \simeq \frac{j\omega\mu_o e^{-jkr}}{4\pi r} \vec{p} \tag{A8}$$

Thus, for small source region $kr' << 1$, the zero-order potential contains only the electric dipole moment.

3. FIRST-ORDER POTENTIAL

The first-order potential is considered next, i.e.,

$$\vec{A}_1 = \frac{jk\mu_o}{4\pi r^2}\left(1 - \frac{j}{kr}\right) e^{-jkr} \int (\vec{r} \cdot \vec{r}')\, \vec{J}\, dv \qquad \text{(A9)}$$

After several vector operations, the integrand in $\vec{A}_1$ can be expressed as

$$\int (\vec{r} \cdot \vec{r}')\, \vec{J}\, dv = \vec{m} \times \vec{r} + \frac{1}{2} j\omega\, \vec{\vec{p}} \cdot \vec{r} \qquad \text{(A10)}$$

where $\vec{m}$ is the magnetic dipole moment

$$\vec{m} = \frac{1}{2} \int \vec{r}' \times \vec{J}(\vec{r}')\, dv \qquad \text{(A11)}$$

and $\vec{\vec{p}}$ is the dyadic form of electric quadrupole moments

$$(\vec{\vec{p}})_{x_i x_j} = \vec{i}_i \vec{i}_j \int x_i' x_j' \rho\, dv \qquad \text{(A12)}$$

Hence

$$\vec{A}_1 = \frac{jk\mu_o}{4\pi r^2}\left(1 - \frac{j}{kr}\right) e^{-jkr}\left[\vec{m} \times \vec{r} + \frac{1}{2} j\omega\, \vec{\vec{p}} \cdot \vec{r}\right] \qquad \text{(A13)}$$

Note that the above representation is appropriate only for a source that is electrically small.

4. SECOND-ORDER POTENTIAL

The expansion of vector potential $\vec{A}_2$ can be written from equation (A2) as

$$\vec{A}_2 = -\frac{jk\mu_o}{4\pi}(5) h_2^{(2)}(kr) \int \vec{J}(\vec{r}')\, j_2(kr')\, p_2(\cos\gamma)\, dv \qquad \text{(A14)}$$

where

$$j_2(kr') \approx \frac{8(kr')^2}{5 \cdot 4 \cdot 3 \cdot 2} \quad , \quad \text{for } kr' << 1 \quad ;$$

$$h_2^{(2)}(kr) = \left[-\frac{j}{kr} - \frac{3}{(kr)^2} + \frac{3j}{(kr)^3} \right] e^{-jkr} ,$$

$$p_2(\cos\gamma) = \frac{1}{2} (3 \cos^2\gamma - 1) ,$$

and

$$\cos\gamma = \frac{\vec{r} \cdot \vec{r}'}{rr'}$$

The integrand is expanded as

$$(\vec{J}) j_2(kr') \; p_2(\cos\gamma) = \frac{(\vec{J})(kr')^2}{15} \frac{1}{2} \left[3 \left(\frac{\vec{r} \cdot \vec{r}'}{rr'} \right)^2 - 1 \right]$$

$$= \frac{k^2}{30} \left[\frac{3}{r^2} \vec{J}(\vec{r} \cdot \vec{r}')^2 - (r')^2 \vec{J} \right] \qquad \text{(A15)}$$

Using the vector identity,

$$\vec{J}(\vec{r}' \cdot \vec{r}) = \frac{1}{2} \left[(\vec{r}' \times \vec{J}) \times \vec{r} + \vec{J}(\vec{r}' \cdot \vec{r}) + \vec{r}'(\vec{r} \cdot \vec{J}) \right] \qquad \text{(A16)}$$

the integrand becomes

$$\frac{k^2}{30} \left\{ \frac{3}{r^2} \frac{1}{2} \left[(\vec{r}' \cdot \vec{r})(\vec{r}' \times \vec{J}) \times \vec{r} + \vec{J}(\vec{r}' \cdot \vec{r})^2 + \vec{r}'(\vec{r} \cdot \vec{J})(\vec{r}' \cdot \vec{r}) \right] - (r')^2 \vec{J} \right\}$$

The magnetic quadrupole is defined in dyadic form as

$$\vec{\vec{m}} = \frac{1}{2} \int [(\vec{r}' \times \vec{J})\vec{r}' + \vec{r}'(\vec{r}' \times \vec{J})] \, dv \qquad \text{(A17)}$$

Substitution of this definition into the integrand in equation (A15) gives rise to

$$\vec{A}_2 = -\frac{jk\mu_o h_2^{(2)} k^2}{24\pi} \left\{ \frac{3}{r^2} (\vec{\vec{m}} \cdot \vec{r}) \times \vec{r} + \frac{3}{2r^2} \int \left[\left(\vec{r}' \times (\vec{r}' \times \vec{J}) \times \vec{r} \right) \times \vec{r} + \vec{J}(\vec{r}' \cdot \vec{r})^2 + \vec{r}'(\vec{r} \cdot \vec{J})(\vec{r}' \cdot \vec{r}) \right] dv - \int (r')^2 \vec{J} \, dv \right\} \qquad \text{(A18)}$$

Since the magnetic quadrupole is of main interest, the second-order potential contributed by magnetic quadrupole moment is specifically written as

$$\vec{A}_{m.q.} = - \frac{jk^3 \mu_o h_2^{(2)}(kr)}{8\pi r^2} (\vec{m} \cdot \vec{r}) \times \vec{r} \qquad \text{(A19)}$$

5. FIELDS OF DIPOLE MOMENTS

After the vector potential is obtained, the fields can be expressed through standard procedure of solving Maxwell's equations. That is

$$\vec{H} = \frac{1}{\mu_o} \nabla \times \vec{A}, \qquad \text{(A20)}$$

and

$$\vec{E} = \frac{1}{j\omega\varepsilon_o} \nabla \times \vec{H} \qquad \text{(A21)}$$

Substitution of equation (A8) and the magnetic dipole term in equation (A13) into the above equations gives rise to

$$\vec{H}_1 = - \frac{j\omega}{4\pi r} e^{-jkr} \left[(jk + \frac{1}{r})(\vec{1}_r \times \vec{p}_1) + (jk + \frac{1}{r} + \frac{1}{jkr^2})(\vec{m}_1/c) \right.$$
$$\left. - (jk + \frac{3}{r} + \frac{3}{jkr^2})(\vec{1}_r \cdot \vec{m}_1/c)\vec{1}_r \right] , \qquad \text{(A22)}$$

and

$$\vec{E}_1 = - \frac{j\omega\sqrt{\mu/\varepsilon}}{4\pi r} e^{-jkr} \left[-(jk + \frac{1}{r})(\vec{1}_r \times \vec{m}_1/c) + (jk + \frac{1}{r} + \frac{1}{jkr^2}) \vec{p}_1 \right.$$
$$\left. - (jk + \frac{3}{r} + \frac{3}{jkr^2})(\vec{1}_r \cdot \vec{p}_1)\vec{1}_r \right] \qquad \text{(A23)}$$

where the vector fields E_1 and H_1 are subscripted to denote that they are contributed only by the electric and magnetic dipole moment vectors p_1 and m_1.

6. FIELDS OF QUADRUPOLE MOMENTS

If only the quadrupole terms in the vector potential expansion are substituted in equation (A20), the magnetic field due to electric and magnetic quadrupoles is

$$\vec{H}_2 = \frac{k\omega}{8\pi r} e^{-jkr} \left[\left(jk + \frac{3}{r} - \frac{3}{jkr^2} \right) \vec{1}_r \times (\vec{\vec{p}}_2 \cdot \vec{1}_r) - \left(jk + \frac{5}{r} + \frac{12}{jkr^2} - \frac{12}{k^2 r^3} \right) \vec{1}_r \left(\frac{\vec{1}_r \cdot \vec{\vec{m}}_2 \cdot \vec{1}_r}{c} \right) + \left(jk + \frac{2}{r} + \frac{3}{jkr^2} + \frac{3}{k^2 r^3} \right) \left(\frac{\vec{\vec{m}}_2}{c} \cdot \vec{1}_r \right) \right] \quad \text{(A24)}$$

The electric field due to quadrupole moments is

$$\vec{E}_2 = \frac{k\omega\sqrt{\mu/\varepsilon}}{8\pi r} e^{-jkr} \left[- \left(jk + \frac{3}{r} - \frac{3}{jkr^2} \right) \vec{1}_r \times \left(\frac{\vec{\vec{m}}_2}{c} \cdot \vec{1}_r \right) - \left(jk + \frac{5}{r} + \frac{12}{jkr} - \frac{12}{k^2 r^3} \right) \vec{1}_r (\vec{1}_r \cdot \vec{\vec{p}}_2 \cdot \vec{1}_r) + \left(jk + \frac{2}{r} + \frac{3}{jkr^2} + \frac{3}{k^2 r^3} \right) (\vec{\vec{p}}_2 \cdot \vec{1}_r) \right] \quad \text{(A25)}$$

The above fields are valid at any field point but are appropriate only when the source region is small, i.e., $kr' << 1$.

APPENDIX B

DERIVATION OF MULTIPOLE COEFFICIENTS IN SPHERICAL HARMONICS

In a source-free region, an electromagnetic field can be expanded as the superposition of multipole fields. The multipole coefficients are to be derived in the following paragraphs.

Using the MKS system and assuming the time factor $e^{j\omega t}$, the Maxwell equations in frequency domain are given by

$$\nabla\times\vec{E} = -j\omega\mu_o\vec{H} \tag{B1}$$

$$\nabla\times\vec{H} = \vec{J} + j\omega\varepsilon_o\vec{E} \tag{B2}$$

$$\nabla\cdot\vec{E} = \rho/\varepsilon_o \tag{B3}$$

$$\nabla\cdot\vec{H} = 0 \tag{B4}$$

Taking the curl of equation (B2), and using equations (B1) and (B4), yields

$$(\nabla^2 + k^2)\vec{H} = -\nabla\times\vec{J} \tag{B5}$$

Define a function $\vec{E}'$,

$$\vec{E}' = \vec{E} + \frac{\vec{J}}{j\omega\varepsilon_o} \tag{B6}$$

Note that $\vec{E}' = \vec{E}$ in source-free region.

Taking the curl of equation (B1) and using equations (B2) and (B3), it follows that

$$(\nabla^2 + k^2)\vec{E}' = -\nabla \times \nabla \times \frac{\vec{J}}{j\omega\varepsilon_o} \tag{B7}$$

Equations (B5) and (B7) are known as the vector Helmholtz equation. A complete set of vector solutions for the Helmholtz equations can be formed by two sets of electromagnetic multipole fields (ref. 8). The first set is

$$\vec{E}_{\ell,m} = g_{\ell,m}(kr)\ \vec{X}_{\ell,m}(\theta,\phi) \tag{B8}$$

and

$$\vec{H}_{\ell,m} = -\frac{1}{j\omega\mu_o}\nabla \times \vec{E}_{\ell,m}$$

$$= -\frac{1}{j\omega\mu_o}\nabla \times g_{\ell,m}(kr)\ \vec{X}_{\ell,m}(\theta,\phi) \tag{B9}$$

where $\vec{X}_{\ell,m}$ are the vector spherical harmonics (ref. 8) and $g_{\ell,m}$ are the radial functions to be determined. Another set is

$$\vec{H}_{\ell,m} = f_{\ell,m}(kr)\ \vec{X}_{\ell,m}(\theta,\phi) \tag{B10}$$

and

$$\vec{E}_{\ell,m} = \frac{1}{j\omega\varepsilon_o}\nabla \times \vec{H}_{\ell,m}$$

$$= \frac{1}{j\omega\varepsilon_o}\nabla \times f_{\ell,m}(kr)\ \vec{X}_{\ell,m}(\theta,\phi) \tag{B11}$$

where

$$\ell = 0,1,2,3,\ldots$$

$$m = -\ell,-\ell+1,\ldots,0,1,\ldots\ell$$

The vector spherical harmonics are defined (ref. 8) as

$$\vec{X}_{\ell,m} = -\frac{j}{\sqrt{\ell(\ell+1)}}\left(\vec{r} \times \nabla Y_{\ell,m}(\theta,\phi)\right) \tag{B12}$$

where $Y_{\ell,m}$ are the spherical harmonics in terms of associated Legendre polynomials as

$$Y_{\ell,m}(\theta,\phi) = \sqrt{\frac{2\ell + 1(\ell - m)!}{4\pi(\ell + m)!}}\, P_{\ell}^{m}(\cos\theta)\, e^{jm\phi} \tag{B13}$$

The orthonormality of both functions can be expressed as:

$$\int_0^{2\pi}\int_0^{\pi} Y^{*}_{\ell,m}(\theta,\phi)\, Y_{\ell',m'}(\theta,\phi)\, \sin\theta\, d\theta\, d\phi = \begin{cases} 1, & \ell = \ell' \text{ and } m = m' \\ 0, & \text{otherwise} \end{cases} \tag{B14a}$$

and

$$\int_0^{2\pi}\int_0^{\pi} \vec{X}^{*}_{\ell',m'}(\theta,\phi)\, \vec{X}_{\ell,m}(\theta,\phi)\, \sin\theta\, d\theta\, d\phi = \begin{cases} 1, & \ell = \ell' \text{ and } m = m' \\ 0, & \text{otherwise} \end{cases} \tag{B14b}$$

The radial function $f_{\ell,m}$ in equation (B10) can be determined as follows. Substituting equation (B10) into equation (B5), taking scalar product of both sides with $\vec{X}^{*}_{\ell,m}$ and then integrating over all angles will lead to

$$\int_0^{2\pi}\int_0^{\pi} \vec{X}^{*}_{\ell,m}(\theta,\phi) \cdot (\nabla^2 + k^2)\, f_{\ell,m}(kr)\, \vec{X}_{\ell,m}(\theta,\phi)\, \sin\theta\, d\theta\, d\phi$$

$$= -\int\int \vec{X}^{*}_{\ell,m}(\theta,\phi) \cdot \nabla \times \vec{J}\, \sin\theta\, d\theta\, d\phi \tag{B15}$$

The left-hand side becomes

$$\text{LHS} = \int_0^{2\pi}\int_0^{\pi} \vec{X}^{*}_{\ell,m}(\theta,\phi) \cdot \vec{X}_{\ell,m}(\theta,\phi)\, \sin\theta\, d\theta\, d\phi \cdot \left[\frac{d^2}{dr^2} + \frac{2}{r}\frac{d}{dr} + k^2 - \frac{\ell(\ell+1)}{2}\right] f_{\ell,m}(kr) = \left[\frac{d^2}{dr^2} + \frac{2}{r}\frac{d}{dr} + k^2 - \frac{\ell(\ell+1)}{r^2}\right] f_{\ell,m}(kr) \tag{B16}$$

because of orthonormality. Hence, equation (B15) can be written as

$$\left[\frac{d^2}{dr^2} + \frac{2}{r}\frac{d}{dr} + k^2 - \frac{\ell(\ell+1)}{r^2}\right] f_{\ell,m}(kr) = -\iint \vec{X}^*_{\ell,m}(\theta,\phi) \cdot \nabla \times \vec{J} \sin\theta d\theta d\phi \tag{B17}$$

Note that the Green's function $G(r,r')$ for the differential equation

$$\left[\frac{d^2}{dr^2} + \frac{2}{r}\frac{d}{dr} + k^2 - \frac{\ell(\ell+1)}{2}\right] G(r,r') = -\frac{1}{r^2}\delta(r - r') \tag{B18}$$

with the boundary conditions of finiteness at the origin and outgoing waves at infinity is known to have two possible solution forms:

$$G(r,r') = \begin{cases} -jkj_\ell(kr')\, h_\ell^{(2)}(kr) , & r > r' \\ -jkj_\ell(kr)\, h_\ell^{(2)}(kr') , & r < r' \end{cases} \tag{B19}$$

where j_ℓ, $h_\ell^{(2)}$ are spherical Bessel functions and Hankel functions of the second kind.

Thus, the solution for equation (B17) for $r > r'$ is

$$\begin{aligned} f_{\ell,m}(kr) &= -jkh_\ell^{(2)}(kr) \int_0^\infty r'^2 j_\ell(kr') \int_0^{2\pi}\int_0^{\pi} \vec{X}^*_{\ell,m}(\theta',\phi') \\ &\quad \cdot \nabla' \times \vec{J} \cdot \sin\theta'\, dr' d\theta' d\phi' \\ &= -jkh_\ell^{(2)}(kr) \int_V r'^2 j_\ell(kr')\, \vec{X}^*_{\ell,m} \cdot \nabla' \times \vec{J}\, dv \end{aligned} \tag{B20}$$

Using equation (B12) and appropriate vector identity it follows that

$$\begin{aligned} f_{\ell,m}(kr) = \frac{\ell k^2 h_\ell^{(2)}(kr)}{j\sqrt{\ell(\ell+1)}} \int_V Y^*_{\ell,m}(\theta',\phi') \Big\{ &\rho(\vec{r}')\frac{d}{dr'}[r' j_\ell(kr')] \\ &+ \frac{jk}{c}[\vec{r}' \cdot \vec{J}(\vec{r}')] j_\ell(kr') \Big\}\, dv \end{aligned} \tag{B21}$$

Define the electric multipole coefficients $p_{\ell,m}$ by

$$p_{\ell,m} = \frac{(2\ell+1)!!}{k^{\ell}(\ell+1)} \int Y^{*}_{\ell,m}(\theta',\phi') \left\{ \rho(\vec{r}') \frac{d}{dr'} [r' j_{\ell}(kr')] + \frac{jk}{c} [\vec{r} \cdot \vec{J}(\vec{r}')] j_{\ell}(kr') \right\} dv \qquad \text{(B22)}$$

which approaches the electrostatic multipole coefficients or the quasi-static definition in Appendix D.

The magnetic field in equation (B10) is then given by

$$\vec{H}_{\ell,m} = \frac{ck^{\ell+2}}{j(2\ell+1)!!} \left(\frac{\ell+1}{\ell}\right)^{\frac{1}{2}} h^{(2)}_{\ell}(kr)\, p_{\ell,m} \vec{X}_{\ell,m}(\theta,\phi) \qquad \text{(B23)}$$

where $(2\ell+1)!! = (2\ell+1)(2\ell-1)\ldots5\cdot3\cdot1$.

By similar procedure, $g_{\ell,m}(kr)$ in equation (B8) can be shown to be

$$g_{\ell,m}(kr) = -jkh^{(2)}_{\ell}(kr) \int_0^{\infty} r'^2 j_{\ell}(kr') \int_0^{2\pi}\int_0^{\pi} \vec{X}_{\ell,m}(\theta',\phi') \cdot \frac{\nabla' \times \nabla' \times \vec{J}(r')}{j\omega\varepsilon_o} \sin\theta'\, dr'\, d\theta'\, d\phi'$$

$$= -\frac{jkh^{(2)}_{\ell}(kr)}{j\omega\varepsilon_o} \int_V r'^2 j_{\ell}(kr')\, \vec{X}_{\ell,m}(\theta',\phi')\, \nabla' \times \nabla' \times \vec{J}(\vec{r}')\, dv \qquad \text{(B24)}$$

Using equation (B12) and appropriate vector identities, it follows that

$$g_{\ell,m}(kr) = \frac{kh^{(2)}_{\ell}(kr)}{j\sqrt{\ell(\ell+1)}\,\omega\varepsilon_o} \int Y^{*}_{\ell,m}(\theta',\phi')\, j_{\ell}(kr')\, \nabla' [\vec{r}' \times \vec{J}(\vec{r}')]\, dv \qquad \text{(B25)}$$

Define the magnetic multipole coefficients as

$$m_{\ell,m} = -\frac{(2\ell+1)}{k^{\ell}(\ell+1)} \int Y^{*}_{\ell,m}(\theta',\phi')\, j_{\ell}(kr')\, \nabla' \cdot [\vec{r}' \times \vec{J}(\vec{r}')]\, dv \tag{B26}$$

By using the identity with $\vec{J}(\vec{r}') = 0$ on the integration surface

$$\begin{aligned}
\int f(\vec{r}')\, \nabla' \cdot \left(\vec{r}' \times \vec{J}(\vec{r}')\right) dv &= -\int \nabla f(\vec{r}') \cdot [\vec{r}' \times \vec{J}(\vec{r}')]\, dv \\
&\quad + \int \nabla' \cdot [f(r')\, \vec{r}' \times \vec{J}(\vec{r}')]\, dv \\
&= -\int \nabla' f(\vec{r}') \cdot [\vec{r}' \times \vec{J}(\vec{r}')]\, dv \\
&\quad + \int_{A} [f(r')\, \vec{r}' \times \vec{J}(\vec{r}')] \cdot dA \\
&= -\int \nabla' f(\vec{r}') \cdot [\vec{r}' \times \vec{J}(\vec{r}')]\, dv
\end{aligned} \tag{B27}$$

equation (B26) becomes

$$m_{\ell,m} = \frac{(2\ell+1)!!}{k^{\ell}(\ell+1)} \int_{V} \nabla' Y^{*}_{\ell,m}(\theta',\phi')\, j_{\ell}(kr') \cdot [\vec{r}' \times \vec{J}(\vec{r}')]\, dv \tag{B28}$$

The electric field in equation (B8) can now be written as

$$\vec{E}_{\ell,m} = \frac{jk^{\ell+2} c\mu_{o}}{(2\ell+1)!!} \left(\frac{\ell+1}{\ell}\right)^{\frac{1}{2}} h^{(2)}_{\ell}(kr)\, m_{\ell,m} \vec{X}_{\ell,m}(\theta,\phi) \tag{B29}$$

APPENDIX C

EXPRESSION OF VECTOR SPHERICAL HARMONICS $\vec{X}_{\ell,m}$ AND $\nabla X h_\ell^{(2)} \vec{X}_{\ell,m}$ IN SPHERICAL COORDINATES

1. $\vec{X}_{\ell,m}$ EXPANDED IN SPHERICAL COORDINATES

The vector spherical harmonics used in multipole fields are defined (ref. 8) by

$$\vec{X}_{\ell,m}(\theta,\phi) = -\frac{j}{\sqrt{\ell(\ell+1)}} (\vec{r} \times \nabla) Y_{\ell,m}(\theta,\phi)$$

$$= \frac{1}{\sqrt{\ell(\ell+1)}} \vec{L} Y_{\ell,m}(\theta,\phi) \qquad \text{(C1)}$$

where

$$Y_{\ell,m}(\theta,\phi) = \sqrt{\frac{(2\ell+1)(\ell-m)!}{4\pi(\ell+m)!}} P_\ell^m(\cos\theta)\, e^{jm\phi} \qquad \text{(C2)}$$

After somewhat lengthy operations, equation (C1) can be expanded into only θ and ϕ components:

$$\vec{X}_{\ell,m}(\theta,\phi) = \frac{1}{\sqrt{\ell(\ell+1)}} \left\{ \vec{I}_\theta \left[-m \csc\theta\, Y_{\ell,m}(\theta,\phi) \right] + j\vec{I}_\phi \left[m \cot\theta\, Y_{\ell,m}(\theta,\phi) \right.\right.$$

$$\left.\left. + \sqrt{(\ell+m)(\ell-m+1)}\, e^{-j\phi}\, Y_{\ell,m-1}(\theta,\phi) \right] \right\} \qquad \text{(C3)}$$

Noting that

$$Y_{\ell,-m}(\theta,\phi) = (-1)^m Y^*_{\ell,m}(\theta,\phi) \qquad \text{(C4)}$$

and

$$\vec{X}_{\ell,-m}(\theta,\phi) = -\frac{j}{\sqrt{\ell(\ell+1)}} (\vec{r} \times \nabla) Y_{\ell,-m}(\theta,\phi) \qquad \text{(C5)}$$

$\vec{X}_{\ell,-m}$ can be related to $\vec{X}_{\ell,m}$ by

$$\vec{X}_{\ell,-m} = -\frac{j(-1)^m}{\sqrt{\ell(\ell+1)}}(\vec{r}\times\nabla)\,Y^*_{\ell,m}(\theta,\phi)$$

$$= (-1)^{m+1}\,\vec{X}^*_{\ell,m} \qquad \text{(C6)}$$

For reference purposes, some lowest orders of the $Y_{\ell,m}(\theta,\phi)$ and the spherical harmonic vectors are explicitly written in the following functions of θ and ϕ

$$Y_{1,0} = \sqrt{\frac{3}{4\pi}}\cos\theta,$$

$$Y_{1,2} = -\sqrt{\frac{3}{8\pi}}\sin\theta\, e^{j\phi},$$

$$Y_{2,0} = \sqrt{\frac{5}{4\pi}}\left(\frac{3}{2}\cos^2\theta - \frac{1}{2}\right),$$

$$Y_{2,1} = -\sqrt{\frac{15}{8\pi}}\sin\theta\cos\theta\, e^{j\phi},$$

and

$$Y_{2,2} = \frac{1}{4}\sqrt{\frac{15}{2\pi}}\sin^2\theta\, e^{j2\phi} \qquad \text{(C7)}$$

$$\vec{X}_{1,0}(\theta,\phi) = \vec{1}_\phi j\sqrt{\frac{3}{8\pi}}\sin\theta,$$

$$\vec{X}_{1,1}(\theta,\phi) = \frac{1}{4}\sqrt{\frac{3}{\pi}}\,e^{j\phi}\left(\vec{1}_\theta + j\cos\theta\vec{1}_\phi\right),$$

$$\vec{X}_{2,0}(\theta,\phi) = \vec{1}_\phi j\sqrt{\frac{15}{8\pi}}\sin\theta\cos\theta,$$

$$\vec{X}_{2,1}(\theta,\phi) = \frac{1}{4}\sqrt{\frac{5}{\pi}}\,e^{j\phi}\left(\cos\theta\vec{1}_\theta + j\cos 2\theta\vec{1}_\phi\right),$$

and

$$\vec{X}_{2,2}(\theta,\phi) = -\frac{1}{4}\sqrt{\frac{5}{\pi}}\sin\theta\, e^{j2\phi}\,(\vec{1}_\theta + j\cos\theta\vec{1}_\phi) \qquad \text{(C8)}$$

2. $\nabla X h_\ell \vec{X}_{\ell,m}(\theta,\phi)$ IN SPHERICAL COORDINATES

By vector identity

$$\nabla X h_\ell^{(2)}(kr)\, \vec{X}_{\ell,m}(\theta,\phi) = \nabla h_\ell^{(2)}(kr) \times \vec{X}_{\ell,m}(\theta,\phi) + h_\ell^{(2)}(kr) \nabla \times \vec{X}_{\ell,m}(\theta,\phi) \tag{C9}$$

By the recurrence formula,

$$\nabla h_\ell^{(2)}(kr) = \vec{I}_r \frac{\partial h_\ell^{(2)}(kr)}{\partial r} = \vec{I}_r k \left[h_{\ell-1}^{(2)}(kr) - \frac{\ell+1}{kr} h_\ell^{(2)}(kr) \right] \tag{C10}$$

Since $\vec{X}_{\ell,m}$ is independent of r and has no r-component, as shown in equation (C3), it can be written as $\vec{I}_\theta X_\theta + \vec{I}_\phi X_\phi$ and its curl becomes:

$$\nabla \times \vec{X}_\ell = \frac{\vec{I}_r}{r^2 \sin\theta} \left[\frac{\partial (r \sin\theta\, X_\phi)}{\partial \theta} - \frac{(\partial r X_\phi)}{\partial \phi} \right] + \frac{1}{r} (X_\theta \vec{I}_\phi - X_\phi \vec{I}_\theta)$$

$$= \frac{\vec{I}_r}{r} \left(\frac{\partial X_\phi}{\partial \theta} + \cot\theta\, X_\phi - \csc\theta \frac{\partial X_\theta}{\partial \phi} \right) + \frac{1}{r} (-X_\phi \vec{I}_\theta + X_\theta \vec{I}_\phi) \tag{C11}$$

Combining equations (C9) to (C11) results in the desired expansion:

$$\nabla X h_\ell^{(2)}(kr)\, \vec{X}\ (\theta,\phi) = \frac{h_\ell^{(2)}(kr)}{r} \left(\frac{\partial X_\phi}{\partial \theta} + \cot\theta\, X_\phi - \csc\theta \frac{\partial X_\theta}{\partial \phi} \right) \vec{I}_r$$

$$+ \left[k h_{\ell-1}^{(2)}(kr) - \frac{\ell}{r} h_\ell^{(2)}(kr) \right] (-X_\phi \vec{I}_\theta + X_\theta \vec{I}_\phi) \tag{C12}$$

For $m < 0$, equation (C6) can be used to show that

$$\nabla X h_\ell^{(2)}\, \vec{X}_{\ell,-m} = (-1)^{m+1}\, \nabla X h_\ell^{(2)}\, \vec{X}^*_{\ell,m} \tag{C13}$$

With the aid of equation (C8), the results of the operations in equation (C12) are tabulated below for reference purposes.

ℓ	m	$\nabla X\, h_\ell^{(2)}(kr)\, X_{\ell,m}(\theta,\phi)$
1	0	$j\sqrt{\frac{3}{8\pi}}\left[2\cos\theta\,\frac{h_1^{(2)}}{r}\,\vec{I}_r - \sin\theta\left(kh_0^{(2)} - \frac{1}{r}\,h_1^{(2)}\right)\vec{I}_\theta\right]$
	1	$\frac{j}{4}\sqrt{\frac{3}{\pi}}\,e^{j\phi}\left[\frac{h_1^{(2)}}{r}\csc\theta(\cos 2\theta - 1)\vec{I}_r + \left(kh_0^{(2)} - \frac{1}{r}\,h_1^{(2)}\right)(\cos\theta\vec{I}_\theta + j\vec{I}_\phi)\right]$
2	0	$j\sqrt{\frac{15}{8\pi}}\left[\frac{h_2^{(2)}}{r}(\cos 2\theta + \cos^2\theta)\,\vec{I}_r - \left(kh_1^{(2)} - \frac{2}{r}\,h_2^{(2)}\right)\sin\theta\cos\theta\vec{I}_\theta\right]$
	1	$-\frac{j}{4}\sqrt{\frac{5}{\pi}}\,e^{j\phi}\left[\frac{h_2^{(2)}}{r}(3\sin 2\theta)\vec{I}_r + \left(kh_1^{(2)} - \frac{2}{r}\,h_2^{(2)}\right)(-j\cos 2\theta\vec{I}_\theta + \cos\theta\vec{I}_\phi)\right]$
	2	$\frac{j}{4}\sqrt{\frac{5}{\pi}}\,e^{j2\phi}\left[\frac{h_2^{(2)}}{r}\,3\sin^2\theta\,\vec{I}_r + \left(kh_1^{(2)} - \frac{2}{r}\,h_2^{(2)}\right)(\sin\theta\cos\theta\vec{I}_\theta + j\sin\theta\vec{I}_\phi)\right]$

APPENDIX D

ASYMPTOTIC RELATIONSHIP BETWEEN MULTIPOLE MOMENTS AND MULTIPOLE COEFFICIENTS

1. ASYMPTOTIC MULTIPOLE COEFFICIENTS

The electric and magnetic multipole coefficients are derived in Appendix B as

$$p_{\ell,m} = \frac{(2\ell+1)!!}{k^{\ell}(\ell+1)} \int Y^{*}_{\ell,m}(\theta',\phi') \left\{ [kr' j_{\ell-1}(kr') - \ell j_{\ell}(kr')] \rho + \frac{jk}{c} (\vec{r}' \cdot \vec{J})\, j_{\ell}(kr') \right\} dv \qquad \text{(D1)}$$

and

$$m_{\ell,m} = \frac{(2\ell+1)!!}{k^{\ell}(\ell+1)} \int \nabla' \left[Y^{*}_{\ell,m}(\theta',\phi')\, j_{\ell}(kr') \right] \cdot (\vec{r}' \times \vec{J})\, dv \qquad \text{(D2)}$$

where integrations are over the source region designated by the primed spherical coordinates, and

$$(2\ell+1)!! = (2\ell+1)(2\ell-1)\ldots 5 \cdot 3 \cdot 1 \qquad \text{(D3)}$$

The $Y_{\ell,m}(\theta',\phi')$ are spherical harmonics and the $j_{\ell}(kr')$ are spherical Bessel functions with $\ell = 1,2,3,\ldots$, and $m = -\ell,-\ell+1,\ldots\ell$.

When the frequency approaches zero, or $kr'_{max} << 1$, the spherical Bessel function can be approximated by

$$j_{\ell}(kr') \cong \frac{(kr')^{\ell}}{(2\ell+1)!!} \left\{ 1 - \frac{\frac{1}{2}(kr')^2}{1!(2\ell+3)} + \frac{\left[\frac{1}{2}(kr')^2\right]^2}{2!(2\ell+3)(2\ell+5)} \cdots \right\} \qquad \text{(D4)}$$

Retaining only the first term of $j_{\ell}(kr')$ the electric and magnetic coefficients in their asymptotic form can be reduced to

$$p_{\ell,m} \simeq \int (r')^{\ell}\, Y^{*}_{\ell,m}\, \rho\, dv, \qquad \text{(D5)}$$

and

$$m_{\ell,m} \simeq \frac{1}{\ell+1} \int \nabla' \left[Y^{*}_{\ell,m} (r')^{\ell} \right] \cdot (\vec{r}' \times \vec{J})\, dv \qquad \text{(D6)}$$

By expressing the integrand in terms of rectangular coordinates, the $p_{\ell,m}$ and $m_{\ell,m}$ in equations (D5) and (D6) can be written as linear combinations of multipole moments. Examples for electric dipole, magnetic dipole, electric quadrupole, and magnetic quadrupole coefficients are shown below. Since dipoles are of main concern, more extensive derivations are given.

2. ELECTRIC DIPOLE

The electric dipole coefficient in spherical harmonics is given by

$$p_{1,m} = \frac{3}{2k} \int Y^{*}_{1,m} \left[\rho (kr' j_0 - j_1) + \frac{jk}{c} (\vec{r}' \cdot \vec{J})\, j_1 \right] dv \qquad \text{(D7)}$$

where $m = -1, 0, 1$. Expanding as equation (D4) and retaining only the kr terms for the spherical Bessel functions, the asymptotic form of equation (D7) becomes

$$p_{1,m} \simeq \int Y^{*}_{1,m}(\theta', \phi')\, r'\, \rho(r', \theta', \phi')\, dv \qquad \text{(D8)}$$

Use of the expression $Y^{*}_{\ell,m}$ in Appendix B gives

$$Y^{*}_{1,1}(\theta', \phi') = -\sqrt{\frac{3}{8\pi}} \sin\theta'\, e^{-j\phi'},$$

$$Y^{*}_{1,0}(\theta', \phi') = \sqrt{\frac{3}{4\pi}} \cos\theta',$$

and

$$Y^{*}_{1,-1}(\theta',\phi') = - Y_{1,1}(\theta',\phi') \tag{D9}$$

Meanwhile, the following relationships

$$x' = r' \sin\theta' \cos\phi' ,$$

$$y' = r' \cos\theta' \sin\phi' ,$$

and

$$z' = r' \cos\theta' \tag{D10}$$

are applied to the definition of the electric dipole moments,

$$p_x = \int x'\rho \, dv ,$$

$$p_y = \int y'\rho \, dv ,$$

and

$$p_z = \int z'\rho \, dv \tag{D11}$$

A straightforward rearrangement shows that the asymptotic coefficients are related to the moments as

$$p_{1,1} = - \sqrt{\frac{3}{8\pi}} (p_x - jp_y) ,$$

$$p_{1,0} = \sqrt{\frac{3}{4\pi}} p_z ,$$

and

$$p_{1,-1} = \sqrt{\frac{3}{8\pi}} (p_x + jp_y) \tag{D12}$$

3. MAGNETIC DIPOLE

The magnetic dipole moment and coefficient have similar relationship as the electric dipole. The magnetic dipole coefficient in spherical harmonics definition is given by

$$m_{1,m} = \frac{3}{2k} \int \nabla' \left[Y^*_{1,m}(\theta',\phi') \, j_1(kr') \right] \cdot (\vec{r}' \times \vec{J}) \, dv \qquad \text{(D13)}$$

where m = -1,0,1.

Note that

$$Y^*_{1,1} \, j_1(kr') \approx \frac{kr'}{3} \left(- \sqrt{\frac{3}{8\pi}} \sin\theta \, e^{-j\phi} \right)$$

$$= - \sqrt{\frac{3}{8\pi}} \frac{k}{3} (x' - jy') \qquad \text{(D14)}$$

when only the first term is retained. The gradient becomes

$$\nabla' \left[Y^*_{1,1} \, j_1(kr') \right] \approx - \sqrt{\frac{3}{8\pi}} \frac{k}{3} (\vec{I}_{x'} - j\vec{I}_{y}) \qquad \text{(D15)}$$

Similarly,

$$\nabla' \left[Y^*_{1,0} \, j_1(kr') \right] \approx \frac{k}{3} \sqrt{\frac{3}{4\pi}} \vec{I}_{z'} \qquad \text{(D16)}$$

Thus the magnetic dipole coefficients are in their asymptotic forms:

$$m_{1,1} \approx - \frac{1}{2} \sqrt{\frac{3}{8\pi}} \int (\vec{I}_{x'} - \vec{I}_{y'}) \cdot (\vec{r}' \times \vec{J}) \, dv \, , \qquad \text{(D17)}$$

and

$$m_{1,0} \approx \frac{1}{2} \sqrt{\frac{3}{4\pi}} \int \vec{I}_{z'} \, (\vec{r}' \times \vec{J}) \, dv \qquad \text{(D18)}$$

Noting that the multipole moments are defined as

$$m_x = \frac{1}{2} \int \vec{I}_x \cdot (\vec{r}' \times \vec{J}) \, dv \qquad \text{(D19)}$$

$$m_y = \frac{1}{2} \int \vec{I}_y \cdot (\vec{r}' \times \vec{J}) \, dv \qquad \text{(D20)}$$

$$m_z = \frac{1}{2} \int \vec{I}_z \cdot (\vec{r}' \times \vec{J}) \, dv \qquad \text{(D21)}$$

it becomes straightforward to show that the magnetic dipole coefficients are related to magnetic dipole moments as

$$m_{1,1} = -\sqrt{\frac{3}{8\pi}}\,(m_x - jm_y)\ , \tag{D22}$$

$$m_{1,0} = \sqrt{\frac{3}{4\pi}}\,m_z\ , \tag{D23}$$

and

$$m_{1,-1} = \sqrt{\frac{3}{8\pi}}\,(m_x + jm_y) \tag{D24}$$

The above series expansions show that the dipole coefficients in general contain dipole moments and higher-order moments. However, the dipole moments become the dominant terms for small sources or low frequencies.

4. ELECTRIC QUADRUPOLE

The electric quadrupole coefficient is given by

$$p_{2,m} = \frac{5}{k^2}\int Y^*_{2,m}(\theta',\phi')\left[\rho\ kr'\ j_1(kr') - 2j_2(kr') + \frac{jk}{c}\,(\vec{r}'\cdot\vec{J})\ j_2(kr')\right] dv \qquad \text{for } m = \pm 2, \pm 1, 0 \tag{D25}$$

Using equation (D4) and retaining the $(kr')^2$ term in the integrand,

$$p_{2,m} \approx \int (r')^2\ Y^*_{2,m}\,\rho\,dv \tag{D26}$$

Using the expression of $Y^*_{2,m}$ in Appendix B and transforming spherical coordinates into the rectangular coordinates, the asymptotic quadrupole coefficients become related to the rectangular moments as

$$p_{2,2} = \frac{1}{4}\sqrt{\frac{15}{2\pi}}\,(p_{xx} - p_{yy} - j2p_{xy}) \tag{D27}$$

$$p_{2,1} = -\sqrt{\frac{15}{8\pi}}\,(p_{xz} - jp_{yz}) \tag{D28}$$

$$p_{2,0} = \frac{1}{2}\sqrt{\frac{5}{4\pi}}\,(2p_{zz} - p_{xx} - p_{yy}) \tag{D29}$$

$$p_{2,-1} = \sqrt{\frac{15}{8\pi}}\,(p_{xz} + jp_{yz}) \tag{D30}$$

$$p_{2,-2} = \frac{1}{4}\sqrt{\frac{15}{2\pi}}\,(p_{xx} - p_{yy} + j2p_{xy}) \tag{D31}$$

5. MAGNETIC QUADRUPOLE

The magnetic quadrupole coefficients are defined as

$$m_{2,m} = \frac{5}{k^2}\int \nabla'\left[Y^*_{2,m}(\theta',\phi')\, j_2(kr')\right] \cdot (\vec{r}' \times \vec{J})\, dv \tag{D32}$$

Keeping only the first term of $j_2(kr')$ expansion

$$m_{2,m} \simeq \frac{1}{3}\int \nabla'(r'^2 Y^*_{2,m}) \cdot (\vec{r}' \times \vec{J})\, dv \tag{D33}$$

Following the same steps performed earlier, and using the definitions for magnetic quadrupole moments,

$$m_{x_i,x_j} = \frac{1}{2}\int \left[x_i(\vec{r}' \times \vec{J}) \cdot \vec{1}_j + x_j(\vec{r}' \times \vec{J}) \cdot \vec{1}_i\right] dv \tag{D34}$$

the desired relationships are obtained as follows:

$$m_{2,2} = \frac{1}{6}\sqrt{\frac{15}{2\pi}}\,(m_{xx} - m_{yy} - j2m_{xy}) \tag{D35}$$

$$m_{2,1} = -\frac{2}{3}\sqrt{\frac{15}{8\pi}}\,(m_{xz} - jm_{yz}) \tag{D36}$$

$$m_{2,0} = \frac{1}{3}\sqrt{\frac{5}{4\pi}}\,(2m_{zz} - m_{xx} - m_{yy}) \tag{D37}$$

$$m_{2,-1} = \frac{2}{3}\sqrt{\frac{15}{8\pi}}\,(m_{xz} + jm_{yz}) \tag{D38}$$

$$m_{2,-2} = \frac{1}{6}\sqrt{\frac{15}{2\pi}}\,(m_{xx} - m_{yy} + j2m_{xy}) \tag{D39}$$

APPENDIX E

TOTAL RADIATED POWER OF MULTIPOLES

The total radiated power is defined as the integration of Poynting vector in radial direction over a spherical surface of radius r:

$$P = \frac{1}{2}\int_0^{2\pi}\int_0^{\pi} \vec{E} \times \vec{H}^* \cdot \hat{I}_r r^2 \sin\theta \, d\theta \, d\phi \tag{E1}$$

where the fields expressed in multipole coefficients are:

$$\vec{E} = \sum_{\ell=1}^{\infty}\left[\frac{jk^{\ell+2}c\mu_o}{(2\ell+1)!!}\left(\frac{\ell+1}{\ell}\right)^{\frac{1}{2}} h_\ell^{(2)}(kr) \sum_{m=-\ell}^{\ell} m_{\ell,m}\vec{X}_{\ell,m} + \frac{1}{j\omega\varepsilon_o}\frac{k^{\ell+2}c}{j(2\ell+1)!!}\left(\frac{\ell+1}{\ell}\right)^{\frac{1}{2}} \sum_{m=-\ell}^{\ell} p_{\ell,m}\nabla \times h_\ell^{(2)}(kr)\vec{X}_{\ell,m}\right] \tag{E2}$$

$$\vec{H} = \sum_{\ell=1}^{\infty}\left[\frac{k^{\ell+2}c}{j(2\ell+1)!!}\left(\frac{\ell+1}{\ell}\right)^{\frac{1}{2}} h_\ell^{(2)}(kr) \sum_{m=-\ell}^{\ell} p_{\ell,m}\vec{X}_{\ell,m} + \frac{j}{\omega\mu_o}\frac{jk^{\ell+2}c\mu_o}{(2\ell+1)!!}\left(\frac{\ell+1}{\ell}\right)^{\frac{1}{2}} \sum_{m=-\ell}^{\ell} m_{\ell,m}\nabla \times h_\ell^{(2)}\vec{X}_{\ell,m}\right] \tag{E3}$$

and, $h_\ell^{(2)}$, $m_{\ell,m}$, $p_{\ell,m}$, and $\vec{X}_{\ell,m}$ are defined in Appendix B.

Define coefficients a_ℓ and b_ℓ as

$$a_\ell = \frac{jk^{\ell+2}c\mu_o}{(2\ell+1)!!}\left(\frac{\ell+1}{\ell}\right)^{\frac{1}{2}} \tag{E4}$$

$$b_\ell = \frac{k^{\ell+2}c}{j(2\ell+1)!!}\left(\frac{\ell+1}{\ell}\right)^{\frac{1}{2}} \tag{E5}$$

and the fields as

$$\vec{E}_1 = \sum_{\ell,m} a_\ell h_\ell^{(2)}(r)\, m_{\ell,m}\, \vec{X}_{\ell,m} \tag{E6}$$

$$\vec{E}_2 = \sum_{\ell,m} \frac{b_\ell}{j\omega\varepsilon_o}\, p_{\ell,m} \nabla \times h_\ell^{(2)}\, \vec{X}_{\ell,m} \tag{E7}$$

$$\vec{H}_1 = \sum_{\ell,m} \frac{j}{\omega\mu_o}\, a_\ell\, m_{\ell,m} \nabla \times h_\ell^{(2)}\, \vec{X}_{\ell,m} \tag{E8}$$

$$\vec{H}_2 = \sum_{\ell,m} b_\ell h_\ell^{(2)}\, p_{\ell,m}\, \vec{X}_{\ell,m} \tag{E9}$$

so that the fields can be represented as

$$\vec{E} = \vec{E}_1 + \vec{E}_2 \tag{E10}$$

$$\vec{H} = \vec{H}_1 + \vec{H}_2 \tag{E11}$$

Substitute equations (E10) and (E11) into equation (E1) and decompose P into four parts

$$P = P_1 + P_2 + P_3 + P_4 \tag{E12}$$

where

$$P_1 = \frac{1}{2} \iint \vec{E}_1 \times \vec{H}_1^* \cdot \vec{1}_r r^2 \sin\theta\, d\theta\, d\phi \tag{E13}$$

$$P_2 = \frac{1}{2} \iint \vec{E}_1 \times \vec{H}_2^* \cdot \vec{1}_r r^2 \sin\theta\, d\theta\, d\phi \tag{E14}$$

$$P_3 = \frac{1}{2} \iint \vec{E}_2 \times \vec{H}_1^* \cdot \vec{1}_r r^2 \sin\theta\, d\theta\, d\phi \tag{E15}$$

$$P_4 = \frac{1}{2} \iint \vec{E}_2 \times \vec{H}_2^* \cdot \vec{1}_r r^2 \sin\theta\, d\theta\, d\phi \tag{E16}$$

Note that the vector identity

$$(\vec{A} \times \vec{B}) \cdot \vec{C} = \vec{A} \cdot (\vec{B} \times \vec{C})$$
$$= \vec{B} \cdot (\vec{C} \times \vec{A}) \qquad \text{(E17)}$$

can be used in the integrand of P_1, after equations (E6) and (E8) are used. First,

$$\vec{X}_{\ell,m} \times (\nabla \times h_\ell^{(2)} \vec{X}_{\ell,m})^* \cdot \vec{1}_r = \vec{X}_{\ell,m} \cdot \left[(\nabla \times h_\ell \vec{X}_{\ell,m})^* \times \vec{1}_r\right] \qquad \text{(E18)}$$

then from Appendix C

$$(\nabla \times h_\ell^{(2)} \vec{X}_{\ell,m}) \times \vec{1}_r = h_\ell'(r) \vec{X}_{\ell,m} \qquad \text{(E19)}$$

where

$$h_\ell'(r) = k h_{\ell-1}^{(2)} - \frac{\ell}{r} h_\ell^{(2)} \qquad \text{(E20)}$$

Hence the vector operations in the integrand of P_1 become

$$\vec{X}_{\ell,m} \times (\nabla \times h_\ell^{(2)} \vec{X}_{\ell,m})^* \cdot 1_r = \vec{X}_{\ell,m} \cdot h_\ell'(r) \vec{X}^*_{\ell,m} \qquad \text{(E21)}$$

By orthonormality of $\vec{X}_{\ell,m}$, the integrated result is

$$P_1 = -\frac{j}{2\omega\mu_o} \sum_{\ell,m} |a_\ell|^2 |m_{\ell,m}|^2 \left[h_\ell^{(2)}\right](h_\ell')^* r^2 \qquad \text{(E22)}$$

The quantities P_2 and P_3 involve cross products of fields that are produced by two independent sets of electric and magnetic densities. Their net outflow of powers has been demonstrated to be zero for the dipoles and quadrupoles. For the present purpose, P_2 and P_3 are identically zero for the first two lowest-order poles.

The evaluation of P_4 is similar to P_1. It is obtained as

$$P_4 = \frac{j}{2\omega\varepsilon_o} \sum_{\ell,m} |b_\ell|^2 |p_{\ell,m}|^2 \, h_\ell^{(2)*} \, h_\ell' \, r^2 \qquad \text{(E23)}$$

For the purpose of providing some examples, the dipole and quadrupole terms are combined from equations (E22) and (E23) as

$$P \simeq -\frac{jr^2}{2\omega\mu_o} \sum_{\ell=1}^{2} \sum_{m=-\ell}^{\ell} \left[|a_\ell|^2 |m_{\ell,m}|^2 \, h_\ell^{(2)} (h_\ell')^* - \frac{\mu_o}{\varepsilon_o} |b_\ell|^2 |p_{\ell,m}|^2 \, h_\ell^{(2)*} h_\ell' \right] \qquad \text{(E24)}$$

Examples are given below for electric dipole, magnetic dipole, and a combined $\vec{p}\times\vec{m}$ dipole.

Example 1. Radiated Power of an Electric Dipole Centered Along x-Axis

The electric dipole coefficients in Appendix D can be used in equation (E24) to give

$$P = \frac{jr^2}{2\omega\varepsilon_o} \left(\frac{k^3 \, c\sqrt{2}}{3} \right)^2 \left(|p_{1,1}|^2 + |p_{1,-1}|^2 \right) \cdot h_1^{(2)*} \, h_1'$$

Note that

$$h_o^{(2)} = \frac{j}{kr} e^{-jkr}$$

and

$$h_1^{(2)} = -\frac{1}{kr} \left(1 - \frac{j}{kr}\right) e^{-jkr}$$

The use of equation (E20) gives

$$h_1' = k h_o^{(2)} - \frac{h_1^{(2)}}{r} = \left[\frac{j}{r} + \frac{1}{kr^2} - \frac{j}{k^2 r^3} \right] e^{-jkr}$$

Simple substitutions give rise to

$$P = -\frac{j2k^4 c}{9\varepsilon_o} |p_{1,1}|^2 \left[j + \frac{1}{k^3 r^3} \right]$$

For an electrically small dipole with $p_y = 0$

$$|p_{1,1}|^2 \cong \frac{3}{8\pi} |p_x|^2$$

$$P \simeq - \frac{jk^4 c}{12\pi\varepsilon_o} |p_x|^2 \left[j + \frac{1}{k^3 r^3} \right]$$

Example 2. Radiated Power of a Magnetic Dipole Centered Along y-Axis

The magnetic dipole coefficients in Appendix D give

$$P = - \frac{jr^2}{2\omega\mu_o} \left(\frac{k^3 \mu_o c\sqrt{2}}{3} \right)^2 \left(|m_{1,1}|^2 + |m_{1,-1}|^2 \right) h_1^{(2)} \cdot (h_1')^*$$

$$= \frac{j2k^4 c\mu_o}{9} |m_{1,1}|^2 \left[-j + \frac{1}{k^3 r^3} \right]$$

For a small magnetic dipole with $m_x = 0$

$$|m_{1,1}|^2 \cong \frac{3}{8\pi} |m_y|^2$$

$$P \simeq \frac{jk^4 c\mu_o}{12\pi} |m_y|^2 \left[-j + \frac{1}{k^3 r^3} \right]$$

Example 3. Radiated Power of a $\vec{p}\times\vec{m}$ Combination

By imposing the p cross m condition, $cp_{1,1} = -m_{1,1}$, the results of last two examples can be combined to give

$$P_{p\times m} = \frac{4k^2 c|p_{1,1}|^2}{9\varepsilon_o} \simeq \frac{k^4 c}{6\pi\varepsilon_o} |p_x|^2$$

which is purely real and independent of the distance r.

APPENDIX F

MULTIPOLE MOMENTS OF THE TRANSMISSION-LINE MEDIUS

1. TRANSMISSION-LINE MEDIUS

The transmission-line MEDIUS has a flat section of length 2L (region II), a slant section at the source end with angle 2α (region I), and a slant section at the load end with angle $2\alpha_2$ (region III). The transmission line is sketched as follows:

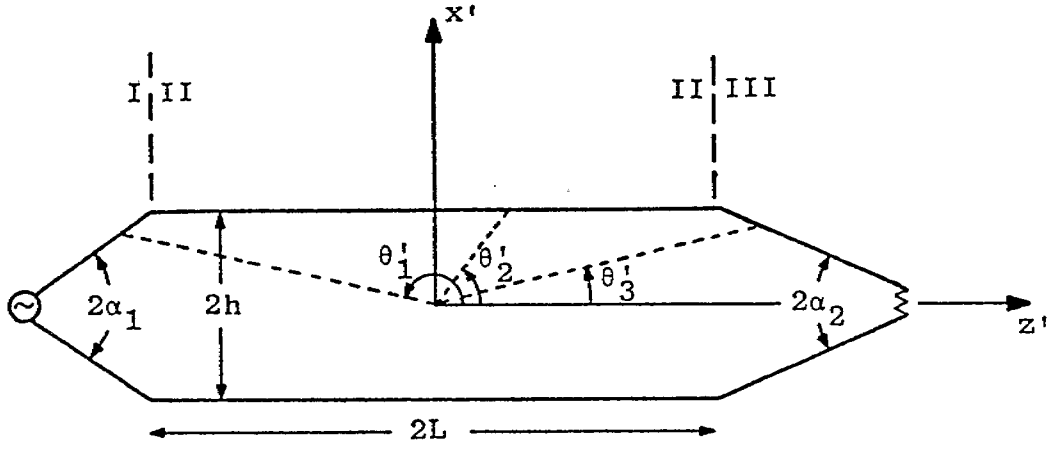

It is assumed that there is no mismatch along the entire line. Under this assumption, the current and charge distribution will be given first in this appendix. The definitions of multipole coefficients will then be defined for the purpose of applying to the transmission line. Finally, the dipole and quadrupole moments of both electric and magnetic types will be formulated.

2. CURRENT AND CHARGE DISTRIBUTIONS

The current distribution on the structure is assumed to take the forms (all variables are unprimed in the following equations without risk of confusion):

$$\vec{I}_{\pm} = \begin{cases} I_o[\sin(\alpha_1)\vec{I}_x \pm \cos(\alpha_1)\vec{I}_z]e^{-jk(z+L)\sec(\alpha_1)+jkL} & \text{in I} \\ \pm I_o \vec{I}_z & \text{in II} \\ I_o[-\sin(\alpha_2)\vec{I}_x \pm \cos(\alpha_2)\vec{I}_z]\ e^{-jk(z-L)\sec(\alpha_2)-jkL} & \text{in III} \end{cases}$$

$$\text{for } x \gtrless 0 \qquad \text{(F1)}$$

The charge distribution can be obtained by the continuity equation as:

$$q_{\pm} = \begin{cases} \pm\frac{I_o}{c}\ e^{-jk(z+L)\sec(\alpha_1)+jkL} & \text{in I} \\ \pm\frac{I_o}{c}\ e^{-jkz} & \text{in II} \\ \pm\frac{I_o}{c}\ e^{-jk(z-L)\sec(\alpha_2)-jkL} & \text{in III} \end{cases}$$

$$\text{for } x \gtrless 0 \qquad \text{(F2)}$$

3. MULTIPOLE MOMENTS

The multipole moments in quasi-static approximation are defined as

$$\vec{p} = \int \vec{r}\ \rho\, dv \qquad \text{(F3)}$$

$$\vec{m} = \frac{1}{2}\int \vec{r} \times \vec{J}\, dv \qquad \text{(F4)}$$

$$(\vec{\vec{p}})_{x_i x_j} = \int x_i x_j\, \rho\, dv \qquad \text{(F5)}$$

$$(\vec{\vec{m}})_{x_i x_j} = \frac{1}{2}\int \left[x_i(\vec{r} \times \vec{J})_{x_j} + x_j(\vec{r} \times \vec{J})_{x_i}\right] dv \qquad \text{(F6)}$$

for electric dipole moment $\vec{p}$, magnetic dipole moment $\vec{m}$, electric quadrupole moment $(\vec{\vec{p}})_{x_i x_j}$, and magnetic quadrupole moment $(\vec{\vec{m}})_{x_i x_j}$, respectively.

The multipole coefficients in spherical harmonics are given by

$$p_{\ell,m} = \frac{(2\ell+1)!!}{k^{\ell}(\ell+1)} \int Y^{*}_{\ell,m} \left\{ \rho \left[kr\, j_{\ell-1} - \ell j_{\ell} \right] + \frac{jk}{c} (\vec{r}' \cdot \vec{J})\, j_{\ell} \right\} dv \qquad \text{(F7)}$$

$$m_{\ell,m} = \frac{(2\ell+1)!!}{k^{\ell}(\ell+1)} \int \nabla(Y^{*}_{\ell,m} j_{\ell}) \cdot (\vec{r} \times \vec{J})\, dv \qquad \text{(F8)}$$

where $p_{\ell,m}$ is the electric multipole coefficient, $m_{\ell,m}$ is the magnetic multipole coefficient. The dipole coefficient consists of three components with index $\ell = 1$ and $m = -1,0,1$. The quadrupole coefficient has five components with index $\ell = 2$ and $m = -2,-1,0,1,2$. The formulation of multipole moments and coefficients for the transmission line are given below.

4. ELECTRIC DIPOLE MOMENT

The electric dipole moment for the MEDIUS can be expressed according to equation (F3) as

$$\vec{p}^{(1)} = \int (x\vec{1}_x + z\vec{1}_z)\, q(z) \sqrt{1 + \left(\frac{dx}{dz}\right)^2}\, dz \qquad \text{(F9)}$$

where

$$x = \begin{cases} z \tan(\alpha_1) + L \tan(\alpha_1) + h\,, & \text{in I} \\ h\,, & \text{in II} \\ -z \tan(\alpha_2) + L \tan(\alpha_2) + h\,, & \text{in III} \end{cases} \qquad \text{(F10)}$$

$$\frac{dx}{dz} = \begin{cases} \tan(\alpha_1) & \text{in I} \\ 0 & \text{in II} \\ -\tan(\alpha_2) & \text{in III} \end{cases} \qquad \text{(F11)}$$

Let the dipole moment $\vec{p}$ in equation (F9) be treated in three distinct regions I, II, and III as

$$\vec{p}^{(1)} = \vec{p}_1^{(1)} + \vec{p}_2^{(1)} + \vec{p}_3^{(1)} \qquad \text{(F12)}$$

Their x-components may be integrated only along the upper part of the transmission line as

$$\vec{p}_1^{(1)} = \vec{I}_x(2) \int_{-L-h\cot(\alpha_1)}^{-L} \left\{ [z \tan(\alpha_1) + L \tan(\alpha_1) + h] \; q_+(z) \sec(\alpha_1) \right\} dz \qquad \text{(F13)}$$

$$\vec{p}_2^{(1)} = \vec{I}_x(2) \int_{-L}^{L} h q_+(z) \, dz \qquad \text{(F14)}$$

$$\vec{p}_3^{(1)} = \vec{I}_x(2) \int_{L}^{L+h\cot(\alpha_1)} \left\{ [-z \tan(\alpha_2) + L \tan(\alpha_2) + h] \, q_+(z) \sec(\alpha_2) \right\} dz \qquad \text{(F15)}$$

After making use of equation (F2), the $\vec{p}_1^{(1)}$ and $\vec{p}_3^{(1)}$ can be simplified by the function

$$f_1(k,\alpha) = \int_{-L-h\cot(\alpha)}^{-L} \left\{ [z \tan(\alpha) + L \tan(\alpha) + h] \sec(\alpha) \right\} e^{-j[k(z+L)\sec(\alpha)+kL]} dz \qquad \text{(F16)}$$

After integration, it becomes

$$f_1(k,\alpha) = \frac{\sin(\alpha)[1 - e^{jkh\csc(\alpha)} + jkh \csc(\alpha)] e^{jkL}}{k^2} \qquad \text{(F17)}$$

Thus

$$\vec{p}_1^{(1)} = \frac{2I_o}{c} f_1(k,\alpha_1)\,\vec{I}_x \tag{F18}$$

Noting that $f_1(-k,\alpha) = f_1^*(k,\alpha)$, equation (F15) can be written as

$$\vec{p}_3^{(1)} = \frac{2I_o}{c} f_1^*(k,\alpha_2)\vec{I}_x \tag{F19}$$

The $\vec{p}_2^{(1)}$ in equation (F14) is readily obtained as

$$\vec{p}_2^{(1)} = \frac{4I_o h}{ck} \sin(kL)\,\vec{I}_x \tag{F20}$$

For the case $\alpha_1 = \alpha_2 = \alpha$,

$$\begin{aligned}\vec{p}_1^{(1)} + \vec{p}_3^{(1)} &= \frac{4I_o}{c} \mathrm{Re}\left(f_1(k,\alpha)\right)\vec{I}_x \\ &= \vec{I}_x \frac{4I_o h}{ck}\left\{\left[\frac{2\sin\left(\frac{kh\csc(\alpha)}{2}\right)\sin\left(kL + \frac{kh\csc(\alpha)}{2}\right)}{kh}\sin(\alpha)\right]\right. \\ &\quad \left. - \sin(kL)\right\}\end{aligned} \tag{F21}$$

The total dipole moment becomes

$$\begin{aligned}\vec{p}^{(1)} &= \vec{p}_1^{(1)} + \vec{p}_2^{(1)} + \vec{p}_3^{(1)} \\ &= \vec{I}_x \frac{8I_o}{ck^2} \sin(\alpha) \sin\left[\frac{kh\csc(\alpha)}{2}\right] \sin\left[kL + \frac{kh\csc(\alpha)}{2}\right]\end{aligned} \tag{F22}$$

Before the magnetic dipole moment is formulated, it is worth noting that the z-component in equation (F9) is identically zero due to the fact that the charge distribution is antisymmetric with respect to the z axis.

5. MAGNETIC DIPOLE MOMENT

The magnetic dipole moment for the transmission line is, according to equation (F4),

$$\vec{m}^{(1)} = -\vec{I}_y \frac{1}{2} \int (xI_z - zI_x) \sqrt{1 + \left(\frac{dx}{dz}\right)^2}\, dz \qquad \text{(F23)}$$

where the currents I_x, I_z are defined in equation (F1). The integrand can be decomposed making use of equations (F10) and (F11) as

$$(xI_z - zI_x) \sqrt{1 + \left(\frac{dx}{dz}\right)^2} = \begin{cases} I_o[L \tan(\alpha_1) + h]\, e^{-jk(z+L)\sec(\alpha_1)+jkL}, & \text{in I} \\ I_o\, h\, e^{-jkz}, & \text{in II} \\ I_o[L \tan(\alpha_2) + h]\, e^{-jk(z-L)\sec(\alpha_2)-jkL}, & \text{in III} \end{cases} \qquad \text{(F24)}$$

Again, let equation (F23) be written in regions I, II, and III as

$$\vec{m}^{(1)} = \vec{m}_1^{(1)} + \vec{m}_2^{(1)} + \vec{m}_3^{(1)} \qquad \text{(F25)}$$

$$m_1^{(1)} = -\vec{I}_y \int_{-L-h\cot(\alpha_1)}^{-L} I_o[L \tan(\alpha_1) + h]\, e^{-jk(z+L)\sec(\alpha_1)+jkL}\, dz \qquad \text{(F26)}$$

$$\vec{m}_2^{(1)} = -\vec{I}_y \int_{-L}^{L} I_o h\, e^{-jkz}\, dz \qquad \text{(F27)}$$

$$\vec{m}_3^{(1)} = -\vec{I}_y \int_{L}^{L+h\cot(\alpha_2)} I_o[L \tan(\alpha_2) + h]\, e^{-jk(z-L)\sec(\alpha_2)-jkL}\, dz \qquad \text{(F28)}$$

Define a function as was done in equation (F16),

$$f_2(k,\alpha) = \int_{-L-h\cot(\alpha)}^{-L} [L \tan(\alpha) + h]\, e^{-jk(z+L)\sec(\alpha)+jkL}\, dz$$

$$= \frac{j[h \cos(\alpha) + L \sin(\alpha)]}{k} e^{jkL} \left[1 - e^{jkh\csc(\alpha)}\right] \qquad \text{(F29)}$$

Noting that $f_2(-k,\alpha) = f_2^*(k,\alpha)$, equation (F25) can be written as

$$\vec{m}_1^{(1)} = -\vec{I}_y I_o f_2(k,\alpha_1) \tag{F30}$$

$$\vec{m}_2^{(1)} = -\vec{I}_y \frac{2I_o h}{k} \sin(kL) \tag{F31}$$

$$\vec{m}_3^{(1)} = -\vec{I}_y I_o f_2^*(k,\alpha_2) \tag{F32}$$

For the case $\alpha_1 = \alpha_2 = \alpha$

$$\vec{m}_1^{(1)} + \vec{m}_3^{(1)} = -2I_o \vec{I}_y \mathrm{Re}[f_2(k,\alpha)]$$

$$= -\vec{I}_y 4I_o [L + h\cot(\alpha)] \frac{\sin(\alpha)}{k} \cdot \sin\left[\frac{kh\csc(\alpha)}{2}\right] \cos\left[kL + \frac{kh\csc(\alpha)}{2}\right] \tag{F33}$$

Thus the total magnetic dipole moment in equation (F25) becomes

$$\vec{m}^{(1)} = -\hat{y}\frac{2I_o}{k}\left\{h \sin(kL) + 2[L \sin(\alpha) + h\cos(\alpha)] \cdot \sin\left[\frac{kh\csc(\alpha)}{2}\right] \cdot \cos\left[kL + \frac{kh\csc(\alpha)}{2}\right]\right\} \tag{F34}$$

6. ELECTRIC QUADRUPOLE MOMENT

The electric quadrupole moment is defined in dyadic form as

$$\vec{\vec{p}}^{(2)} = \int \vec{r}\,\vec{r}\,\rho\, dv \tag{F35}$$

where $\vec{r} = x\vec{I}_x + z\vec{I}_y$ for the transmission line. Assuming $\alpha_1 = \alpha_2 = \alpha$ the antisymmetry of the charge distribution requires that the components $p_{x,x}^{(2)}$ and $p_{y,y}^{(2)}$ vanish. The nonzero components are $p_{x,z}^{(2)}$ and $p_{z,x}^{(2)}$. By the definition,

$$p_{x,z}^{(2)} = \int x\, z\, q(z) \sqrt{1 + \left(\frac{dx}{dz}\right)^2}\, dz = p_{z,x}^{(2)} \tag{F36}$$

it can be shown that contribution from the lower part is equal to that of the upper part of the structure.

Let

$$p_{x,z}^{(2)} = p_1^{(2)} + p_2^{(2)} + p_3^{(2)} \tag{F37}$$

and integrate only along the upper part of the transmission line,

$$p_1^{(2)} = \frac{2I_o}{c} \int_{-L-h\cot(\alpha_1)}^{-L} z\,[z\,\tan(\alpha_1) + L\,\tan(\alpha_1) + h]\; e^{-jk(z+L)\sec(\alpha_1)+jkL} \cdot \sec(\alpha_1)\, dz \tag{F38}$$

$$p_2^{(2)} = \frac{2I_o}{c} \int_{-L}^{L} hz\, e^{-jkz}\, dz \tag{F39}$$

$$p_3^{(2)} = \frac{2I_o}{c} \int_{L}^{L+h\cot(\alpha_2)} z[-z\,\tan(\alpha_2) + L\,\tan(\alpha_2) + h]\; e^{-jk(z-L)\sec(\alpha_2)-jkL} \cdot \sec(\alpha_2)\, dz \tag{F40}$$

where $p_1^{(2)}$ and $p_3^{(2}$ can be expressed with a common function:

$$f_3(k,\alpha) = \int_{-L-h\cot(\alpha)}^{-L} z[z\,\tan(\alpha) + L\,\tan(\alpha) + h]\,\sec(\alpha) \cdot e^{-jk(z+L)\sec(\alpha)+jkL}\, dz$$

$$= \frac{e^{jkL}\tan(\alpha)}{k}\left[-jLh\cot(\alpha) + \frac{h\cot(\alpha) - L}{k\,\sec(\alpha)} - \frac{2j}{k^2\sec^2(\alpha)}\right]$$

$$+ \frac{e^{jkh\csc(\alpha)}\tan(\alpha)}{k}\left[\frac{L + h\cot(\alpha)}{k\,\sec(\alpha)} + \frac{2j}{k^2\sec^2(\alpha)}\right] e^{jkL} \tag{F41}$$

Note that

$$f_3(-k,\alpha) - f_3^*(k,\alpha) \tag{F42}$$

Hence

$$p_1^{(2)} = \frac{2I_o}{c} f_3(k,\alpha) \tag{F43}$$

$$p_2^{(2)} = \frac{j4hI_oL}{ck}\left[\cos(kL) - \frac{\sin(kL)}{kL}\right] \tag{F44}$$

$$p_3^{(2)} = -\frac{2I_o}{c} f_3^*(k,\alpha_2) \tag{F45}$$

For $\alpha_1 = \alpha_2 = \alpha$,

$$p_1^{(2)} + p_3^{(2)} = \frac{j4I_o}{c}\,\mathrm{Im}[f_3(k,\alpha)]$$

$$= \frac{j4I_o}{c}\frac{\tan(\alpha)}{k}\left\{-Lh\cot(\alpha)\cos(kL) + \frac{2h}{k}\cot(\alpha)\cos(\alpha)\right.$$

$$\cdot \cos\left[\frac{kh\csc(\alpha)}{2}\right]\sin\left[\frac{kh\csc(\alpha)}{2} + kL\right]$$

$$+ \frac{2L}{k}\cos(\alpha)\sin\left[\frac{kh\csc(\alpha)}{2}\right]\cos\left[\frac{kh\csc(\alpha)}{2} + kL\right]$$

$$\left. - \frac{4}{k^2}\cos^2(\alpha)\sin\left[\frac{kh\csc(\alpha)}{2}\right]\sin\left[\frac{kh\csc(\alpha)}{2} + kL\right]\right\} \tag{F46}$$

7. MAGNETIC QUADRUPOLE MOMENT

The magnetic quadrupole moment of the transmission line is defined in dyadic form as

$$\vec{\vec{m}}^{(2)} = \frac{1}{2}\int \vec{r}(\vec{r}\times\vec{I}) + (\vec{r}\times\vec{I})\,\vec{r}\,dy \tag{F47}$$

where $\vec{r} = x\vec{i}_x + z\vec{i}_z$ and $\vec{I} = I_x\vec{i}_x + I_z\vec{i}_z$. Note that $\vec{\vec{m}}^{(2)}$ is a symmetric dyad, and only $m_{y,z}$ and $m_{z,y}$ are nonzero. For example:

$$m_{x,y} = m_{y,x} = \frac{1}{2} \int (xz\ I_x - x^2 I_z)\ dz \qquad \text{(F48)}$$

where the contributions from the lower and upper parts of the structure cancel each other. Thus, $m_{x,y} = m_{y,x} = 0$.

The two nonzero components are

$$m^{(2)}_{y,z} = m^{(2)}_{z,y} = \frac{1}{2} \int (z^2 I_x - xz\ I_z)\ dz \qquad \text{(F49)}$$

Let $m^{(2)}_{y,z} = m^{(2)}_1 + m^{(2)}_2 + m^{(2)}_3$ and integrate only along the upper part of the structure,

$$m^{(2)}_1 = -I_o \int_{-L-h\cot(\alpha_1)}^{-L} z[L \sin(\alpha_1) + h \cos(\alpha_1)] \sec(\alpha_1) e^{-jk(z+L)\sec(\alpha_1)} \cdot e^{jkL}\ dz \qquad \text{(F50)}$$

$$m^{(2)}_2 = -I_o \int_{-L}^{L} (h)(z)\ e^{-jkz}\ dz \qquad \text{(F51)}$$

$$m^{(2)}_3 = -I_o \int_{L}^{L+h\cot(\alpha_1)} z[L \sin(\alpha_2) + h \cos(\alpha_2)] \sec(\alpha_2) e^{-jk(z-L)\sec(\alpha_2)} \cdot e^{-jkL}\ dz \qquad \text{(F52)}$$

To simplify these expressions, a function is defined as

$$f_4(k,\alpha) = \int_{-L-h\cot(\alpha)}^{-L} z[L \sin(\alpha) + h \cos(\alpha)] \sec(\alpha) \cdot e^{-jk(z+L)\sec(\alpha)+jkL}\ dz \qquad \text{(F53)}$$

$$f_4(k,\alpha) = \frac{[L \sin(\alpha) + h \cos(\alpha)]\, e^{jkL}}{k^2 \sec(\alpha)} \Big\{ 1 - jkL \sec(\alpha)$$

$$+ [jkL \sec(\alpha) + jkh \csc(\alpha) - 1]\; e^{jkh\csc(\alpha)} \Big\} \qquad \text{(F54)}$$

Note that

$$f_4(-k,\alpha) = f_4^*(k,\alpha) \qquad \text{(F55)}$$

Thus the integrated results are

$$m_1^{(2)} = -I_o\, f_4(k,\alpha_1) \qquad \text{(F56)}$$

$$m_2^{(2)} = \frac{j2hI_o}{k^2} [\sin(kL) - kL \cos(kL)] \qquad \text{(F57)}$$

$$m_3^{(2)} = I_o\, f_4^*(k,\alpha_2) \qquad \text{(F58)}$$

For the case $\alpha_1 = \alpha_2 = \alpha$,

$$m_1^{(2)} + m_3^{(2)} = -j2I_o\, \mathrm{Im}[f_4(k,\alpha)]$$

$$= -j2I_o \frac{L \sin(\alpha) + h \csc(\alpha)}{k^2 \sec(\alpha)} \Big\{ - 2 \sin \frac{kh \csc(\alpha)}{2}$$

$$\cos\left[\frac{kh \csc(\alpha)}{2} + kL\right] - 2\, kL \sec(\alpha) \sin \frac{kh \csc(\alpha)}{2}$$

$$\sin\left[\frac{kh \csc(\alpha)}{2} + kL\right] + kh \csc(\alpha) \cos[kL + kh \csc(\alpha)] \Big\}$$

(F59)

The dipole and quadrupole moments of the transmission line ave been formulated in this Appendix. Their corresponding oefficients associated with spherical harmonics are given in the in text.

APPENDIX G

MULTIPOLE COEFFICIENTS OF THE COMBINED LINEAR AND CIRCULAR CURRENT ELEMENTS

1. THE COMBINED CURRENT ELEMENTS

A linear current element of length 2h and a circular current element of diameter 2b are arranged to have the coincident center at the coordinate origin as shown in the figure:

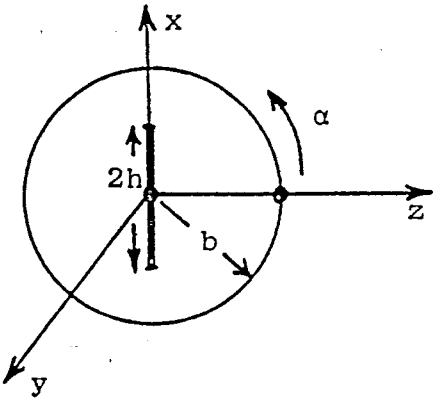

2. MULTIPOLE COEFFICIENTS OF THE LINEAR ELEMENT

The current and charge distribution of a linear current element can be written (ref. 9) as

$$\vec{I}(x') = \vec{1}_x I_o \left\{ \sin k(h - |x'|) + A\left[\cos(kx') - \cos(kh)\right] + B\left[\cos\left(\frac{kx'}{2}\right) - \cos\left(\frac{kh}{2}\right)\right] \right\} \qquad \text{(G1)}$$

$$q(x') = \frac{jI_o}{c}\left[\pm\cos k(h - |x'|) + A \sin(kx') + \frac{B}{2}\sin\left(\frac{kx'}{2}\right)\right]$$

$$\text{for} \quad x' \gtrless 0 \qquad \text{(G2)}$$

where the coefficients A and B are functions of wire diameter and length.

To obtain multipole coefficients reference should be made to the definitions in Appendix B. For the linear element, all the magnetic multipole coefficients are identically zero because

$$\vec{x}' \times \vec{I}(x') = 0$$

where the coordinate x is primed to denote the source region.

As for electric multipoles, all the coefficients of orders higher than octupoles are assumed negligibly small for the time being. The electric quadrupole coefficients are defined as

$$p_{2,m} = \frac{5}{k^2} \int Y^*_{2m}(\theta',\phi')\, q(x')[kr'\, j_1(kr') - 2j_2(kr')]\, dx' \tag{G3}$$

where the primed r, θ, and ϕ denote the source region using the conventional spherical coordinate system. Since Y^*_{20} and Y^*_{22} are even while q(x') is odd along the x' axis, it is readily shown that

$$p_{2,0} = p_{2,2} = p_{2,-2} = 0$$

Also, $Y^*_{21} = 0$ at $\theta' = \pi/2$. As a result,

$$p_{2,1} = p_{2,-1} = 0$$

These results confirm the well-known fact that a center-fed linear element has zero quadrupole field.

The electric dipole coefficient $p_{1,0}$ is equal to zero, because $Y^*_{10} = 0$ at $\theta' = \pi/2$. Therefore, the only nonzero coefficients are

$$p_{1,1} = -p_{1,-1} = \frac{-3}{k}\sqrt{\frac{3}{8\pi}} \int_0^h q(x')[kx'\, j_o(kx') - j_1(kx')]\, dx' \tag{G4}$$

3. MULTIPOLE COEFFICIENTS OF CIRCULAR LOOP

The current and charge distribution for the loop is given (ref. 9) by

$$\vec{I} = \vec{I}_\alpha \sum_{-\infty}^{\infty} I_n\, e^{-jn\alpha} = \vec{I}_\alpha I_o\left[\frac{1}{a_o} + 2\sum_{1}^{\infty}\frac{\cos(n\alpha)}{a_n}\right] \tag{G5}$$

$$q = -\frac{1}{j\omega b}\frac{\partial(\vec{I}\cdot\vec{I}_\alpha)}{\partial\alpha}$$

$$= \frac{1}{\omega b}\sum_{-\infty}^{\infty} nI_n\, e^{-jn\alpha}$$

$$= \frac{2I_o}{j\omega b}\sum_{1}^{\infty}\frac{n\,\sin n\alpha}{a_n} \tag{G6}$$

where the coefficients a_n are dependent on the wire diameter and the loop radius.

The electric multipole coefficients are defined as

$$p_{\ell,m} = \frac{(2\ell+1)!!}{k^\ell(\ell+1)}\int Y^*_{\ell,m}\left\{q[kb\, j_{\ell-1}(kb) - \ell j_\ell(kb)]\right.$$

$$\left. + \frac{jk}{c}(\vec{r}'\cdot\vec{I})\, j_\ell(kb)\right\} bd\alpha \tag{G7}$$

The second term of the integrand is zero, because $\vec{r}'\cdot\vec{I} = 0$ for the loop. Also, the integration around the complete loop can be shown to give

$$p_{1,0} = p_{2,0} = p_{2,2} = p_{2,-2} = 0$$

The other nonzero coefficients are

$$p_{1,1} = \frac{3b}{k}(kbj_o - j_1)\int_0^{\pi}\left(-\sqrt{\frac{3}{8\pi}}\right)\sin(\theta)\left[\frac{2I_o}{j\omega b}\sum_1^{\infty}\frac{n\sin(n\theta)}{a_n}\right]d\theta$$

$$= \frac{3b}{k}(kbj_o - j_1)\left(-\sqrt{\frac{3}{8\pi}}\right)\left(\frac{I_o\pi}{j\omega b a_1}\right)$$

$$= -p_{1,-1} \qquad \text{(G8)}$$

and

$$p_{2,1} = \frac{5(kbj_1 - 2j_2)}{k^2}\int_0^{2\pi}-\sqrt{\frac{15}{8\pi}}\sin(\alpha)\cos(\alpha)\left(\frac{2I_o}{j\omega b}\right)\cdot\sum_1^{\infty}\frac{n\sin(n\alpha)}{a_n}\,bd\alpha$$

$$= \frac{5(kbj_1 - 2j_2)}{k^2}\left(-\sqrt{\frac{15}{8\pi}}\right)\frac{2I_o\pi}{j\omega a_2}$$

$$= -p_{2,-1} \qquad \text{(G9)}$$

The magnetic dipole coefficients are given in Appendix B as

$$m_{1,m} = \frac{3}{2k}\int (\nabla Y^*_{1,m} j_1)\cdot(\vec{r}\times\vec{J})\,dv \qquad \text{(G10)}$$

Note that

$$\vec{r}\times\vec{J} = b|\vec{J}|\cdot\begin{cases}\hat{i}_\phi & \phi = 0^\circ\\ -\hat{i}_\phi & \phi = 180^\circ\end{cases} \qquad \text{(G11)}$$

The coefficient $m_{1,0} = 0$, because

$$(\nabla Y^*_{1,0} j_1)_\phi = 0$$

For $m_{1,1}$

$$(\nabla Y^*_{1,1} j_1)_\phi = j\sqrt{\frac{3}{8\pi}}\,\frac{j_1(kb)}{b}\cdot\begin{cases}\vec{I}_\phi\,, & \phi = 0^\circ\\ -\vec{I}_\phi\,, & -\phi = 180^\circ\end{cases} \tag{G12}$$

A substitution and carrying out the integration give rise to

$$m_{1,1} = \frac{j3b}{k}\sqrt{\frac{3}{8\pi}}\,j_1(kb)\,\frac{I_o\pi}{a_o} = m_{1,-1} \tag{G13}$$

because

$$(\nabla Y^*_{1,-1} j_1)_\phi = (\nabla Y^*_{1,1} j_1)_\phi \tag{G14}$$

The magnetic quadrupole coefficients are defined as

$$m_{2,m} = \frac{5}{k^2}\int (\nabla Y^*_{2,m} j_2)\cdot(\vec{r}\times\vec{J})\,dv \tag{G15}$$

The coefficients $m_{2,0}$ and $m_{2,2}$ are zero because

$$(\nabla Y^*_{2,0} j_2)_\phi = 0 \tag{G16}$$

and

$$(\nabla Y^*_{2,2} j_2)_{\phi=0} = (\nabla Y^*_{2,2} j_2)_{\phi=\pi} \tag{G17}$$

For $m_{2,1}$

$$(\nabla Y^*_{2,1} j_2)_\phi = \frac{j\cos(\theta)}{b}\sqrt{\frac{15}{8\pi}}\,j_2(kb)\cdot\begin{cases}\vec{I}_\phi\,, & \phi = 0^\circ\\ -\vec{I}_\phi\,, & -\phi = 180^\circ\end{cases} \tag{G18}$$

Hence,

$$m_{2,1} = \frac{j10}{k^2}\,j_2(kb)\sqrt{\frac{15}{8\pi}}\,\frac{I_o b\pi}{a_1} = m_{2,-2} \tag{G19}$$

because

$$(\nabla Y^*_{2,-1} j_2)_\phi = (\nabla Y^*_{2,1} j_2)_\phi \tag{G20}$$

4. P CROSS M CONDITION FOR A LOOP AND LINEAR DIPOLE COMBINATION

A loop and a linear dipole combination can generate an electric dipole moment and a magnetic dipole moment to satisfy the p cross m condition. The relationship of the currents on both structures is derived here for an electrically small radiation structure.

Consider the loop and linear dipole combination lying in x-z plane as shown in section 1. The linear dipole is centrally fed. The loop is driven at $\alpha = 0$. The diameter of loop is 2b; the length of linear dipole is 2h.

The current on the loop can be rewritten from equation (G5) as

$$\vec{I}_\ell = \vec{1}_\alpha \sum_{-\infty}^{\infty} I_n \, e^{-jn\alpha} \quad , \quad 0 \le \alpha \le 2\pi$$

where I_n are functions of driving voltage, the radius of the wire and the diameter of the loop.

The electric dipole moment and magnetic dipole moment of the loop, in quasi-static definition, can be shown to be

$$\vec{p}_\ell = -j \frac{2\pi b I_1}{\omega} \vec{1}_x$$

and

$$\vec{m}_\ell = I_o \pi b^2 \vec{1}_y \qquad \text{(G21)}$$

The current on the small linear dipole is given by eq. (G2)

$$\vec{I}_d = \vec{1}_x I_d \sin k(h-|x|) \qquad \text{(G22)}$$

The dipole moments of the linear dipole are

$$\vec{p}_d = \hat{i}_x j \frac{2I_d}{k^2 c} [1 - \cos(kh)]$$

and

$$\vec{m}_d = 0 \tag{G23}$$

To have a p cross m condition for the combination, the magnitudes of dipole moments must satisfy

$$|\vec{m}_\ell| = c|\vec{p}_\ell + \vec{p}_d|$$

or

$$I_o \pi b^2 = c\, j\left\{\frac{2I_d}{k^2 c} [1 - \cos(kh)] - \frac{2\pi b I_1}{\omega}\right\} \tag{G24}$$

For the low frequency, $kb << 1$, I_1 can be approximated as

$$I_1 \simeq -k^2 b^2 I_o$$

Hence,

$$\frac{I_d}{I_o} \simeq \left(-j\frac{\pi b^2}{c} - \frac{2\pi b}{\omega} k^2 b^2\right) \Bigg/ \left\{\left(\frac{2}{k^2 c}\right)[1 - \cos(kh)]\right\} \tag{G25}$$

$$\simeq -j\frac{b^2}{h^2} \pi$$